National Library of Canada
Acquisitions and Bibliographic Services Branch
395 Wellington Street
Ottawa, Ontario
K1A 0N4

Bibliothèque nationale du Canada
Direction des acquisitions et des services bibliographiques
395, rue Wellington
Ottawa (Ontario)
K1A 0N4

Your file Votre référence

Our file Notre référence

NOTICE

The quality of this microform is heavily dependent upon the quality of the original thesis submitted for microfilming. Every effort has been made to ensure the highest quality of reproduction possible.

If pages are missing, contact the university which granted the degree.

Some pages may have indistinct print especially if the original pages were typed with a poor typewriter ribbon or if the university sent us an inferior photocopy.

AVIS

La qualité de cette microforme dépend grandement de la qualité de la thèse soumise au microfilmage. Nous avons tout fait pour assurer une qualité supérieure de reproduction.

S'il manque des pages, veuillez communiquer avec l'université qui a conféré le grade.

La qualité d'impression de certaines pages peut laisser à désirer, surtout si les pages originales ont été dactylographiées à l'aide d'un ruban usé ou si l'université nous a fait parvenir une photocopie de qualité inférieure.

Canada

Characterization of Two Eukaryote-Specific Peptide Inserts in Thymidylate Synthase of *Saccharomyces cerevisiae*

Edith M. Munro

A Thesis

in

The Department

of

Biology

Presented in Partial Fulfillment of the Requirements
for the Degree of Master of Science at
Concordia University
Montreal, Quebec, Canada

October 1995

National Library
of Canada

Acquisitions and
Bibliographic Services Branch

395 Wellington Street
Ottawa, Ontario
K1A 0N4

Bibliothèque nationale
du Canada

Direction des acquisitions et
des services bibliographiques

395, rue Wellington
Ottawa (Ontario)
K1A 0N4

Your file Votre référence

Our file Notre référence

ISBN 0-612-10880-5

Canada

ABSTRACT

Characterization of Two Eukaryote-Specific Peptide Inserts in Thymidylate Synthase of *Saccharomyces cerevisiae*

Edith M. Munro

Three mutant forms of yeast thymidylate synthase were generated, in which eukaryote-specific peptide inserts occurring in two surface loops of the enzyme were deleted.

One mutant, in which the sequence spanning residues 91 to 108 was removed and substituted with 6 corresponding residues from the *E.coli* sequence, showed significantly reduced catalytic activity, as demonstrated by the following: i) complementation of thymidylate synthase deficiency in yeast or *E.coli* required high expression levels, ii) increased K_m for the substrate and decreased turnover rates were observed *in situ* using radiochemical assays on permeabilized whole yeast cells, and iii) increased K_m for substrate and cofactor and decreased turnover rates were observed *in vitro* using spectrophotometric assays on purified enzyme.

The other two mutants, both lacking amino acids 124 to 136, substituted in one of the mutants by 5 corresponding residues of the *E.coli* sequence, were unable to complement yeast or *E.coli*. Minute levels of activity were obtained using a biochemical assay. Immunoblot analyses showing that the mutant was expressed at high levels in *E.coli* suggest that the mutation impairs catalytic activity. This mutation has a second effect in yeast since it dramatically reduced levels of expression.

To Gary, David, and Chris

ACKNOWLEDGMENTS

The compilation of this thesis and the work which it entailed were not a single-handed achievement; the list of people to whom I am indebted is lengthy. First and foremost, I must acknowledge my supervisor, Dr. Reg Storms, whose unfailing support, encouragement and patience gave me the confidence to persevere through the completion of this project, which although at times disheartening, proved to be a very fulfilling experience. I am grateful to my advisers, Dr. Jack Kornblatt who diligently kept me abreast of the latest articles relevant to my field, and Dr. Joanne Turnbull who graciously showed me the ropes of protein purification and often provided invaluable guidance. I would like to express my sincere appreciation to Dr. Shane Climie of Allelix Biopharmaceuticals who invited me to perform my kinetic experiments in his lab, and to Dr. Elaine Vandenberg for her assistance in this work. Many thanks to the following professors and to the personnel in their labs for always being so helpful and cooperative when I needed materials, equipment, or advice: Drs. Tsang, Herrington, Gulick, Ibrahim, Newman, Cupples, Kornblatt, Turnbull and Joyce. I would like to thank my colleagues Tom Downing and L. Nagarajan (Raj) for the frequent discussions, suggestions and trouble-shooting sessions which often helped me to overcome obstacles during the course of my work. Finally, very special thanks to Paul Taslimi for the countless ways in which he helped me, and to Dr. Yue Huang who provided me with invaluable theoretical and computer assistance.

TABLE OF CONTENTS

Page

TABLE OF CONTENTS
(Continued)

Page

TABLE OF CONTENTS
(Continued)

Page

LIST OF FIGURES

LIST OF FIGURES
(Continued)

Number **Page**

LIST OF TABLES

INTRODUCTION

General Properties and Structure of Thymidylate Synthase

Thymidylate synthase (TS) catalyzes the reductive methylation of deoxyuridylate (dUMP) to form the DNA precursor, deoxythymidylate (dTMP). The cofactor N^5,N^{10}-methylene-tetrahydrofolate, serving as both the carbon and electron donor for this reaction, is oxidized to 7,8-dihydrofolate in this process. It is subsequently regenerated, first by the reduction of dihydrofolate to tetrahydrofolate by dihydrofolate reductase, followed by a methylation executed by serine transhydroxymethylase, with the concomitant conversion of serine to glycine (Figure 1). Since deoxythymidylate is required for chromosomal replication, and this pathway provides the only *de novo* source of this metabolite, thymidylate synthase is an important target enzyme for anti-neoplastic drug design (Harrap *et al.*, 1989).

The gene encoding thymidylate synthase has been sequenced for over 18 organisms (referenced in Figure 6), which include human, mouse, some yeasts, protozoans and plants, several bacterial species, and viruses that infect either prokaryotic or eukaryotic hosts. The amino acid sequence of the protein is remarkably conserved among such a diversity of species, even though in the protozoans and at least some plants (Cella *et al.*, 1991; Lazar *et al.*, 1993; Luo *et al.*, 1993) it exists as a bifunctional enzyme covalently linked to dihydrofolate reductase.

The protein has been crystallized for five organisms: human (Schiffer *et al.*, 1991), *Escherichia coli* (Matthews *et al.*, 1990a,b; Perry *et al.*, 1990; Montfort *et al.*, 1990; Kamb *et al.*, 1992a,b; Fauman *et al.*, 1994), *Lactobacillus casei* (Hardy *et al.*, 1987; Finer-Moore

Figure 1

The thymidylate synthase cycle. Thymidylate synthase converts dUMP to dTMP, using the cofactor N^5,N^{10}-methylene-tetrahydrofolate as both the methylene donor and subsequently the reductant of the transferred methylene (the transferred hydride and methylene are circled in the diagram). The bi-product, 7,8-dihydrofolate, is reduced to tetrahydrofolate by dihydrofolate reductase, with the concomitant oxidation of the cofactor NADPH. Tetrahydrofolate is then methylated by serine transhydroxymethylase, as a serine is converted to a glycine. Since tetrahydrofolate derivatives serve in a variety of biosyntheses, the activities of thymidylate synthase and dihydrofolate reductase must be precisely co-ordinated, so as not to deplete the cell's supply of this multi-functional precursor. In the protozoans and at least some plants, thymidylate synthase and dihydrofolate reductase exist as a fused bi-functional polypeptide.

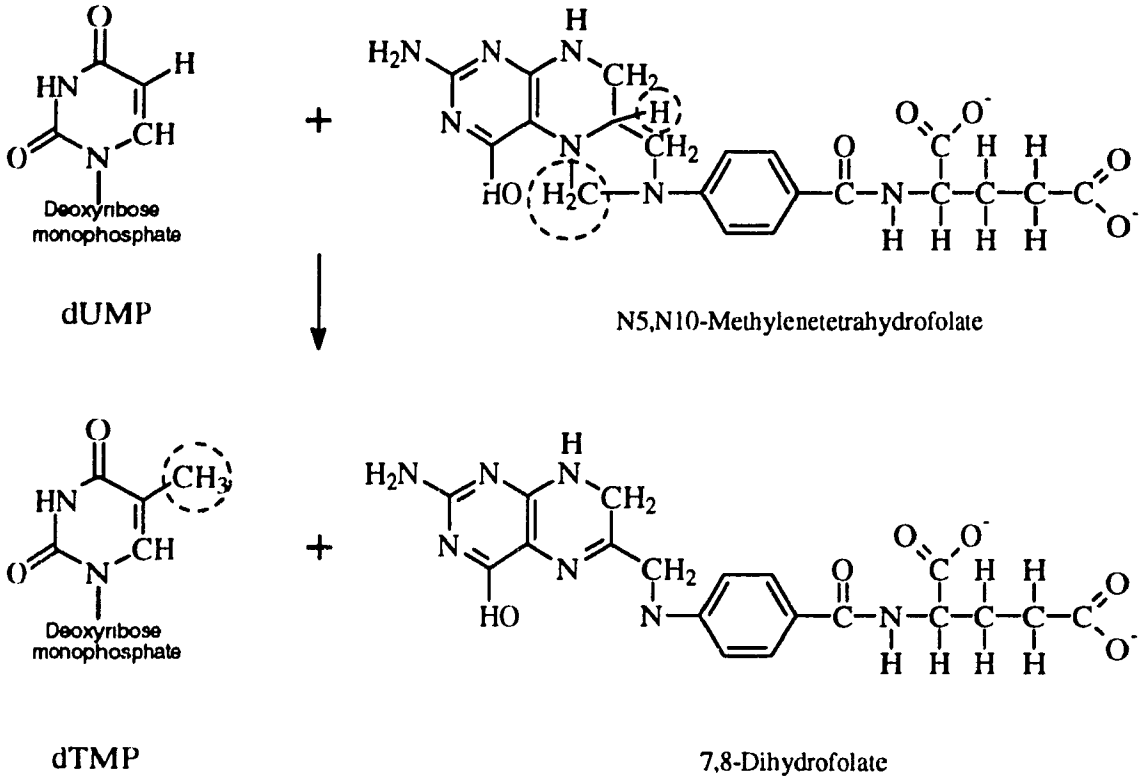
Deoxyribose monophosphate
dUMP
N5,N10-Methylenetetrahydrofolate
Deoxyribose monophosphate
dTMP
7,8-Dihydrofolate

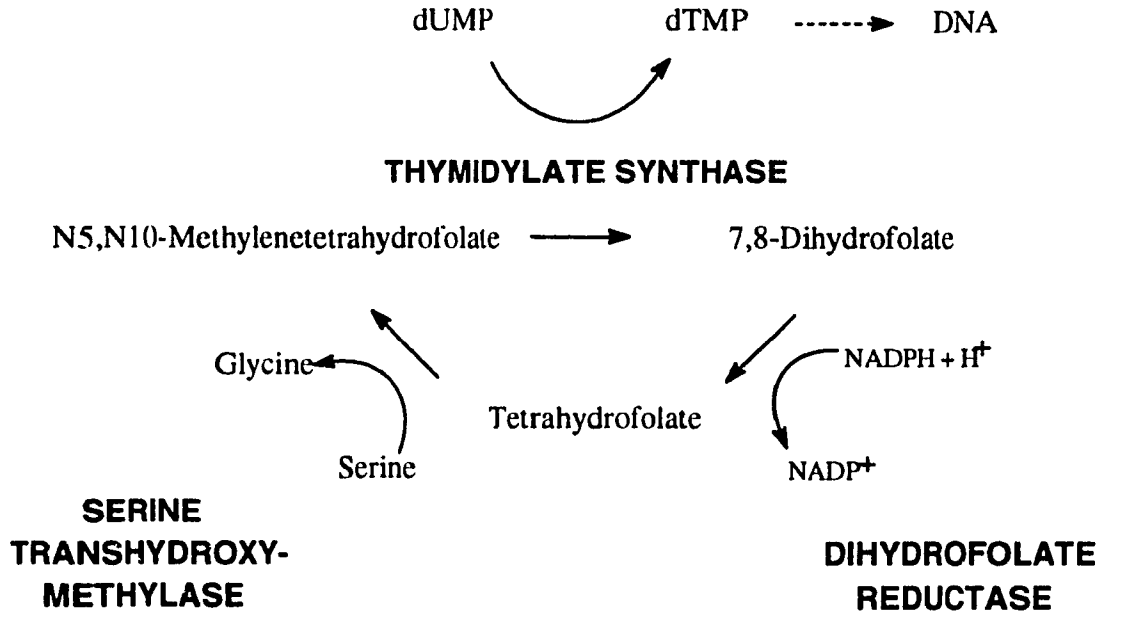
dUMP
dTMP
DNA
THYMIDYLATE SYNTHASE
N5,N10-Methylenetetrahydrofolate
7,8-Dihydrofolate
Glycine
Serine
Tetrahydrofolate
NADPH + H+
NADP+
SERINE TRANSHYDROXY-METHYLASE
DIHYDROFOLATE REDUCTASE

et al., 1993), *Leishmania major* (Knighton *et al.*, 1994), and phage T4 (Finer-Moore *et al.*, 1994). The latter four structures have been solved and show striking similarity, despite the presence of a large helical insert of ca. 50 residues in the *L. casei* enzyme, and the attachment of TS to dihydrofolate reductase in *L. major*. Such conservation of sequence and structure suggests that the characterization of one species should give results generally applicable to the others, although regions of high variability, especially clustered in what is known as the small domain (Figure 2), may play species-specific roles.

TS has been extensively studied, and the use of crystals of the free enzyme as well as the enzyme liganded with one or both substrates or their analogs has revealed much about its structure and mechanism of action (reviewed by Stroud and Finer-Moore, 1993). In addition, the wide array of TS mutants with one or more amino acid substitutions has provided insight as to the roles of some of the conserved residues.

The enzyme is an obligate dimer of two identical subunits (Figure 3), each having an M_r of 30- 35 kilodaltons, depending on the species. There are two active sites, each of which requires the participation of amino acid residues from both subunits (Hardy *et al.*, 1987; Pookanjanatavip *et al.*, 1992). The dimer interface consists mainly of two mostly anti-parallel 6-stranded β-sheets stacked in a β-sandwich conformation. The apposition of the two β-sheets results in intersubunit contact between 25 residues from each subunit *(re E.coli*, Matthews *et al.*, 1990a). These two sheets exhibit an atypical right-handed rotation relative to each other, accommodated by a bulge that partly disrupts the plane of contact (Matthews *et al.*, 1989) . Such stacked β sheets typically contain a high proportion of hydrophobic residues and interactions; TS however, is unusual in that 13 of the 25 interface residues are hydrophilic, many of them forming inter-subunit hydrogen bonds (Matthews *et al.*, 1990).

Figure 2

A. Backbone drawing of an *E. coli* TS monomer liganded with the substrate dUMP and the cofactor analog CB3717 (see Figure 4 for detailed structure). The ligands are shown in red stick form, with dUMP bound directly below CB3717. The last four residues of the flexible C-terminus are colored purple, while the reactive cysteine 146 is yellow. The highly variable small domain, shown in black, has an insert of variable length in most of the other organisms sequenced (see Figure 6). The position of this insert (designated in this work as "EUK1") is indicated in red, as is the position of another insert of 8 residues (designated as "EUK2"), which would be located in the shown surface loop in all eukaryotes. **B**, **C**, and **D** show the same molecule but with the y-axis rotated 45, 90 and 180 degrees respectively.

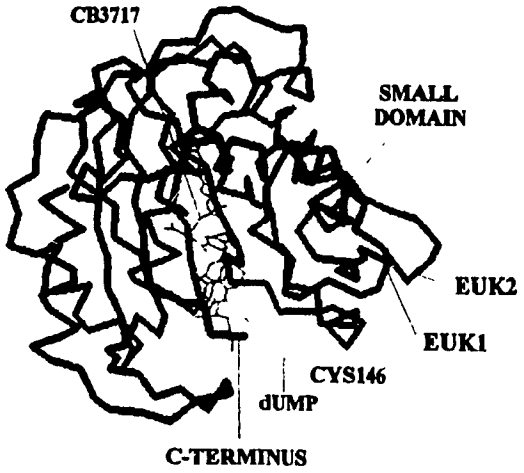

A

B

C

D

Figure 3

A. Backbone drawing of the *E. coli* TS dimer liganded with dUMP and CB3717. The ligands are shown in red stick form. The large hydrophobic α-helix that forms the core of the monomers can be seen as a dense coil in the interior of each subunit. The small domain is coloured dark blue, and the position of the eukaryotic insert "EUK1" is marked in red. The loop which contains the eukaryotic insert "EUK2", and its two flanking helices are shown in black. The position of "EUK2" is marked in red, where the loop is in close proximity to its counterpart on the other subunit at the dimer interface. The catalytic cysteine 146 is shown in yellow, and the last four residues of the C-terminus are coloured purple. **B.** Top view of "A" (the x-axis has been rotated 90 degrees toward the viewer), showing the alignment of the two helices flanking "Loop 2" (coloured black). **C.** Same orientation as "B", but the β-sheets of the two subunits are shown in black and in red, as are the reactive cysteines (shown in ball and stick form) since they are part of the β-sheets. **D.** A different orientation of "C" (the y-axis is rotated 135 degrees), which emphasizes the bulge in the β-sheets, especially noticeable in the left subunit of the dimer.

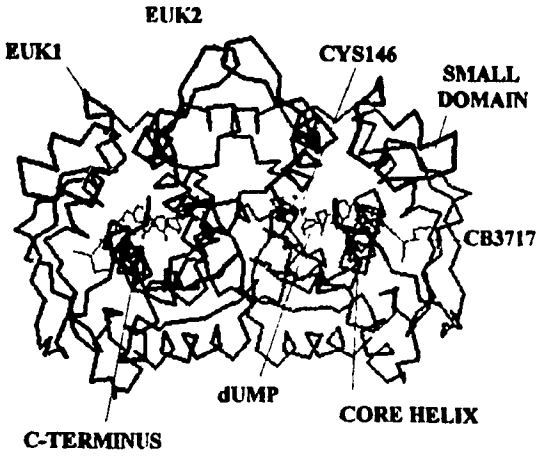
EUK2
EUK1
CYS146
SMALL
DOMAIN
CB3717
dUMP
CORE HELIX
C-TERMINUS

A

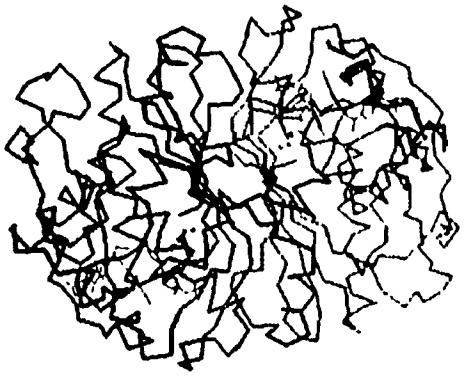

B

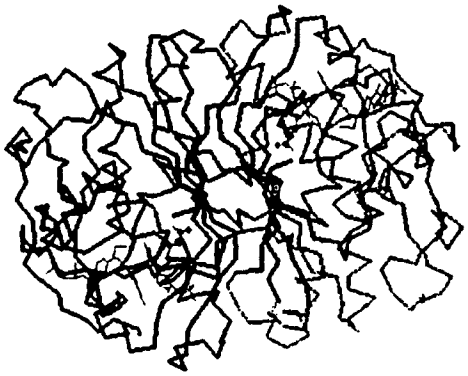

C

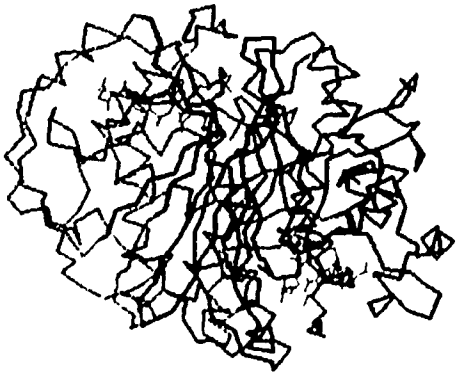

D

The remainder of each subunit is comprised of loops of variable size that are mostly solvent accessible, and 9 to 11 helices ranging in size from 2 to 6 turns. The largest helix is buried and forms the hydrophobic core of each subunit while most of the others are amphipathic. The carboxy terminal is a ribbon structure which, upon binding of substrate and cofactor, undergoes an important conformational change that results in capping the active site cleft and sequestering it from bulk solvent. This conformational change, triggered by the binding of the cofactor (Kamb *et al.*, 1992b), also serves to properly orient the ligands (Montfort *et al.*, 1990; Perry *et al.* 1993), such that the transfer of the carbon unit from cofactor to dUMP is facilitated. Structures of liganded and unliganded *L.casei* TS show that the terminal valine undergoes a displacement of 4Å, the largest observed among the four residues that constitute the carboxy-terminus tail . Studies using mutants at this position indicate that many substitutions are tolerated, but if this terminal residue is deleted, product formation is abolished (Carreras *et al.*, 1992), and the orientation of the substrates differs from those of the wild type enzyme (Perry *et al.*, 1993).

Although the occurrence of such a conformational change is often associated with cooperativity between subunits in multi-site enzymes, no conclusive evidence of such being the case with TS has yet been presented. However, several studies have demonstrated the occurrence of intersubunit communication between catalytic sites. As early as 1974, Aull *et al.* reported that the removal of the C-terminus residue by carboxypepsidase A on one subunit resulted in loss of activity at both enzymic sites. More recently, Bradshaw and Dunlap (1993) have shown that covalent association of one of the active-site cysteines, by chemical modification, enhances substrate binding and dTMP synthesis at the second site. The asymmetry of the TS reaction has been demonstrated by X-ray crystallography, which has

revealed that the TS subunits are asymmetrical when liganded, as well as by kinetic studies which indicate that the two active sites bind dUMP with different affinities (Lockshin and Danenberg, 1979). Several studies have shown that binding of folate makes the second site accessible for dUMP or FdUMP binding (Galivan *et al.*, 1976; Danenberg & Danenberg, 1979; LaPat-Polasko *et al.*, 1990). Dev *et al.* (1994) have presented data suggesting that cofactor only binds significantly at one site, and have proposed that TS may be an "alternate-sites" enzyme: i.e. catalysis at one active site would be coupled to substrate binding at the second site. Finally, in a recent publication Maley *et al.* (1995) have demonstrated that heterodimers with only one functional active site have specific activities that are equivalent to those of the wild type homodimers.

The binding of ligands to TS is mediated by a coordinated hydrogen bond network involving side chains, backbone atoms, and ordered waters that occupy the active site cavity. In addition, the phosphate moiety of dUMP is stabilized by four arginine residues, two from each monomer (Arg 321, 166, 126', 127', *E. coli*), while the glutamate portion of the cofactor interacts electrostatically with a base-rich region of the protein (48-56, *E.coli*), known as the folate-binding loop (Finer-Moore *et al.*, 1990). Finally, highly conserved hydrophobic residues are involved in packing of the pterin and PABA rings of the cofactor, while the pyrimidine ring of the substrate provides a surface upon which the pterin ring stacks (Finer-Moore *et al.*, 1990).

Ligand binding to TS is thought to occur in an ordered *bi-bi* reaction sequence (Danenberg & Danenberg, 1978), with the sequential binding of dUMP followed by cofactor, and release of dihydrofolate followed by dTMP. It has been shown however, that under certain conditions, the polyglutamylated form of the cofactor may bind first (Lu *et al.*, 1984),

without loss of dTMP synthesis activity. Although the pyrimidine ring of dUMP normally forms part of the folate binding site by its interaction with the pterin ring , when folate is polyglutamylated its binding affinity for TS increases such that it is able to bind in the absence of dUMP (Kamb *et al.*, 1992). The ability of dUMP to bind despite occupancy of the active site by the cofactor and the ensuing conformational change, may be attributed to the existence of an equilibrium between the two conformations, which would presumably allow passage of dUMP into the active site cavity during the "open" conformation intervals. An alternate mechanism proposes that dUMP is able to enter the active site via the opposite side of the cavity, since X-ray structures indicate that there is sufficient space for it to do so (Kamb *et al.*, 1992b).

Reaction Mechanism of Thymidylate Synthase

The use of substrate and cofactor derivatives (Figure 4) which form stable covalent complexes with TS has enabled investigators to trap the enzyme in forms that are considered analogs of the steady-state intermediates. This, together with the study of mutants having amino acid substitutions in the catalytic site, has led to the elucidation of the reaction mechanism. The current and generally accepted model (Matthews *et al.*, 1990b; reviewed by Stroud and Finer-Moore, 1993; Lehninger, 1993), advances that the reaction is initiated when the C6 atom of the pyrimidine ring of the substrate undergoes a nucleophilic attack by the S atom of a conserved cysteine residue (Cys146, *E.coli* numbering). It has been shown in several studies that any substitution of this residue, with the possible exception of serine, completely abolishes enzyme activity (Dev *et al.*, 1988; Climie *et al.*, 1990b; Michaels

Figure 4

Ligands of thymidylate synthase. The substrate dUMP (deoxyuridine monophosphate) differs from the product dTMP (deoxythymidine monophosphate) in that it has a hydrogen at C5 whereas dTMP is methylated at that position. The substrate analog F-dUMP has a fluorine at C5, which results in blocking the TS catalysed reaction at the first step (see mechanism, Figure 5). F-dUMP is thus a potent inhibitor of TS, and is used clinically as an anti-cancer drug. The cofactor, CH_2H_4folate (N^5,N^{10}-methylene-tetrahydrofolate), transfers its one-carbon unit from the imidazole ring as a first step of the TS reaction, and later reduces the transferred methylene by donating a hydride from C6 of the pterin ring, thus forming the by-product, H_2folate (7,8-dihydrofolate). The cofactor analog, CB3717 (10-propargyl-5,8-dideazafolate, sometimes abbreviated as PDDF), has a quinazoline ring substituted for the pterin ring, and a propargyl group at N10. CB3717 was initially designed as a TS inhibitor to be used clinically as an anti-proliferative agent, since it prevents dTMP synthesis by its inability to form a covalent bond with dUMP (see mechanism, Figure 5). Both analogs have been extremely useful in elucidating the TS mechanism as they form stable covalent complexes that are considered to mimic the intermediates of the reaction, and are readily crystallized.

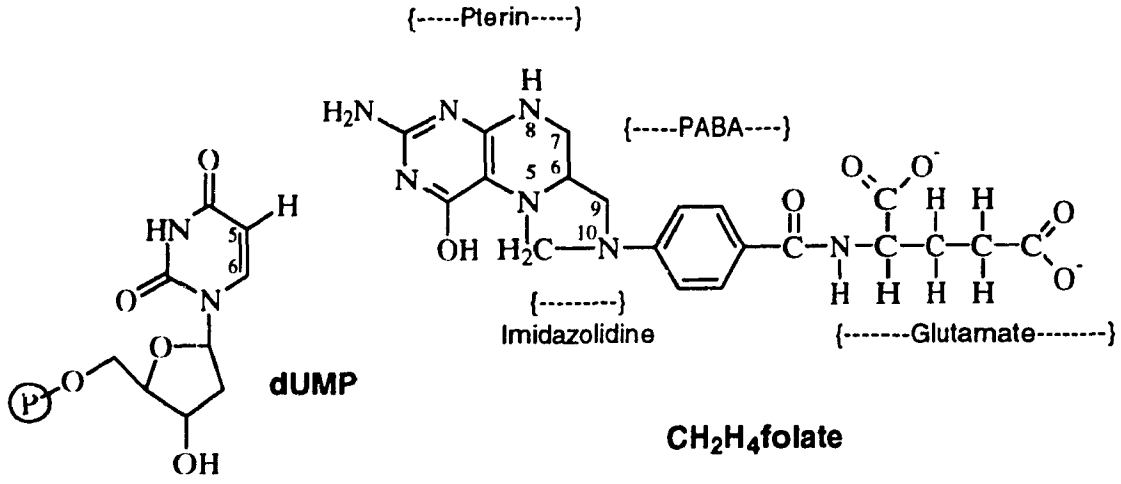

dUMP

CH_2H_4folate

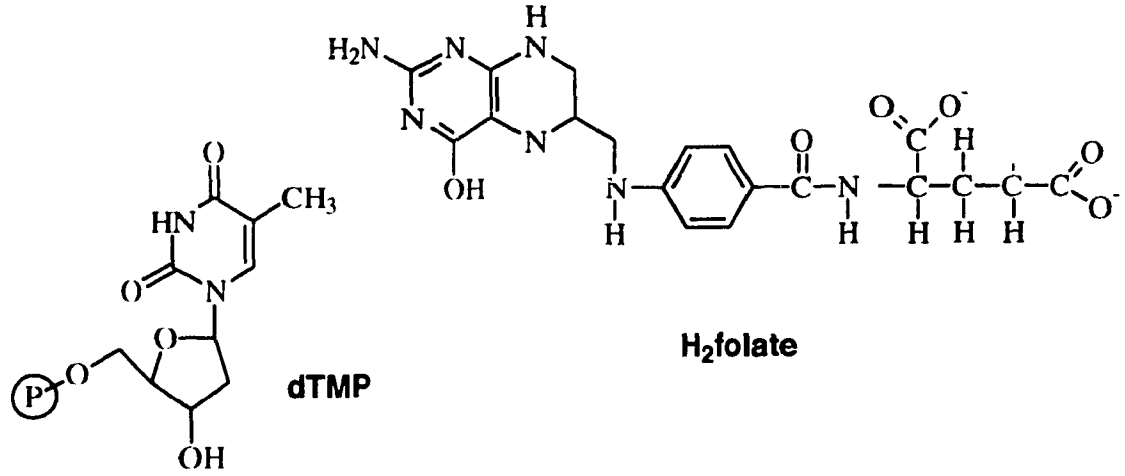

dTMP

H_2folate

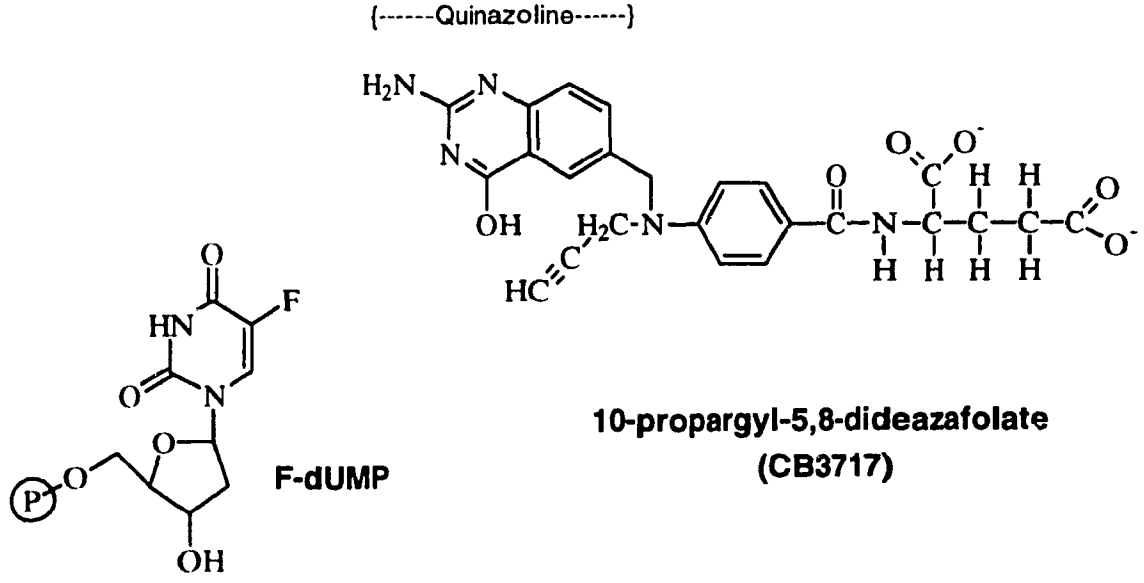

F-dUMP

10-propargyl-5,8-dideazafolate (CB3717)

Figure 5

The currently accepted model for the thymidylate synthase mechanism. C6 of the substrate, dUMP, undergoes a nucleophilic attack by the S atom of a conserved cysteine, which simultaneously loses a proton. The new bond between this cysteine and C6 forces the delocalization of an electron pair between C6 and C5, with the consequent formation of an enolate which is thought to be stabilized by a nearby water molecule, and activation of C5 (I). Meanwhile, upon binding to the enzyme, the imidazolidine ring of the cofactor has opened, with a concomitant proton capture at N-10, resulting in the formation of an iminium ion. The stage is thus set for the condensation of the thiolate anion with the iminium cation at the C5 position, which produces the steady-state covalent ternary complex (II). The abstraction of a proton at C5 ensues, presumably aided by a proximal ordered water molecule, since this hydrogen is poorly acidic. Deprotonation is concurrent with electron movement to, and elimination of, tetrahydrofolate. It is at this step that the substrate analog, F-dUMP, inhibits dTMP formation, since the fluorine which replaces the hydrogen at C5 cannot be abstracted and thus prevents the breakdown of the ternary complex. The final step of the reaction, is a hydride transfer from C6 of the cofactor to the methylene which was transferred in the previous step (III). Electron movement to the enzyme cysteine residue follows, with concomitant disengagement of the product and formation of a double bond between C6 and C5.

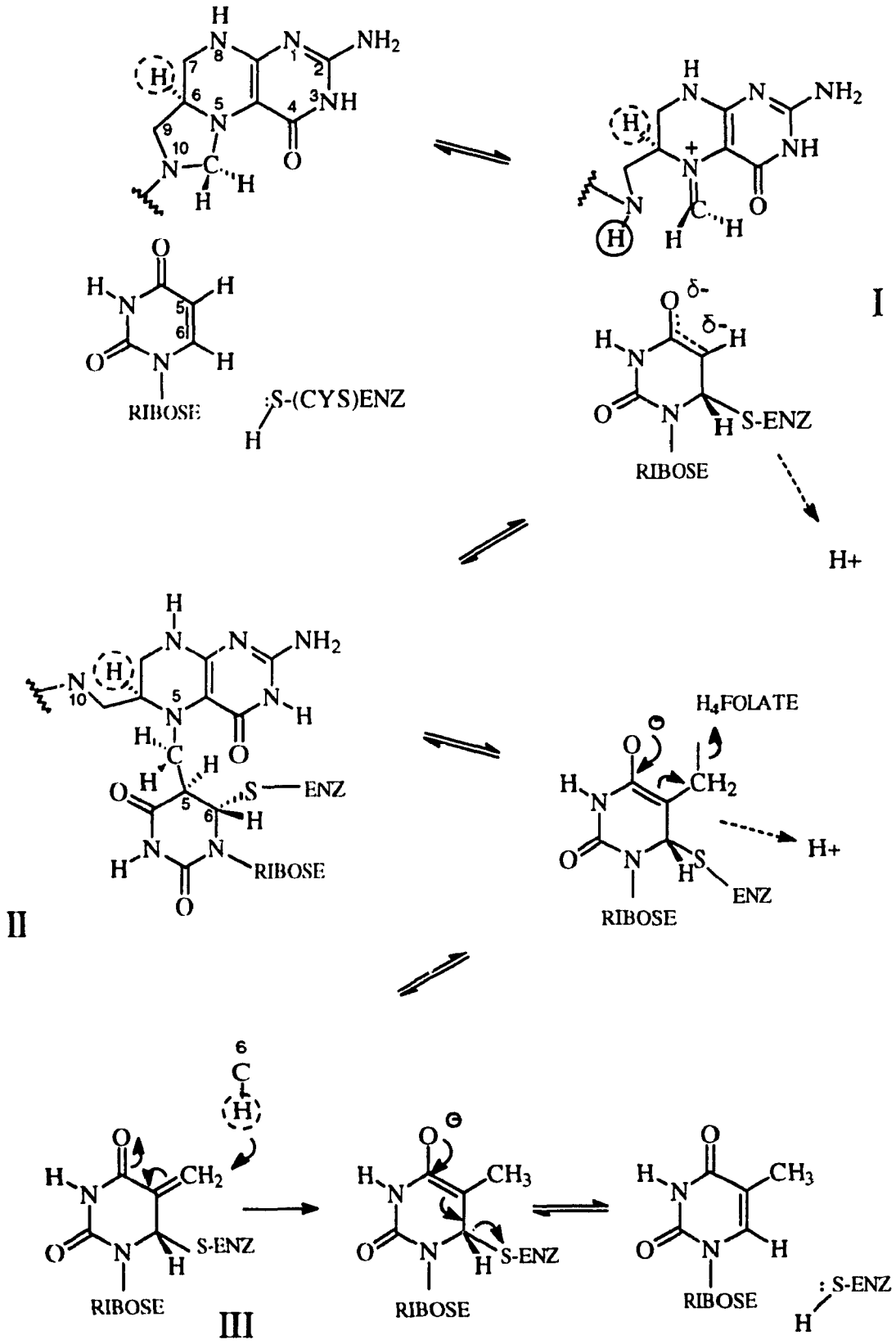
RIBOSE
:S-(CYS)ENZ
S-ENZ
I
δ-
δ-
H+
ENZ
II
H4FOLATE
H+
RIBOSE
III
S-ENZ
RIBOSE
RIBOSE
: S-ENZ

et al., 1990; LaPat-Polasko *et al.*, 1990). The resulting covalent bond between the S and C6 atoms, causes the delocalization of shared electrons between C5 and C6 of the pyrimidine ring and the formation of an enolate which is thought to be stabilized by a proximal ordered water molecule. The nearby cofactor, whose imidazolidine ring has opened following binding to the active site, then condenses with the activated dUMP at the C5 position, with the concomitant formation of the covalent steady-state intermediate (Figure 5, II). The subsequent loss of the proton at position C5 of the pyrimidine ring and elimination of H_4folate completes the transfer of the C unit to the substrate. This weakly acidic proton was long thought to be abstracted by a nearby basic side-chain of the enzyme, but in the failure to identify a plausible candidate, the mechanism which is presently favoured is that the proton is accepted by a water molecule which is ordered through hydrogen bonding to a conserved tyrosine (*L.casei* 146) and an alanine (*L.casei* 196) (Fauman *et al.*, 1994). The second step of the reaction, a stereospecific hydride transfer from C6 of the pterin ring of the cofactor to the transferred methylene, necessitates relative reorientation of the substrate and cofactor, the nature of which has not yet been elucidated. Concurrently, the steady-state intermediate (Figure 5, III) breaks down and the product, dTMP, disengages from the cysteine residue of the enzyme. Product release from the active site is thought to be driven by the displacement of an ordered water molecule by the methyl group of dTMP (Fauman *et al.*, 1994). This water, which is also the putative proton acceptor in the elimination step, is hydrogen bonded to tyrosine 146 and alanine 196 in the TS-dUMP complex, but is disordered in TS bound to dTMP. The decrease in enthalpy resulting from the loss of two hydrogen bonds is presumably sufficient to destabilize the complex, despite the simultaneous increase in entropy.

Modes of Regulation of Thymidylate Synthase Activity

Since dTMP is a DNA precursor, it is crucial that sufficient pools of this metabolite be available at the time when cells undergo a burst of DNA synthesis, the S phase of the cell cycle. Maintenance of high levels of dTMP during the remainder of the cell cycle would appear however, to be an unnecessary energy expenditure, since the only fate of this compound is to be incorporated into DNA. In the eukaryote *S.cerevisiae*, thymidylate synthase expression is cell-cycle regulated (Storms *et al.*, 1984; Greenwood *et al.*, 1986; McIntosh *et al.*, 1988). It has been shown that regulation of the enzyme is coupled to DNA synthesis, with activity and thymidylate synthase-specific transcript peaks both appearing during the S-phase of the cell cycle. Thymidylate synthase levels are thus primarily controlled by regulation of transcription, but the decrease of activity following S-phase suggests that enzyme instability (i.e. loss of activity caused by a post-translational mechanism) also plays a role in its regulation (Greenwood *et al.*, 1986). Studies of human thymidylate synthase (Chu *et al.*, 1991; Keyomarsi *et al.*, 1993) suggest another mechanism of negative regulation, that of "translational detainment" of the mRNA by its binding to unliganded TS protein. Finally, the ability of small molecules such as pyridoxal phosphate and glyceraldehyde-3-phosphate to inhibit human TS activity *in vitro* (Bures *et al.*, 1991) may reflect yet another mode of regulation of the enzyme.

Eukaryote-Specific Peptide Inserts

Although TS exhibits one of the most highly conserved primary sequences known, alignment of these sequences from 18 organisms reveals a salient feature in the eukaryotes: the presence of two oligopeptide inserts (Figure 6) which are conspicuously absent in the prokaryotes (with the exception of *L.casei* and *S. aureus Tn*4003 which have a long insert of 50 residues where the eukaryotes have a 12-residue insert). The first eukaryotic insert is located within a coil that connects two α-helices, and partially lines one side of the active site cleft, but which is not directly implicated in substrate or cofactor binding (Figures 2 and 3). This coil will be referred to in this work as "loop 1". The second eukaryotic insert occurs in a loop which interrrupts two α-helices, but nonetheless allows classical α-helical hydrogen bonding between two residues across the interface of the helices (Matthews *et al.*, 1990a). This loop, henceforth designated as "loop 2", is ordered by two short interacting β-ribbons, and at least in *E.coli* contributes several residues to intersubunit contact (Figure 3). The neck of this loop is also stabilized by an arginine-aspartate salt linkage in *L. casei*, these two residues being completely conserved with the exception of phage T4 in which a glycine replaces the arginine. The eukaryotic inserts appear to be solvent accessible, and it is thus not surprising that their sequences contain a large proportion of hydrophilic residues.

The conservation of these inserts among all the eukaryotic thymidylate synthases so far sequenced suggests that they may play a eukaryote-specific role. In view of the fundamental organizational differences between eukaryotic and prokaryotic cells, several possibilities concerning the function of the eukaryotic inserts should be considered. Since

Figure 6

Alignment of amino acid sequences (89 to 140, numbering based on yeast sequence) of 18 different thymidylate synthases. The alignment of the first 17 species is adapted from Perry *et al.* (1990). The *T. gondii* sequence is taken from Roos (1993) and has been aligned based on the residues which are absolutely conserved among all known sequences. Eukaryotic organisms are represented by sequences 1 to 11, and 18, while the prokaryotic sequences are seen from 12 to 17. All the eukaryotes sequenced to date have inserts of 12 and 8 residues at positions 97 and 124 respectively, which are located in surface loops. The yeast sequence shown in parentheses (top sequences) is the deleted sequence of mutant ΔEUK1, and is replaced by the underlined *E.coli* sequence, EWADEN. The second yeast sequence in parentheses (bottom sequences) is the deletion in mutants ΔEUK2 and ΔEUK3; in ΔEUK3 it is replaced with the underlined *E.coli* sequence, TPDGR. References: *Saccharomyces cerevisiae* (Taylor *et al.*, 1987); *Pneumocystis carinii* (Edman *et al.*, 1989); human (Takeishi *et al.*, 1985); mouse (Perryman *et al.*, 1986); *Herpesvirus saimiri* (Honess *et al.*, 1986); *Herpesvirus atales* (Richter *et al.*, 1988); *Varicella-Zoster* virus (Thompson *et al.*, 1987); *Leishmania major* (Beverley *et al.*, 1986); *Leishmania tropica* (Grumont *et al.*, 1986); *Crithidia fasciculata* (Hughes *et al*, 1989); *Plasmodium falciparum* (Bzik *et al.*, 1987); *Candida albicans* (Singer *et al.*, 1989); *Escherichia coli* (Belfort *et al.*, 1983); *Bacillus subtilis* (Iwakura *et al.*, 1988); *B. subtilis* phage Φ3T (Kenny *et al.*, 1985); coliphage T4 (Chu *et al.*, 1984); *Lactobacillus casei* (Bellisario *et al.*, 1979; Maley *et al.*, 1979a,b); *Staphylococcus aureus* transposon *Tn*4003 (Rouch *et al.*, 1989); *Toxoplasma gondii* (Roos, 1993).

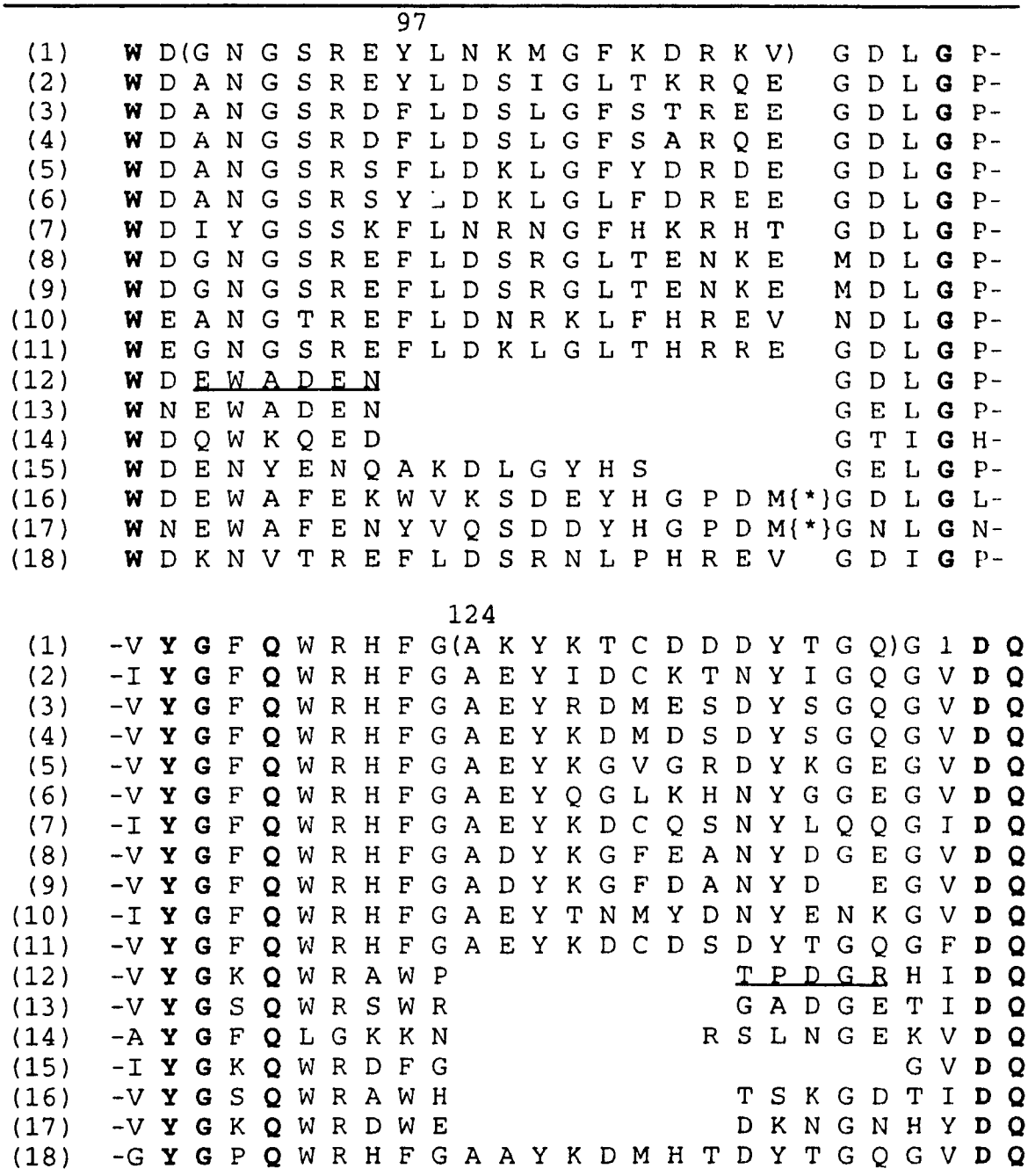

*38 a.a. insert

(1) *Saccharomyces cerevisiae*, (2) *Pneumocystis carinii*, (3) human (4) mouse, (5) *Herpesvirus saimiri*, (6) *Herpesvirus atales*, (7) *Varicella-Zoster* virus, (8) *Leishmania major/tropica*, (9) *Crithidia fasciculata*, (10) *Plasmodium falciparum*, (11) *Candida albicans*, (12) *Escherichia coli*, (13) *Bacillus subtilis*, (14) *B. subtilis* phage Φ3T, (15) coliphage T4, (16) *Lactobacillus casei*, (17) *Staphylococcus aureus* transposon *Tn*4003, (18) *Toxoplasma gondii*.

eukaryotes are compartmentalized while prokaryotes are not, one possible role could be that of a targeting sequence that directs the enzyme to its appropriate cellular compartment, as is often the case in eukaryotic proteins (Sabatini *et al.*, 1982). Localization studies of yeast thymidylate synthase indicating accumulation of the enzyme around the nucleus support this hypothesis (Poon and Storms, 1994). Another function, proposed by Hardy *et al.* (1987), could be that of a suicide sequence (e.g. a protease attack site) enabling post-translational deactivation. In support of this, Garvey and Santi (1985), have shown that in *L. tropica*, the first eukaryotic insert in the bifunctional thymidylate synthase-dihydrofolate reductase protein is susceptible to attack by several proteases *in vitro*, resulting in the loss of thymidylate synthase activity. A third possibility is that of a recognition sequence for protein-protein interaction. It has been postulated that in prokaryotes, enzymes involved in DNA synthesis form "replitase" complexes that channel nucleotides into the DNA replication fork (reviewed by Mathews and Slabaugh, 1986). Whether this occurs in eukaryotes remains a subject of controversy, but it has been shown that folate channeling does occur between the thymidylate synthase and dihydrofolate reductase domains of the *L. major* bifunctional enzyme (Knighton *et al.*, 1994).

It has been suggested that the removal of the large *L. casei* insert corresponding to the first eukaryotic insert would cause very little disturbance of the core enzyme, since the remaining amino and carboxy termini are in close proximity (Hardy *et al.*, 1987). Similarly, it would seem unlikely that the excision of the second eukaryotic insert, found in a loop that is almost closed as a result of the salt linkage constricting its neck, would have any repercussions on enzyme structure or activity. If this were the case, such deletion mutants could be engineered, and tested for complementation in prokaryotic and eukaryotic cells to

determine whether or not the inserts perform a eukaryote-specific function.

Experimental Design

We have constructed deletion mutants of the eukaryote-specific sequences of *S.cerevisiae* thymidylate synthase to address the roles of these inserts in the context of enzyme structure as well as in the context of the cellular environment. The mutant involving the first insert has been designated as "ΔEUK1"; it has a deletion of the 12 residues that comprise the insert (residues #97 to 108, yeast numbering system) as well as 6 residues upstream (#91 to #96), which are replaced by the corresponding 6 residues of *E. coli* (Figures 6 and 7). The rationale for this substitution was two-fold: i) the substituted segment contains a motif, N-G-S-R, that is conserved among most of the eukaryotes and hence may contribute to the putative function of the insert, and ii) mimicking a prokaryotic enzyme in the vicinity of the deletion might maximize our chances of obtaining an enzymatically active mutant.

The second mutant, denoted as "ΔEUK2a", has a 13-residue deletion (#124 to 136), of which the first eight make up the second eukaryote-specific insert. The last 5 residues include a Y-G-Q motif found in several of the eukaryotes. The third mutant, "ΔEUK2b", differs from ΔEUK2a in that these last 5 residues are substituted with the corresponding 5 residues of *E. coli*. ΔEUK2a also carries a point mutation, for reasons to be discussed later.

To determine the effect of these deletions, the first experimental approach was the use of an *in vivo* complementation assay performed in a prokaryotic cell (*E.coli*) as well as a eukaryotic cell (*S.cerevisiae*). Our results indicate that the mutant allele *TMP1-ΔEUK1* is able to complement TS deficiency, in both prokaryotic and eukaryotic systems, in a dose-

Figure 7

Diagrammatic representation of mutants constructed for this study. The eukaryotic inserts EUK1 (Y-L-N-K-M-G-F-K-D-R-K-V) and EUK2 (A-K-Y-K-T-C-D-D) are shown in white within the *TMP1* gene, while the adjacent sequences that were also deleted (G-N-G-S-R-E and D-Y-T-G-Q respectively) are indicated in black. The *E. coli* sequences that were inserted into mutants ΔEUK1 and ΔEUK2b are shown in grey, and are labeled with their corresponding amino acid codes. The point mutation in ΔEUK2a is indicated as a substitution of histidine 121 to aspartate.

TMP1

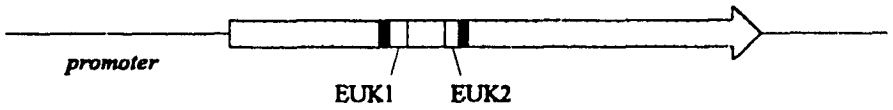

thyA (E.coli)

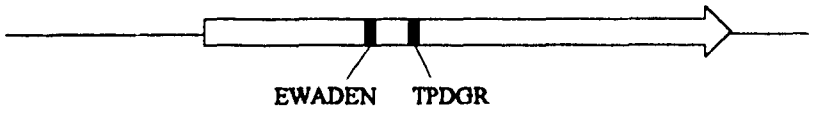

TMP1-ΔEUK1

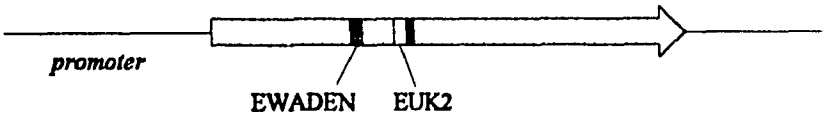

TMP1-ΔEUK2a

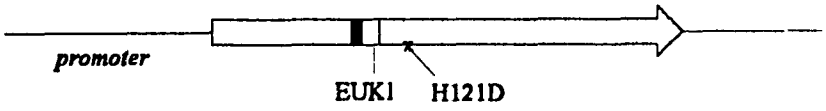

TMP1-ΔEUK2b

dependent manner; that is, the gene must be expressed in high levels in order to support cell growth. The nature of this reduced ability to complement TS-deficient cells was investigated in several ways. Tritium-release assays using permeabilized whole cell systems revealed that the mutant enzyme had a greatly impaired catalytic activity. That this was not due to a decrease in transcription or translation was demonstrated using immunoblot analysis, which indicated that levels of the mutant protein were at least as high as for the wild type protein. Finally, to determine whether the reduced catalytic activity was related to a structural aberration, the enzyme was purified in order to compare its kinetic parameters with those of the wild type. Our results revealed that the mutant enzyme had a decreased binding affinity for both the substrate and the cofactor, as well as a decreased specific activity, which indicates that the mutation does indeed lead to structural anomalies. Moreover, it is unlikely that an impairment of this magnitude would still lead to complementation of TS-deficient yeast cells when the enzyme is expressed in low levels, if the deleted sequence effected another important role, such as targeting. Finally, the fact that normal *in vivo* function can be restored by increasing the levels of expression of the mutant enzyme suggests that yeast TS is not stochiometrically involved in a nucleotide-synthesis complex.

In contrast to *TMP1-ΔEUK1*, the mutant alleles *TMP1-ΔEUK2a* and *TMP1-ΔEUK2b* were unable to rescue TS-deficient bacterial or yeast strains. Immunoblot analysis revealed that, at least in *E. coli*, this inability to complement persisted even when mutant protein levels were as elevated as wild type levels in a high expression system.

Our results demonstrate that the removal of sequences of yeast thymidylate synthase encompassing the eukaryotic inserts, leads to severe impairment of enzyme activity, and suggest that these sequences are essential structural features of the enzyme.

MATERIALS AND METHODS

Generation of Deletion Mutant ΔEUK1

Five plasmids (pEGBl-E1, pEG830-E1, pEG13-E1, pEG50-E1, pEGRBS-E1), each harboring a deletion of the eukaryotic sequence coding for amino acids 91 to 108, replaced by the sequence encoding E-W-A-D-E-N, were constructed. The original mutation, designated as ΔEUK1, was generated by PCR (polymerase chain reaction) amplification of a segment of the *TMP1* gene, using yeast genomic DNA as template. The oligonucleotides used as primers spanned a region of ca. 1 Kb (Figure 8). The resulting PCR product was characterized by agarose gel electrophoresis of *Hind*III and *Pst*I digests, which yielded the expected fragments of 275 and 682 bp, and 381 and 576 bp respectively. The PCR product was then trimmed to a length of 673 bp with *Hind*III and *Bgl*II, and cloned into phagemid Bluescript 2524, resulting in phagemid pEGBl-E1. This construct was transformed into *E.coli* strain XL1-Blue to generate single-stranded DNA which was used as sequencing template to screen for the deletion. Two samples were sequenced through the first 410 bases and last 180 bases of the *Hind*III/*Bgl*II fragment. The DNA sequences showed that no spontaneous mutations were introduced in these regions. The replacement of nucleotides 271 to 324 of the yeast gene with those encoding the corresponding *E. coli* region was confirmed.

To construct the second plasmid, pEG830-E1 (Figure 9), the mutagenized fragment was integrated into the *TMP1* gene, by exchanging the *Hind*III to *Bgl*II fragment of pEGBL-E1, containing ΔEUK1, for the corresponding fragment of the wild type gene on plasmid

pTL830. Ligates were transformed into *thyA⁻ E. coli* strain 264; transformants were initially selected on ampicillin plates supplemented with thymidine, and colonies were patched onto plates without thymidine, to select for thymidine prototrophs. Of 22 patches, 11 were thymidine prototrophs and 11 were auxotrophs. Analysis of *Pvu*II digests revealed that all the auxotrophs harbored pEGB1-E1 DNA. Four prototrophs were screened by careful *Pvu*II restriction analysis and 3 out of 4 harbored the *TMP1 ΔEUK1* allele, as detected by a 333 bp *Pvu*II fragment compared to the 369 bp fragment of wild type controls.

To obtain plasmid pEG13-E1 (Figure 10), a yeast/*E.coli* shuttle vector harboring the *TMP1-ΔEUK1* gene, the mutagenized *TMP1* gene was removed from plasmid pEG830-E1 by *Hind*III/*Sma*I digestion and ligated into the *Hind*III and *Pvu*II sites of the shuttle vector YEp13. Ligates were transformed into *E.coli* strain MC1066; transformants were selected on ampicillin plates and replica-plated on minimal media supplemented with tryptophan and uracil to select for leucine prototrophs. This eliminated transformants harboring religated plasmid pEG830-E1. To screen for colonies containing the *TMP1-ΔEUK1* gene, leucine prototrophs were patched onto tetracycline plates since insertion of the *TMP1-ΔEUK1* gene into YEp13 requires excision of the *tet* gene. Plasmid DNA analysis of the tetracycline sensitive colonies by *Hind*III/*Pvu*II digestion confirmed the presence of the mutagenized *TMP1* gene in 6 of 11 samples tested.

To test low-copy expression of ΔEUK1, the *Hind*III to *Sma*I fragment of pEG830-E1 was ligated into theYCp50 backbone, generated by *Hind*III and *Nru*I digestion. The desired plasmid, pEG50-E1 (Figure 11), was isolated by transformation into *E.coli* strain MC1066, followed by selection on ampicillin plates and replica-plating onto minimal media

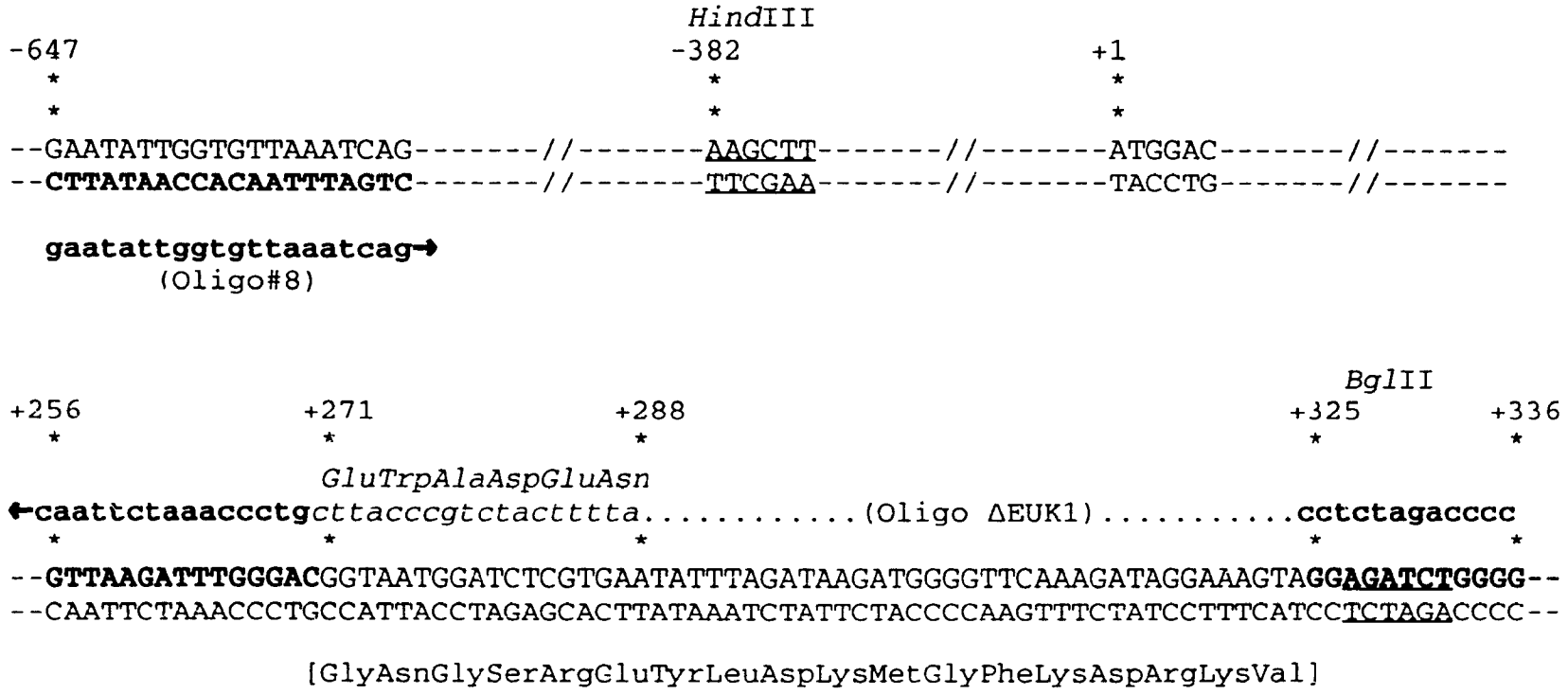

Figure 8. PCR amplification scheme for generation of ΔEUK1. Primers "oligo #8" and "oligo ΔEUK1" are shown as lowercase sequences while the *TMP1* gene and upstream region are in uppercase. Arrows indicate direction of extension. Bold face letters indicate homology between template and primer. Restriction sites used for cloning the PCR product are underlined. Dashed lines indicate unshown sequences. The dotted line represents continuity between bases at positions 288 and 325 in oligo ΔEUK1. The deleted yeast amino acid sequence is shown in square brackets while the *E.coli* insert is shown in italics both as an amino acid sequence and a nucleotide sequence within oligo ΔEUK1.

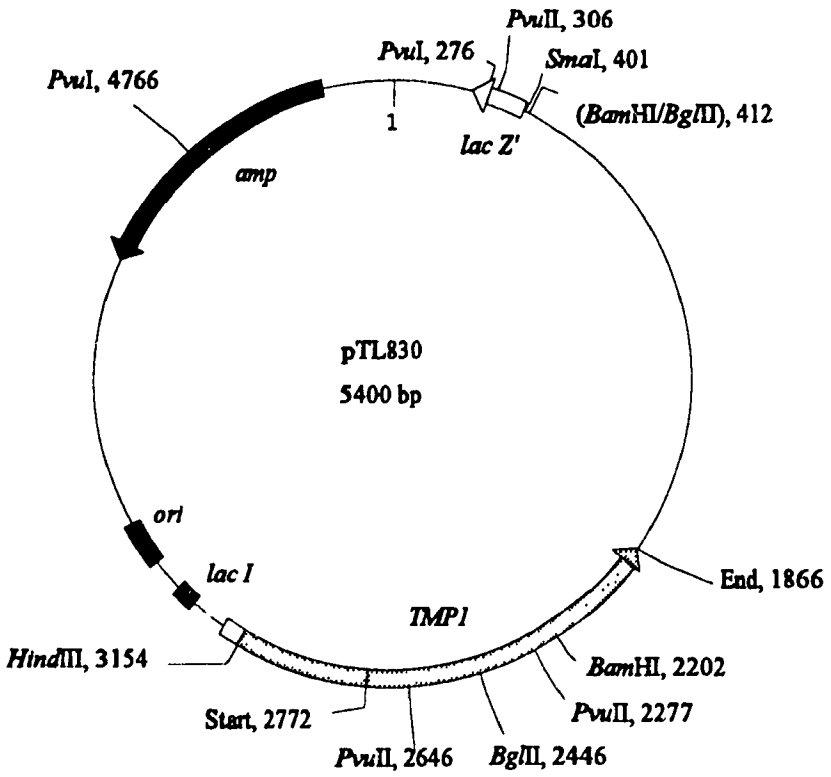

Figure 9. *E. coli* high copy plasmid constructed by ligating a *Hind*III to second *Bgl*II fragment of *TMP1* into the *Hind*III to *Bam*HI backbone of pUC9. Plasmid pEG830-E1 is identical to this except that it harbors *TMP1-ΔEUK1* rather than the *TMP1* wild type gene.

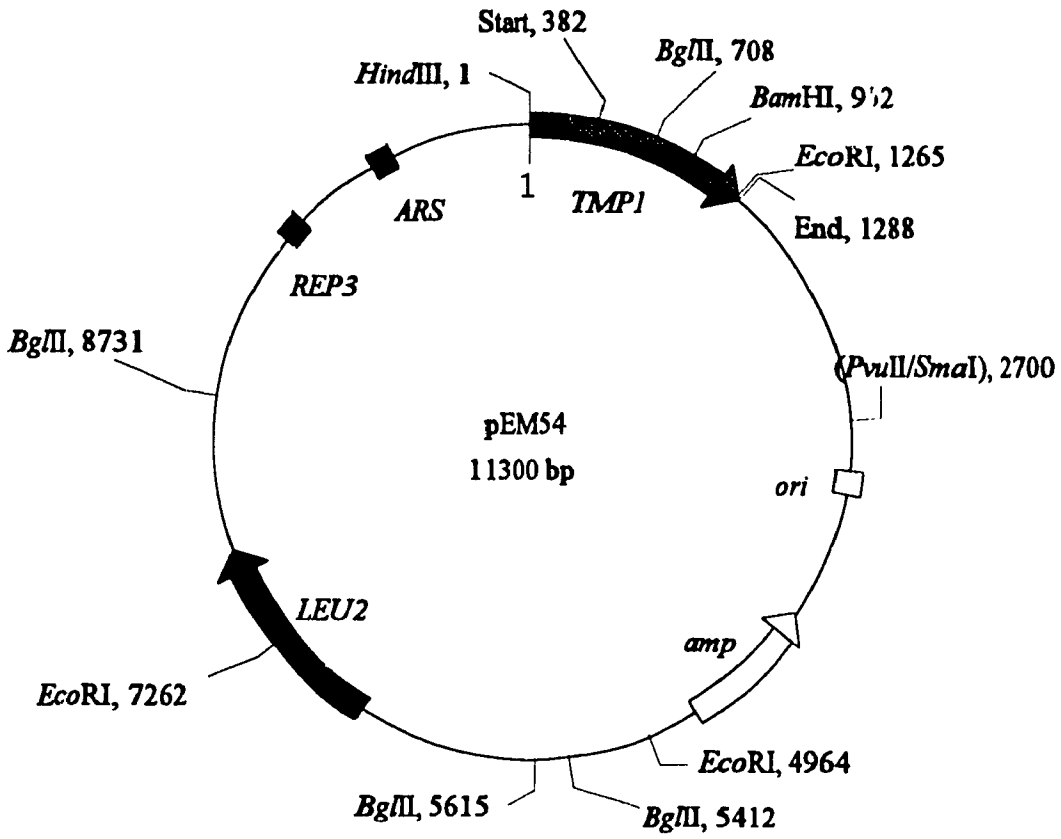

Figure 10. Yeast episomal plasmid constructed by ligating the *Hind*III to *Sma*I fragment of pTL830 into the *Hind*III to *Pvu*II backbone of YEp13. Plasmid pEG13-E1 is identical except that it harbors *TMP1-ΔEUK1* rather than the *TMP1* wild type gene.

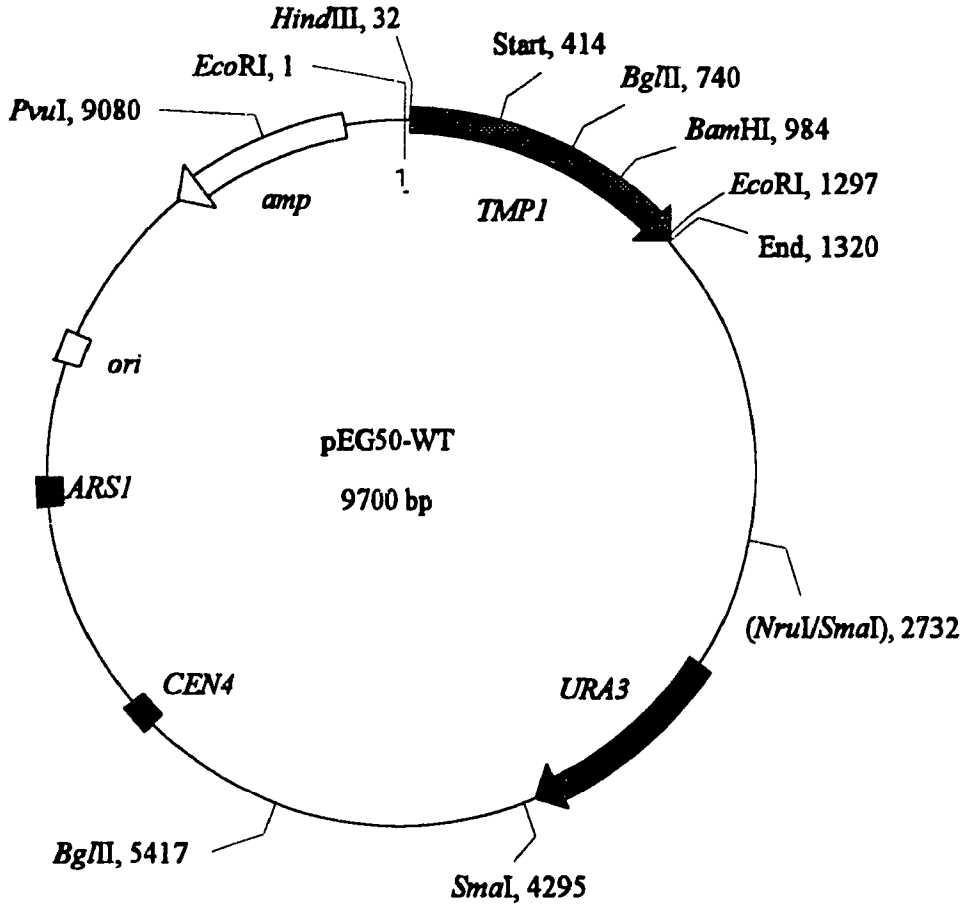

Figure 11. Yeast centromeric plasmid constructed by ligating the *Hind*III to *Sma*I fragment of pTL830 into the *Hind*III to *Nru*I backbone of YCp50. Plasmid pEG50-E1 is identical except that it has *TMP1-ΔEUK1* instead of the *TMP1* wild type gene.

plates supplemented with tryptophan and leucine to select for uracil prototrophs. This eliminated transformants harboring plasmid pEG830-E1 which might have religated despite digestion of the backbone with *Pvu*I. Insertion of the *TMP1-ΔEUK1* gene was determined by testing the uracil prototrophs for tetracycline sensitivity, since the *Nru*I insertion site is located within the *tet* gene of plasmid YCp50. Presence of the *TMP1-ΔEUK1* gene was further confirmed by *Pvu*II and *Bgl*II separate digestions which yielded the expected fragments of 339bp and 9 Kb, and 3.5 and 6.3 Kb respectively. An analogous construct of the wild type *TMP1* gene was made in the same manner by cloning the *Hind*III/*Sma*I fragment of pTL830 into the *Hind*III and *Nru*I sites of YCp50, resulting in plasmid pEG50-WT.

To optimize expression of yeast thymidylate synthase in *E. coli*, the following construct was made. A segment of the *TMP1-ΔEUK1* gene was amplified by PCR, using pEG830-E1 as template and primers spanning ca. 630 bp (Figure 12). The PCR product, containing an *E.coli* ribosomal binding site and a *Hind*III restriction site 14 bp upstream of the start codon, was trimmed to 554 bp with *Hind*III and *Bam*HI. It was then exchanged for the 952 bp *Hind*III/*Bam*HI fragment of pTL830, thus removing the yeast promoter of *TMP1*. Ligates were transformed into *E. coli* strain DH5α and selection was done on ampicillin plates. Verification of the PCR insert was done by screening for a *Hind*III/*Bam*HI fragment of 554 bp versus the original fragment of 952 bp. Analogous constructs were made for wild type *TMP1*, as well as *TMP1-ΔEUK2a* and *TMP1-ΔEUK2b*, using as templates plasmids pTL830, pEG89-E2a and pEG89-E2b respectively. These four new pTL830 derivatives were renamed pEGRBS-WT, pEGRBS-E1, pEGRBS-E2a and pEGRBS-E2b (Figure 13). Plasmids pEGRBS-WT and pEGRBS-E1 were sequenced through the PCR-amplified region

to confirm that they contained either the wild type or ΔEUK1 version of *TMP1* and the ribosomal binding site, as well as to ensure that no other mutations had been introduced during the PCR procedure.

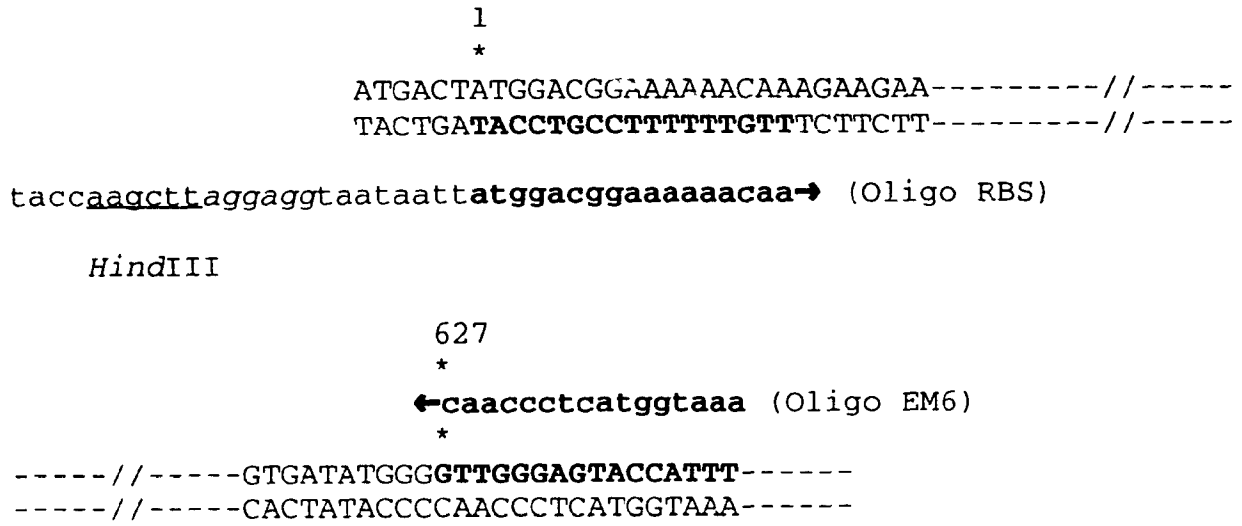

Figure 12. PCR amplification scheme for construction of pEGRBS plasmids to optimize expression of yeast TS in *E.coli*. Primers "oligo EM6" and "oligo RBS" are shown as lowercase sequences while the *TMP1* gene sequences are in uppercase. Arrows indicate direction of extension. Homologous sequences between primer and template are in bold face. The ribosomal binding sequence, AGGAGG, is shown in italics, and the new *Hind*III site is underlined.

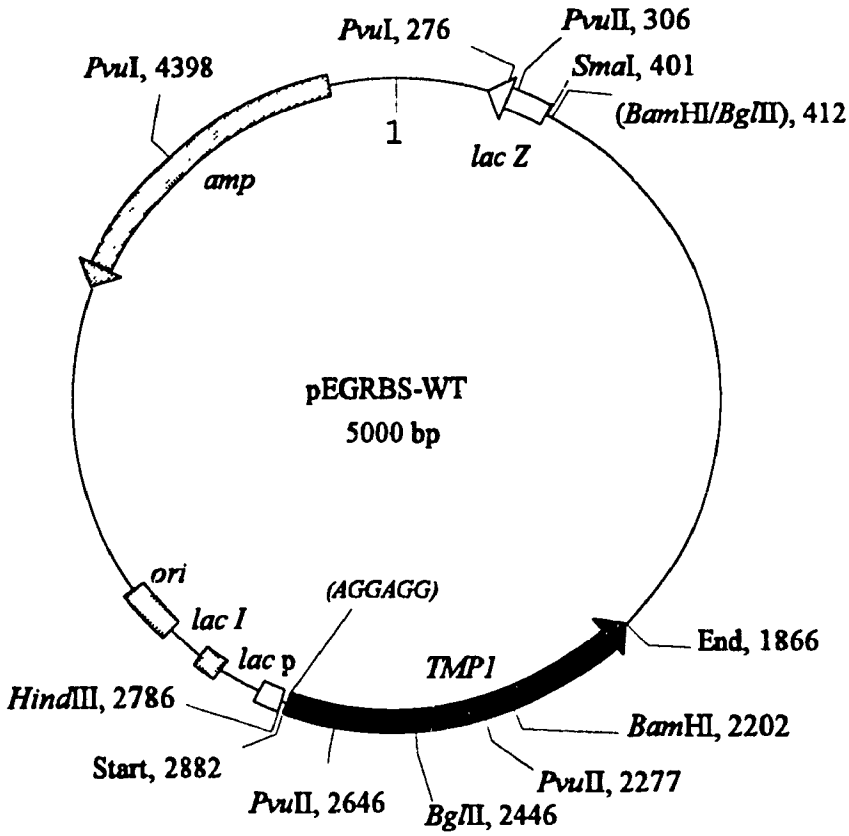

Figure 13. *E. coli* vector constructed from pTL830, to increase expression of yeast TS. The *TMP1* promoter has been dropped and the gene is expressed using the *lac Z* promoter (shown as *lac* p) instead. An *E.coli* ribosomal binding sequence (*AGGAGG*) has been inserted just downstream of the *Hind*III site. Other versions of this plasmid are pEGRBS-E1, pEGRBS-E2a, and pEGRBS-E2b, which are identical to pEGRBS-WT except that they contain the ΔEUK1, 2a and 2b mutations respectively.

Generation of Mutants ΔEUK2a and ΔEUK2b

Mutants ΔEUK2a and ΔEUK2b were generated by the method of Kunkel *et al.* (1987) using a Bio-Rad "Muta-Gene Phagemid *In Vitro* Mutagenesis" kit and following the included protocol. The synthetic primers used for the procedure are shown in Figure 15; phagemids pEM89 (Figure 14) and pEG89-E2a were used as template to generate mutants ΔEUK2a and ΔEUK2b respectively. Single-stranded template of phagemids pEM89, pEG89-E2a and Bluescript 2524 as well as stocks of M13K07 helper phage were prepared according to procedures described by Maniatis *et al.*(1989), and Vieira and Messing (1987).

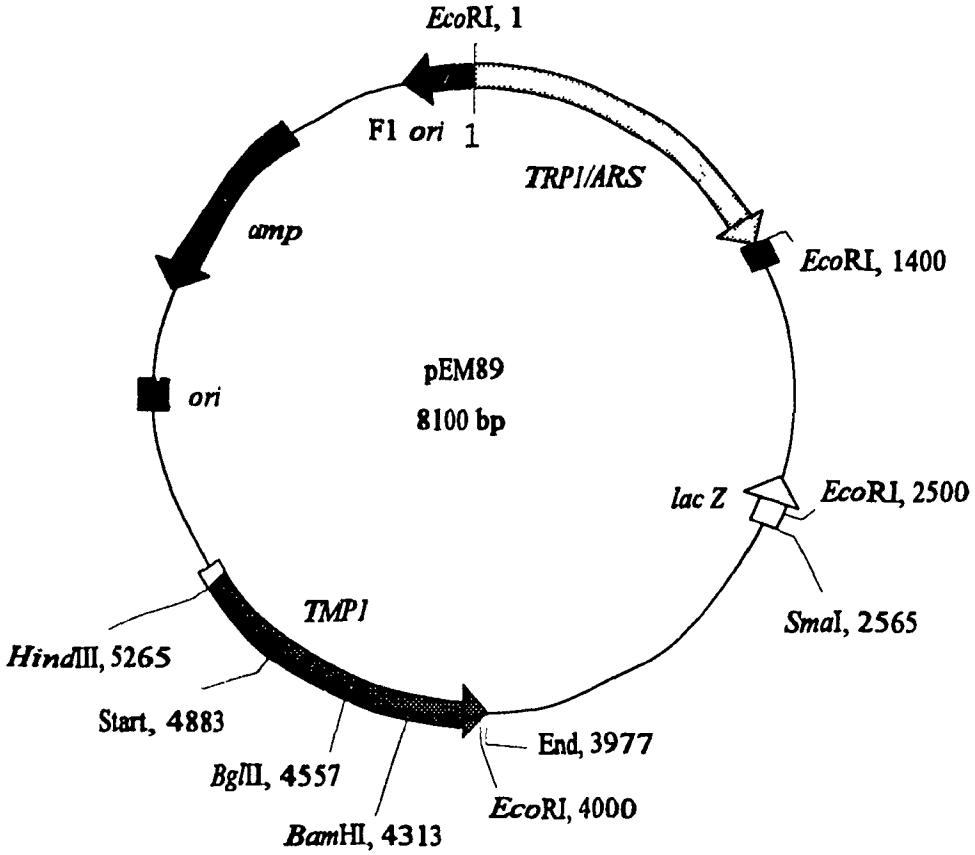

Figure 14. Yeast/*E.coli* shuttle vector constructed by ligating the *Hind*III to *Sma*I fragment of pTL830 into *Hind*III and *Sma*I sites of the *lacZα* segment of pEMBLYr25. Plasmids pEG89-E2a and pEG89-E2b are identical except that they contain *TMP1-ΔEUK2a* and *TMP1-ΔEUK2b* respectively.

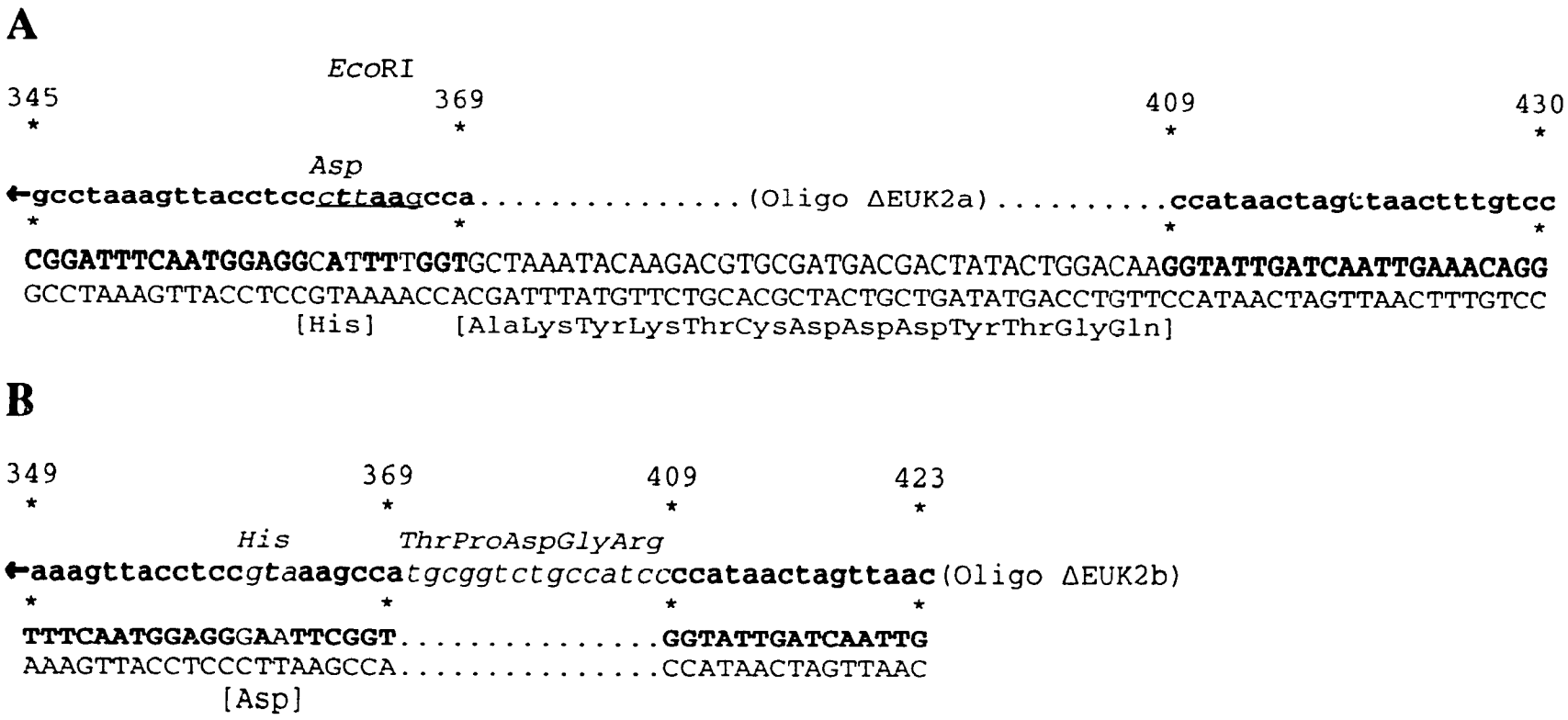

Figure 15. **A.** Sequence of synthetic primer "oligo ΔEUK2a" and complementary regions on the *TMP1* wild type gene. **B.** Sequence of "oligo ΔEUK2b" and complementary regions on the *TMP1-ΔEUK2a* gene used as template. Primer sequences are shown in lowercase letters. Bold face letters indicate homology between template and primer. Arrows indicate direction of extension. The new *Eco*RI site of ΔEUK2a is underlined. All numbers refer to positions on the wild type gene. Dotted lines indicate continuity between bases adjacent to the lines. Square brackets indicate deleted amino acids while inserted amino acids are denoted by italics.

TABLE I: RELEVANT PLASMIDS AND THEIR CHARACTERISTICS

PLASMID NAME	YEAST MARKER	*E.coli* GENES	PARENTAL PLASMID	REPLICATION SEQUENCES	OTHER DNA	SIZE (Kb)	COMMENTS
pTL830	-	*amp* *lac I*	pUC9[a]	pBR322 *ori*	*TMP1*	5.4	*Hind*III to second *Bgl*II fragment of *TMP1* ligated into *Hind*III to *Bam*HI backbone of pUC9
pEG830-E1	-	*amp* *lac I*	pTL830	pBR322 *ori*	*TMP1-ΔEUK1*	5.4	Same as pTL830 but *TMP1* has ΔEUK1 deletion
YEp13[b]	*LEU2*	*amp* *tet*	pBR322	pBR322 *ori* *REP3* *ARS-2μm*	-	10.8	

(Continued)

[a]Vieira and Messing, 1982
[b]Broach *et al.*, 1979; Lagosky *et al.*, 1987

TABLE I *(Continued)*

PLASMID NAME	YEAST MARKER	*E.coli* GENES	PARENTAL PLASMID	REPLICATION SEQUENCES	OTHER DNA	SIZE (Kb)	COMMENTS
pEM54	*LEU2*	*amp*	YEp13	pBR322 *ori* *REP3* *ARS-2μm*	*TMP1*	11.3	*Hind*III to *Sma*I fragment of pTL830 (containing *TMP1*) ligated into *Hind*III to *Pvu*II backbone of YEp13
pEG13-E1	*LEU2*	*amp*	YEp13	pBR322 *ori* *REP3* *ARS-2μm*	*TMP1-ΔEUK1*	11.3	Same as pEM54 but *TMP1* has ΔEUK1 deletion
pEM89	*TRP1*	*amp*	pEMBLYr25[a]	pBR322 *ori* *ARS1* f1 *ori*	*TMP1*	8.1	*Hind*III to *Sma*I fragment of pTL830 (containing *TMP1*) ligated into *Hind*III and *Sma*I sites of the *lacZα* segment of pEMBLYr25

(Continued)

[a]Baldari and Cesareni, 1985; Dente *et al.*, 1983

TABLE I *(Continued)*

PLASMID NAME	YEAST MARKER	*E.coli* GENES	PARENTAL PLASMID	REPLICATION SEQUENCES	OTHER DNA	SIZE (Kb)	COMMENTS
pEG89-E2a	*TRP1*	*amp*	pEM89	pBR322 *ori* *ARS1* fl *ori*	*TMP1-ΔEUK2*a	8.1	Same as pEM89 but *TMP1* has ΔEUK2a deletion
pEG89-E2b	*TRP1*	*amp*	pEG89-E2a	pBR322 *ori* *ARS1* fl *ori*	*TMP1-ΔEUK2b*	8.1	Same as pEM89 but *TMP1* has ΔEUK2b deletion
pNG22[a]	*TRP1* *URA3*	*amp*		pMB1 *ori* *ARS1*			
YCp50[b]	*URA3*	*amp* *tet*	pBR322	pBR322 *ori* *CEN4* *ARS1*		8.0	

(Continued)

[a]Luche and Sumrada, 1990
[b]Rose *et al.*, 1987

TABLE I *(Continued)*

PLASMID NAME	YEAST MARKER	*E.coli* GENES	PARENTAL PLASMID	REPLICATION SEQUENCES	OTHER DNA	SIZE (Kb)	COMMENTS
pEG50-WT	*URA3*	*amp*	YCp50	pBR322 *ori* *CEN4* *ARS1*	*TMP1*	9.7	*Hind*III to *Sma*I fragment of pTL830 (containing *TMP1*) ligated into *Hind*III to *Nru*I backbone of YCp50
pEG50-E1	*URA3*	*amp*	YCp50	pBR322 *ori* *CEN4* *ARS1*	*TMP1*	9.7	Same as pEG50-WT but *TMP1* has ΔEUK1 deletion
pEGRBS-WT	-	*amp*	pTL830	pBR322 *ori*	*TMP1*	5.0	PCR-generated *TMP1* fragment encompassing the region from the start codon to the *Bgl*II site, exchanged for the *Hind*III to *Bgl*II fragment of pTL830. The PCR fragment has a *Hind*III site and *E.coli* ribosomal binding site at the 5' end

(Continued)

TABLE I *(Continued)*

PLASMID NAME	YEAST MARKER	*E.coli* GENES	PARENTAL PLASMID	REPLICATION SEQUENCES	OTHER DNA	SIZE (Kb)	COMMENTS
pEGRBS-E1	-	*amp*	pTL830	pBR322 *ori*	*TMP1-ΔEUK1*	5.0	Same as pEGRBS-WT but *TMP1* has ΔEUK1 deletion
pEGRBS-E2a	-	*amp*	pTL830	pBR322 *ori*	*TMP1-ΔEUK2a*	5.0	Same as pEGRBS-WT but *TMP1* has ΔEUK2a deletion
pEGRBS-E2b	-	*amp*	pTL830	pBR322 *ori*	*TMP1-ΔEUK2b*	5.0	Same as pEGRBS-WT but *TMP1* has ΔEUK2b deletion
Bluescript-2524	-	*amp*	Bluescript-M13-KS[a]	pBR322 *ori* f1 *ori*	$P_{T3,T7}$	4.3	1.4 Kb upstream fragment of *TMP1* ligated into the polylinker region of Bluescript M13-KS, generating unique *Hind*III and *Bgl*II sites

[a]Short *et al.*, 1988

(Continued)

TABLE I *(Continued)*

PLASMID NAME	YEAST MARKER	*E.coli* GENES	PARENTAL PLASMID	REPLICATION SEQUENCES	OTHER DNA	SIZE (Kb)	COMMENTS
pEGBL-E1	-	*amp*	Bluescript-2524	pBR322 *ori* f1 *ori*	$P_{T3,T7}$	4.8	PCR-generated *Hind*III to *Bgl*II fragment of *TMP1* having ΔEUK1 deletion, ligated into *Hind*III to *Bgl*II backbone of Bluescript 2524
pNKY1009[a]	*URA3*	*amp*	YRp7[b]	pMB1 *ori* *ARS1*		9.6	*Bgl*II to *Bam*HI fragment containing *URA3* flanked by 2 *hisG* repeats, ligated into the *Bam*H1 linker inserted in the *Eco*RV site of the *TRP1* gene

[a]Alani *et al.*, 1987
[b]Struhl *et al.*, 1979

TABLE II: STRAINS USED

STRAINS	SPECIES	GENOTYPE	REFERENCE OR SOURCE
MC1066	*E.coli*	*hsdR⁻ leuB6 trpC9830 pyrF674*::Tn 5 (*cam*^{r}) *lacX74 galK galU strA*^{r}	Casadaban *et al.*, 1983
CJ236	*E.coli*	*dut1 ung1 thi1 relA*-1 pCJ105 (*cam*^{r} F')	Kunkel *et al.*, 1987
XL1-Blue	*E.coli*	*supE44 hsdR17 recA1 endA1 gyrA46 thi relA1 lac*⁻ F'[*proAB*$^+$ *lacI*^{q} *lacZ* ΔM15 Tn*10* (*tet*^{r})]	Bullock *et al.*, 1987
264	*E.coli*	*HfrH thi lac thy*Δ64	Belfort and Pedersen-Lane, 1984
DH5α	*E.coli*	*supE44 lacU169* (ϕ80 *lacZ* ΔM15) *hsdR1 recA1 endA1 gyrA96 thi*-1	Hanahan *et al.*,1983
280	*S.cerevisiae*	*MATa tmp1-6 leu2-3,112 ura3-52 trp1-289 tup*⁻	R. Storms
559	*S.cerevisiae*	*MATa tmp1-6 leu2-3,112 tup*⁻	B. Barclay
3236	*S.cerevisiae*	*MATa tmp1-6 leu2-3,112 ura3-52 trp1::hisG tup*⁻	This work
2379	*S.cerevisiae*	*MATa leu2-3,112 ura3-52 trp1*	M. Whiteway
HR125-5D	*S.cerevisiae*	*MATa leu2 ura3-52 trp1 his3 his4*	Hall *et al.*, 1984

TABLE III: NOMENCLATURE OF DELETION MUTANTS FROM *S.cerevisiae* TS

NAME BY CONVENTION	ABBREVIATION
TSΔ97-108,G91E,N92W,G93A,S94D,R95E,E96N	ΔEUK1
TSΔ124-136,H121D	ΔEUK2a
TSΔ124-131,D132T,Y133P,T134D,Q136R	ΔEUK2b

Thymidylate Synthase Assays: Tritium Release Method

Yeast strain 280 transformed either with pEM54 or pEG13-E1 was grown in 7 liters of selective media supplemented with ampicillin (100 µg/ml), streptomycin (50 µg/ml) and tetracycline (50 µg/ml) to prevent bacterial contamination. When cultures reached OD_{600} = 0.2 (ca. 5 x 10^6 cells/ml), they were centrifuged in batches of 350 ml. at 4°C, 6000 rpm (6370 x *g*) for 10 minutes in a Beckman JA-10 rotor. Pellets were resuspended in 2 ml of ice-cold water and centrifuged in a clinical centrifuge for 3-5 minutes. The water was removed by aspiration and cells were stored at -80° C.

For assays of wild type enzyme (expressed from plasmid pEM54), 1 pellet was resuspended in 2.5 ml of water and 260 µl of this cell suspension used per assay. Each aliquot of 260 µl was diluted with 250 µl of 2x Buffer A (40% glycerol, 20 mM β-mercaptoethanol, 20 mM $MgCl_2$, 2 mM EDTA, 40 mM Tris-HCl pH 8, 6% Brij-35 detergent), 10 µl were removed for cell counting, followed by addition of 400 µl of freshly made Buffer B (25 mM $MgCl_2$, 2.5 mM EDTA, 250 mM Tris-HCl pH 8, 200 mM β-mercaptoethanol, 0.2% formaldehyde, 1.8 mM R,S-H_4folate). Reactions were initiated by adding 100 µl of tritium- labelled dUMP, and 160 µl aliquots were removed at different time intervals for each assay (see Table IV). Reactions were terminated by dispensing the 160 µl aliquots into Eppendorf tubes containing 500 µl of 12% activated charcoal in 0.1N HCl. After a 30 minute incubation on ice, the tubes were twice centrifuged at 16,000 x *g* for 30 minutes each, vortexing in between centrifugations, and 100 µl aliquots of the supernatant were dispensed in duplicate into 3.5 ml of Ecolume scintillation cocktail. Dpms were counted

in a Rackbeta Model 1215 scintillation counter, and blank reactions (using all above reagents but no cells) were considered as background and subtracted from all results. A negative control was also done using untransformed strain 280, to ensure that tritium release was not occurring via some other mechanism. For assays of the mutant enzyme (expressed from plasmid pEG13-E1), 11 pellets were resuspended in 220 µl each of ice-cold water, for a final pooled volume of ca. 5 ml, and 550 µl of this cell suspension were used for each assay. The same procedure was followed as for the wild type enzyme, except that dUMP concentrations and time points were different (see Table IV), and aliquots were increased from 160 µl to 210 µl. The cofactor used for these assays was synthesized by Paul Taslimi, by the reduction of folate in the absence of O_2, with modifications as described in his Master's thesis (1995) to the method of O'Dell (1947). The radiochemical [5-^{3}H]-dUMP was purchased from Amersham, and was diluted with various amounts of unlabeled nucleotide to give the radioactivities listed in Table IV.

TABLE IV: PARAMETERS SET FOR KINETIC ASSAYS USING THE TRITIUM RELEASE RADIOCHEMICAL METHOD

	[dUMP] (μM)	Approximate specific activity of dUMP (dpm/pmole)	Time Points (Minutes)
Wild Type:	1.5	900	0, 1, 2, 3, 4
	2.5	550	0, 1, 2, 3, 4
	3.75	550	0, 1, 2, 3, 4
	5	400	0, 1, 2, 3, 4
	10	200	0, 1, 2, 3, 4
	15	150	0, 1, 2, 3, 4
	25	100	0, 2, 4, 6, 8
	100	30	0, 4, 8, 12, 16
Mutant ΔEUK1:	100	40	0, 20, 45, 65, 85
	150	30	0, 20, 45, 65, 85
	200	20	0, 20, 45, 65, 85
	300	20	0, 20, 45, 65, 85
	400	15	0, 20, 45, 65, 85
	500	10	0, 20, 45, 65, 85
	1000	10	0, 20, 45, 65, 85
	2000	5	0, 20, 45, 65, 85

Concentrations of substrate and approximate specific activities of dUMP used for the radiochemical assays on permeabilized yeast cells expressing wild type or mutant TS. The cofactor concentration was maintained at 1.8 mM (racemic mixture) and reactions were performed at 25°C.

Purification of Wild Type and Mutant Enzymes

A 2-liter culture of *E. coli* strain 264 transformed with pEGRBS-WT was grown for 24 hours, in 2XYT media supplemented with ampicillin (100 µg/ml) but containing no thymidine. A 17 g cell pellet was harvested by centrifuging at 6000 rpm (6370 x *g*) for 10 minutes in a Beckman JA-10 rotor, and was resuspended in 80 ml of 20 mM Tris-HCl, pH 7.4, 0.2 mM EDTA, 1 mM PMSF (phenylmethylsulfonyl fluoride). Cells were lysed by sonication at maximum setting using a ½ inch diameter probe, in 12 bursts of 30 seconds each, cooling on ice in between. Cellular debris were then removed by twice centrifuging at 10500 rpm (15188 x *g*), 4°C, for 20 minutes in a JA-17 rotor. The supernatant was decanted and made 10% in glycerol. Henceforth all procedures were carried out at 4°C. The total protein yield of 460 mg (4.3 mg/ml) was loaded onto a Q-sepharose column (2.5 x 8 cm), pre-equilibrated with start buffer (20 mM Tris-HCl, pH 7.4, 0.2 mM EDTA, 10% glycerol), at a flow rate of 2.5 ml/min. The column was washed with 500 ml of start buffer, and TS was eluted with a linear gradient from 0 to 0.8M KCl in start buffer (400 ml total volume). Fractions of 7.5 ml were collected, and the TS peak appeared from 70-140 mM KCl, as determined by tritium release assays and SDS-gel electrophoresis. Fractions 6 to 9 were pooled and dialyzed for 4 hours in 6 liters of dialysis buffer (20 mM KPO_4, pH 7, 0.2 mM EDTA). The dialysate was loaded onto a hydroxyapatite column (2.5 x 8 cm), pre-equilibrated with 25 mM KPO_4, pH 7, 0.5 mM EDTA, at a flow rate of 0.8 ml/min. The column was washed with 400 ml of equilibration buffer, and TS was eluted with a linear gradient from 25 to 350 mM KPO_4, pH 7, 0.5 mM EDTA (200 ml total volume). Fractions

of 7 ml were collected, and the TS peak appeared from 200 to 350 mM KPO_4, as determined by tritium release assays and SDS-gel electrophoresis. Fractions 18 to 28 were pooled, dialyzed overnight in 6 liters of 20 mM KPO_4, pH 7, 0.2 mM EDTA, concentrated to 2.8 µg/µl on PEG 20000, and stored at -80°C.

For the mutant enzyme, a 4-liter culture of *E. coli* 264 transformed with pEGRBS-E1 was grown and harvested in the same manner as the wild type culture. The purification procedure was essentially the same as for the wild type enzyme except for the following. The TS peak eluted from the Q-sepharose column from 300-500 mM KCl, co-eluting with the main protein peak. TS fractions from the hydroxyapatite column (14-27) occurred from 110-220 mM KPO_4, and these still contained a large number of contaminating bands. The fractions were pooled, and dialyzed overnight in 6 liters of buffer containing 20% glycerol, 50 mM TEOLA (triethanolamine) pH 7, 1 mM EDTA and 80 mM KCl. The dialysate was then made 4 mM in dUMP and incubated at 4°C for 1.5 hours prior to loading onto a Cibacron-blue sepharose column (1.6 x 7 cm) previously equilibrated with buffer containing 20% glycerol, 50 mM TEOLA, 1 mM EDTA, 4 mM dUMP and 80 mM KCl, at a flow rate of 0.5 ml/min. The column was washed with 100 ml of equilibration buffer, and TS was eluted with a linear gradient from 0.25 to 2 M KCl (150 ml) in equilibration buffer. TS emerged as a broad peak from 0.5 to 2 M KCl and the cleanest fractions were pooled into 7 samples which were dialyzed separately in 20 mM KPO_4, 0.2 mM EDTA and then concentrated on PEG 20000. The 7 pools were tested for activity to ensure that specific activity was equivalent among all samples before pooling into one homogeneous batch, which yielded ca. 23 mg of protein concentrated at 3 mg/ml. SDS-PAGE gels of the various

purification stages for both wild type and mutant enzymes are shown in Figure 21.

Spectrophotometric Assays

Spectrophotometric assays (Pogolotti *et al.*, 1986) were performed at 25°C in black quartz cuvettes with a CARY3E UV-Visible spectrophotometer by Varian Instruments. To determine K_m for the substrate dUMP, reactions were done in a 1 ml volume of TS-assay buffer (pH 7.4) containing 50 mM TES (N-tris[hydroxymethyl]methyl-2-aminoethanesulfonic acid), 25 mM $MgCl_2$, 6.5 mM HCHO, 1 mM EDTA, 75 mM β-mercaptoethanol, 100 μM of 6R-CH_2-H_4folate; dUMP concentrations varied from 2.5 to 125 μM for the wild type enzyme and from 10 μM to 2 mM for the mutant. Reactions were initiated by the addition of enzyme, 13 μg in the case of the wild type and 84 μg for the mutant. Reactions were followed by monitoring the appearance of 7,8-dihydrofolate (Abs_{340}), and rates were calculated by linear regression analysis using CARY3E software. Linear ranges were taken over 2-4 minute time spans for the wild type and 25-30 minutes for the mutant. Assays to determine K_m for the cofactor were done similarly, with dUMP concentrations held at 50 μM for the wild type and 300 μM for the mutant, while cofactor concentrations were varied from 1.25 to 200 μM for the wild type and 10 to 200 μM for the mutant.

The cofactor (6R,S)-CH_2-H_4folate was prepared (see Appendix A) from tetrahydrofolate purchased from Sigma. The active concentration of cofactor (6R-CH_2-H_4folate) was determined spectrophotometrically by measuring the total 7,8-dihydrofolate produced by excess thymidylate synthase in TS assay buffer containing 150 μM dUMP, and

using $\varepsilon_{340} = 6400\ M^{-1}cm^{-1}$ (see Appendix A).

Generation of a *TRP1* Disruption Mutant of Yeast Strain 280

The chromosomally encoded *TRP1* gene of yeast strain 280 had a high reversion frequency to the Trp^+ phenotype, and was therefore disrupted. This was achieved by gene replacement at the *TRP1* chromosomal locus of yeast strain 280, by integrative transformation of a *trp1::hisG-URA3-hisG* fragment from plasmid pNKY1009 (Table I and Figure 16, Alani *et al.*, 1987).

A complete *Bgl*II/*Eco*RI digest of the plasmid was transformed into strain 280, and Ura^+ transformants were selected on YNB plates supplemented with tryptophan and leucine at 50 µg/ml and dTMP at 200 µg/ml. Five colonies were picked, and to ensure that they were recombinants rather than transformants harboring uncut plasmid, they were grown to saturation in 10 ml of YEPD media with dTMP, and plated onto tryptophan selection plates. After one week, no Trp^+ revertants appeared, compared to 25 revertants on a control plate of untreated yeast strain 280, suggesting that all 5 colonies were recombinants of the *TRP1* locus. Two colonies were grown overnight in 2 ml of YEPD with dTMP, harvested by centrifugation, resuspended in water and spread on YNB plates supplemented with tryptophan, leucine, uracil, dTMP, and 1 mg/ml FOA (fluoro-orotic acid) to select for FOA resistance. FOA resistant colonies are Ura^- since FOA sensitivity is due to the activity of the *URA3* gene product which decarboxylates innocuous 5-fluoro-orotidylate to produce toxic 5-fluoro-uridylate (Boeke *et al.*, 1984). This is thus a convenient method of selecting for

colonies in which the *hisG* repeats have recombined, causing excision of the *URA3* gene and hence restoring the *ura3-52* dependent Ura$^-$ phenotype in the strain. Finally, several FOA resistant colonies were picked and tested for their original phenotype, Trp$^-$, Ura$^-$, Tmp$^-$, and Leu$^-$. The resulting yeast strain was designated 3236.

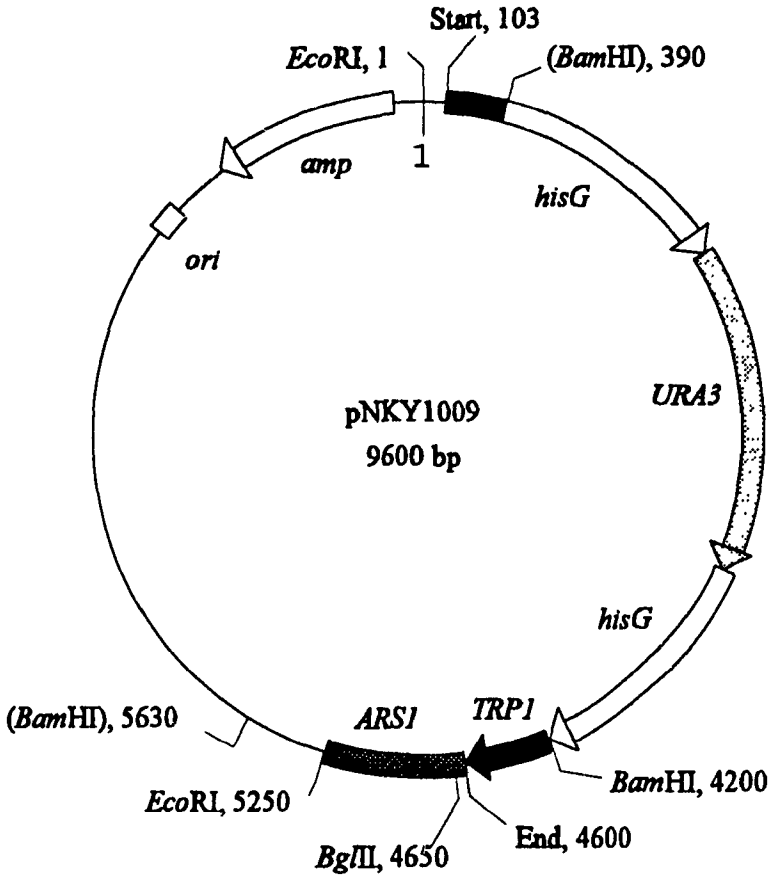

Figure 16. Plasmid used to generate the *TRP1* gene disruption of yeast 3236. The plasmid was cut with *Eco*RI and *Bgl*II to excise the *TRP1* gene and induce recombination with the chromosomally-encoded *TRP1* gene of yeast strain 280. The *URA3* gene allows for selection of recombinants, and the *hisG* repeats cause subsequent excision of the *URA3* gene, which is detected by FOA resistance, and which conveniently restores the *ura3-52* allele as a selectable marker in the strain.

Other Procedures

Yeasts were transformed according to the method of Schiestl and Gietz (1989), except that lithium chloride was used instead of lithium acetate. *E.coli* were transformed by the calcium chloride procedure described by Maniatis *et al.* (1989).

Small scale preparations of plasmid DNA were performed by several methods, which included 1) the alkali lysis method in Maniatis *et al.* 2) an adaptation of the protocol in the Promega "Magic Miniprep" kit supplied by Bio/Can Scientific and 3) the Wizard Miniprep kit which was used to prepare double-stranded template for sequencing.

DNA digestions and ligations were performed by standard protocols in Maniatis *et al.*, using enzymes and buffers purchased from Bio/Can Scientific. For the ligations, a ratio of insert to recipient vector of 10:1 was usually used, and the vectors were dephosphorylated with calf intestinal phosphatase to minimize re-circularization of the original plasmid.

PCR amplifications were accomplished by the method described by Mullis and Faloona (1987) and later modified by Saiki *et al.* (1988), using a Bio/Can Scientific Hybaid Thermal Reactor. Yeast bank DNA or plasmid DNA were used as template, with a 1000-fold excess of primers (65 picomoles of each primer). The reactions were carried out in 100 µl volumes, using 5 units of *Taq* polymerase and 0.2 mM deoxyribonucleotides. The denaturation temperature was programmed at 95°C for 3 minutes initially and 18 seconds for each subsequent cycle, hybridization at 55°C for 1 minute, and primer extension at 72°C for 1 minute. The rate of change of temperature was set at "RAMP 3", and the cycle was repeated 30 times. For asymmetric amplification to generate sequencing template, the same

procedure was followed, but 50 picomoles of one primer and 3 picomoles of the other were used.

DNA sequencing was carried out by the dideoxyribonucleotide chain-terminating method of Sanger *et al.* (1977) using a Pharmacia "T7-Sequencing Kit" or a USB "Sequenase Version 2.0 Kit" and following the included protocol. Acrylamide gels (6%) with urea were prepared according to procedures of Maniatis *et al.* The templates used were either single stranded phagemid generated *in vivo*, single-stranded DNA fragments amplified by asymmetric PCR, or denatured double-stranded DNA prepared with the Promega Wizard Miniprep Kit.

Protein concentrations were estimated following the protocol included with the Bio-Rad Protein Assay Kit (Bradford, 1976), and BSA was used for the standard curve. Proteins were analyzed by SDS-PAGE using 12% gels stained with Coomassie blue R250. Immunoblot analyses were performed as described in the doctoral thesis of Dr. Pak Poon (1993), using the stock ot TS antibodies also prepared by Dr. Poon.

Culture Media

Yeasts were grown in YEPD medium consisting of 1% Bacto-yeast extract, 2% Bacto-peptone, and 2% dextrose, supplemented with deoxythymidine monophosphate (200 µg/ml) in the case of Tmp$^-$ strains. Selection media (YNBD) consisted of 1.75 g/l of yeast nitrogen base (Difco) without amino acids, 5 g/l ammonium sulfate, and 2% dextrose, supplemented with 50 µg/ml of the required amino acids and 20 µg/ml of uracil when

necessary. To increase growth rates, selection was at times maintained using drop out media which is similar to YNBD except that all amino acids and nitrogenous bases are supplemented except those used for the selection, as described by Ausubel *et al.* (1989).

E. coli were grown in double-strength YT media consisting of 1.6% Bacto-tryptone, 1.0 % yeast extract (Bacto) and 0.5% NaCl, adjusted to pH 7, with 2% agar (Sigma) added for plates. Transformants were selected by supplementing the medium with ampicillin (100 µg/ml). Selective pressure for F' factors was maintained by supplementation with tetracycline (20 µg/ml) for strain XL1-blue and chloramphenicol (100 µg/ml) for strain CJ236. For selection of M13K07-infected cells, 70 µg/ml of kanamycin was added. *E. coli* strain 264 was grown in 2XYT media supplemented with thymidine (50 µg/ml). Thymidine prototrophs of this strain were selected on minimal medium consisting of 10.5 g/l dibasic potassium phosphate, 4.5 g/l monobasic potassium phosphate, 1 g/l ammonium sulfate, 0.5 g/l sodium citrate, 0.2% glucose and 1 mM magnesium sulfate, supplemented with thiamine (2 µg/ml) and ampicillin (100 µg/ml).

Figure 17

Sequencing gels of primer regions of ΔEUK1 , ΔEUK2a , ΔEUK2b and RBS constructs. Relevant sequences are bracketted with black arrows. The loading order is A C G T from left to right.

A. CAATTCTAAACCCTG*CTTACCCGTCTACTTTTA*CCTCTAGACCCC

The italicized sequence is the *E.coli* insert in ΔEUK1, the underlined sequence is the *Bgl*II cloning site.

B. GCCTAAAGTTACCTCCGTTAAGCCACCATAACTAGTTAAC

The new *Eco*RI site of ΔEUK2a is underlined.

C. AAAGTTACCTCCGTAAAGCCA*TGCGGTCTGCCATCC*CC

The italicized sequence is the *E.coli* insert in ΔEUK2b.

D. CCAAGCTT*AGGAGG*TAATAATTATGGACGGAAAAAACAA

The italicized sequence is the *E.coli* ribosomal binding sequence introduced into all 4 pEGRBS plasmids. The underlined sequence is the new *Hind*III cloning site and the bold face codon is the START site.

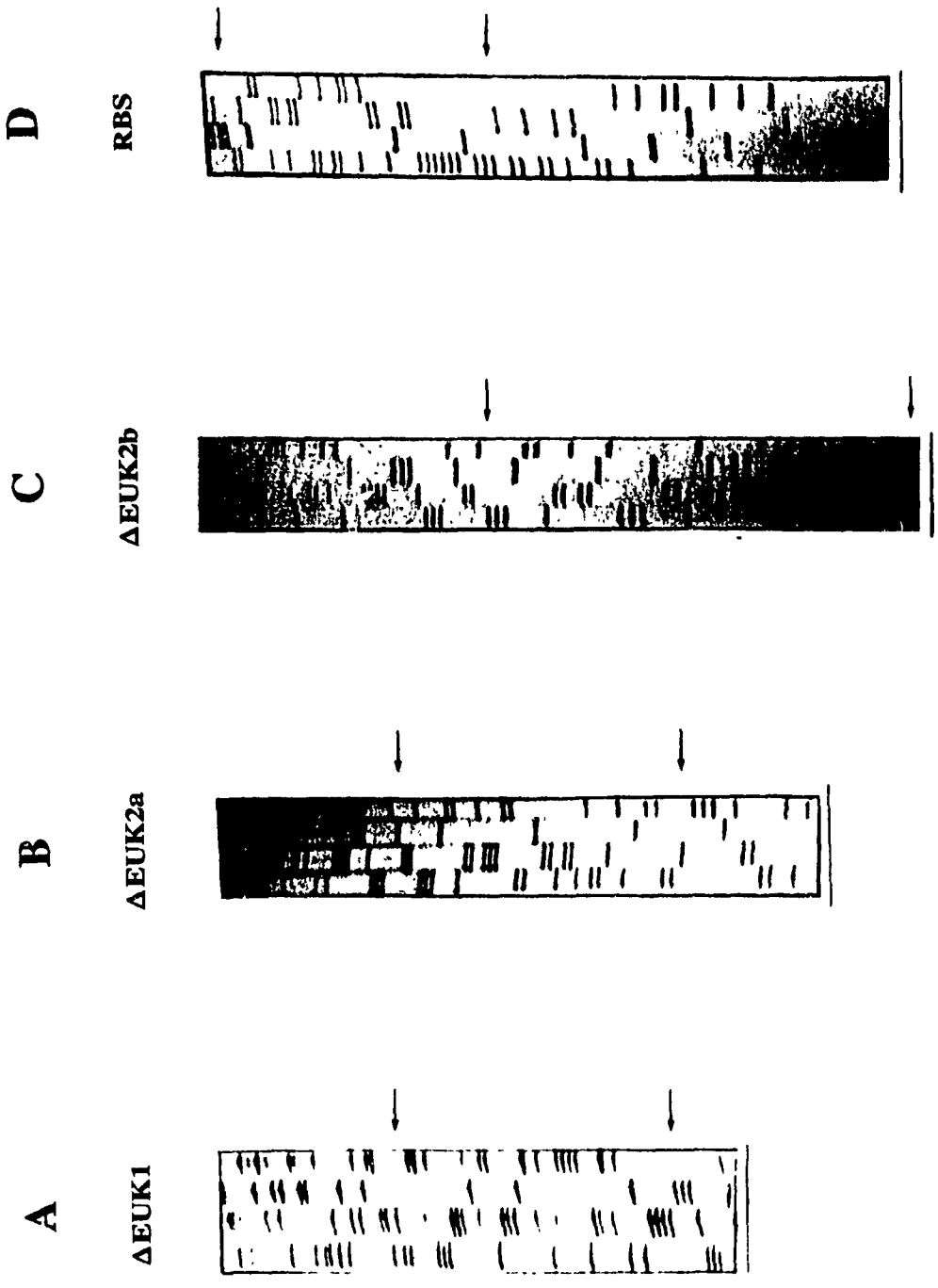
D
RBS
C
ΔEUK2b
B
ΔEUK2a
A
ΔEUK1

RESULTS

Section I: Mutant ΔEUK1

In order to investigate the function of the peptide insert at position 97 to 108 in yeast thymidylate synthase, the mutant denoted as ΔEUK1 was constructed. This mutant has a deletion of 18 amino acids, from #91 to #108 inclusively, which encompasses the so-called eukaryotic insert from #97 to #108. In addition, the six preceding residues are substituted by the corresponding sequence of *E. coli*, E-W-A-D-E-N (see Figures 6, 7 and Table III), since they contain a conserved motif of N-G-S-R in the eukaryotes which we felt might contribute to the hypothetical role of the insert. Furthermore, we hoped that emulation of the *E.coli* enzyme in this region would increase the likelihood of obtaining a functional mutant.

Complementation of Mutant ΔEUK1 in *E. coli* and *S.cerevisiae*

To determine whether mutant ΔEUK1 had any activity, the initial approach was to test its ability to complement *E.coli* and *S.cerevisiae* strains that were deficient for thymidylate synthase activity. The mutant allele was cloned into several types of vectors and transformed into appropriate strains of *E. coli* and *S.cerevisiae* (Table V).

Plasmids pTL830 and pEG830-E1 are pUC derived constructs which are expressed in very high copy levels in *E.coli* but cannot be propagated in yeast since they have neither markers nor replication origins for yeast. Both the wild type and mutant *TMP1* gene

complemented the thyA$^-$ *E.coli* strain 264 when expressed from these vectors. Plasmids pEM54 and pEG13-E1 are yeast episomal plasmids derived from YEp13 and are expressed in multi-copy levels in both yeast and *E.coli*. Only the wild type *TMP1* gene complemented *E.coli* strain 264 in these plasmids, but both the wild type and mutant *TMP1* gene complemented Tmp$^-$ yeast strain 559. Plasmids pEG50-WT and pEG50-E1 are yeast centromeric plasmids derived from YCp50 and are expressed in one or two copies per cell in yeast but multi-copy levels in *E.coli*. The wild type *TMP1* gene complemented both *E.coli* and yeast when expressed in this vector, while the mutant did not complement *E.coli* and complemented yeast only weakly. Growth results of *E.coli* and *S.cerevisiae* harboring these plasmids and patched onto selective media with and without thymidylate are shown in Figure 18.

Figure 18

A. Various transformants of *E.coli* strain 264 on minimal media with ampicillin. Colonies grown on rich media with ampicillin and thymidine were picked and patched onto plates that lacked thymidine (1a, 2a) and then onto plates with thymidine (1b, 2b).

Top:
1. pTL830 (high copy *E.coli* plasmid harboring wild type *TMP1*)
2. pEG830-E1 (same as 1. but harboring *TMP1-ΔEUK1*)
3. pEG830-E1 (same as 2. but different isolate)
4. YEp13 (*E.coli* /yeast shuttle vector - no *TMP1* gene)

Bottom:
1. pEM54 (*E.coli*/yeast shuttle with wild type *TMP1*)
2. pEG13-E1 (same as 1. but with *TMP1-ΔEUK*
3. YEp13 (no *TMP1* gene)
4. pEG50-WT (*E.coli*/yeast centromeric shuttle w. *MP1*)
5. pEG50-E1 (same as 4. but with *TMP1-ΔEUK1*)
6. YCp50 (same as 4. and 5. but without a *TMP1* gene)

B. Various transformants of yeast strain 559 on selection media. Colonies grown on selection plates supplemented with thymidylate were patched onto plates without (1a, 2a) and with thymidylate (1b, 2b).

Top:
1. pEM54 (*E.coli*/yeast shuttle with wild type *TMP1*)
2. pEG13-E1 (same as 1. but with *TMP1-ΔEUK1*)
3. YEp13 (same as 1. and 2. but without a *TMP1* gene)

Bottom:
1. pEG50-WT (*E.coli*/yeast centromeric shuttle with wild type *TMP1*)
2. pEG50-E1 (same as 1. but with *TMP1-ΔEUK1*)
3. YCp50 (same as 1. and 2. but without a *TMP1* gene)

A

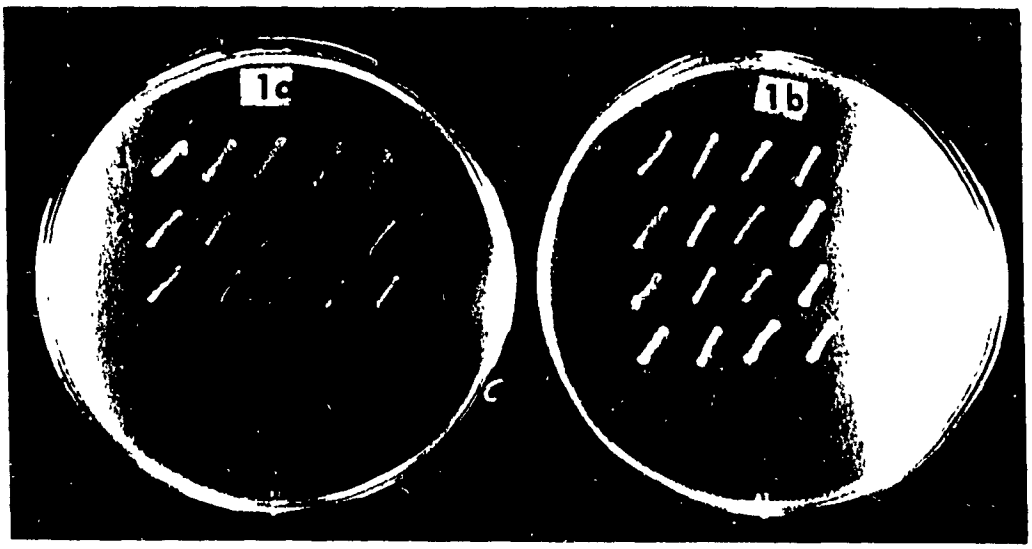

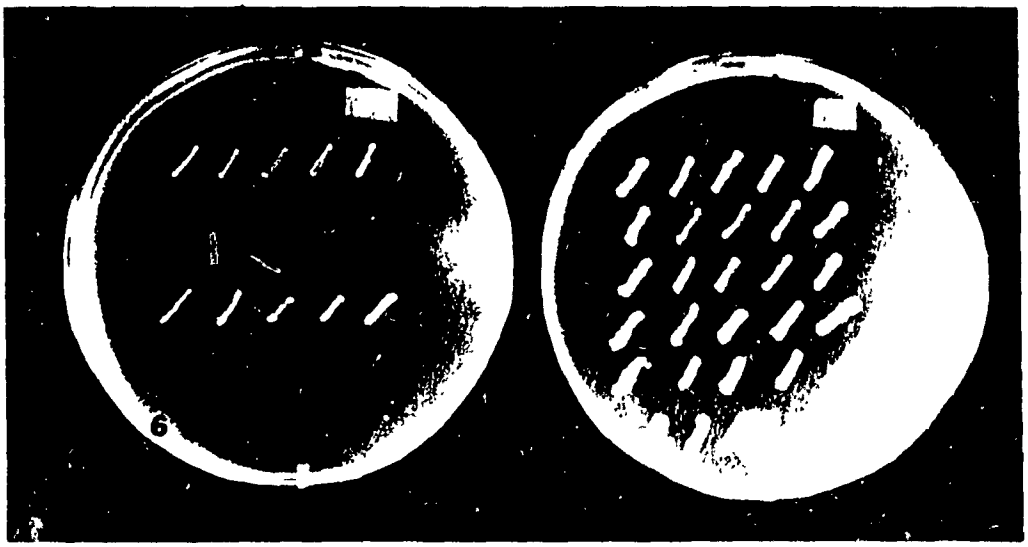

B

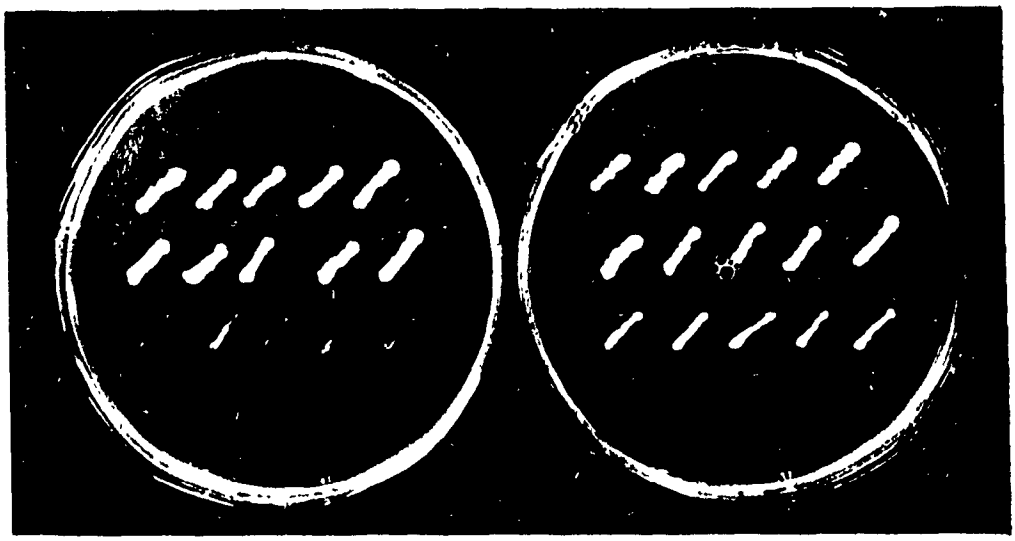

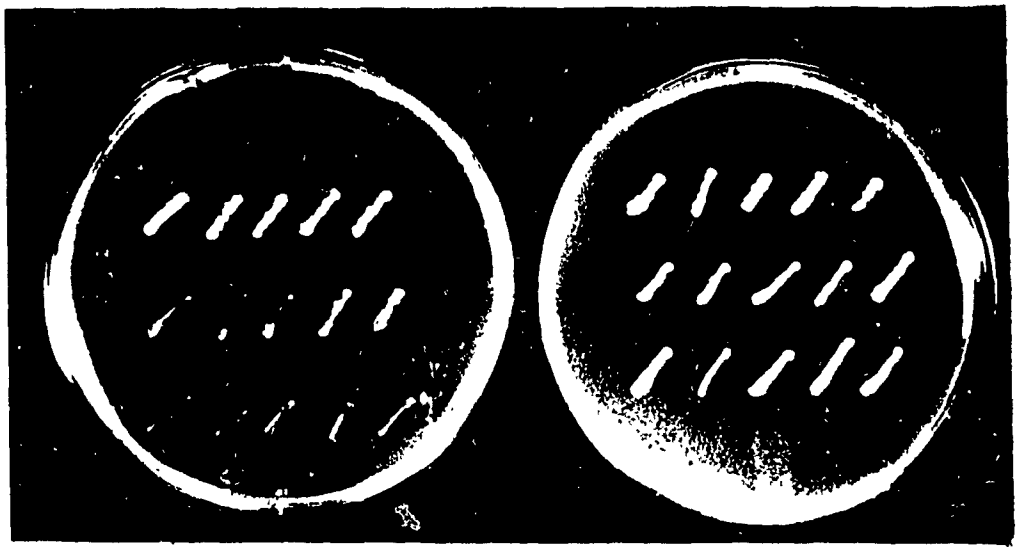

TABLE V: COMPLEMENTATION RESULTS FOR MUTANT ΔEUK1

Vector	*TMP1* Gene	*E.coli* (thy A$^-$)	*S.cerevisiae* (Tmp$^-$)
pTL830	wild type	+++	n/a*
pEG830-E1	ΔEUK1	++	n/a*
pEM54	wild type	+++	+++
pEG13-E1	ΔEUK1	-	+++
YEp13	none	-	-
pEG50-WT	wild type	+++	+++
pEG50-E1	ΔEUK1	-	+
YCp50	none	-	-

*Not applicable since this is not a yeast vector.

Ability to complement was assessed by patching single colony transformants grown with thymidine (for *E.coli*) or thymidylate (for yeast) onto minimal media plates without these supplements (see Figure 18).

+++ Good healthy growth; thick, uniform patches
++ Moderate growth; thin patches
+ Weak growth; mottled patches
- No growth; absence of patches

Kinetic Characterization of Mutant ΔEUK1 Using Permeabilized Whole Yeast Cells

Since the complementation results suggested that high levels of mutant enzyme were required for adequate biological activity both in *E. coli* and yeast, the biochemical activity of ΔEUK1 was tested by attempting a kinetic comparison with the wild type enzyme. The mutant and wild type enzymes were expressed from the same type of plasmid (pEM54 and pEG13-E1 respectively) in the yeast strain 280, under selective conditions. Cells were harvested and permeabilized and assays were performed *in situ*, using the tritium release radiochemical method of Kammen (1966) as modified by Bisson and Thorner (1977). In this assay, dUMP tritiated at the C5 position is used as substrate, and the amount of tritium released by thymidylate synthase in the first step of the reaction is quantitated. Preliminary experiments indicated that the mutant enzyme had much lower activity, hence ca. 10 times more cells were used for the assays as for the wild type enzyme in order to produce adequate amounts of product. In addition, the range of substrate concentrations used was higher and the time span of the assays was longer (see Table IV). Reaction rates were calculated from the linear portion of the time course plots, and expressed as picomoles of protons released per minute per 10^9 cells. Michaelis-Menten curves were generated using the Enzfitter Program (Figure 19 and Table VI) and the results indicated a 20-fold increase in substrate K_m and 100-fold decrease in V_{max} for the cells expressing the mutant enzyme as compared to those expressing the wild type. Immunoblots of thymidylate synthase from both cultures showed that expression of the mutant enzyme was at least as high as that of the wild type (Figure 20).

TABLE VI: MICHAELIS-MENTEN KINETICS FOR TRITIUM RELEASE ASSAYS USING PERMEABILIZED WHOLE CELLS

	[dUMP] μM	Rate* pmol H+/min/10^9 cells ($x10^{-3}$)	Calculated ($x10^{-3}$)
Wild type	1.5	0.58	0.85
	2.5	1.03	1.32
	3.75	1.79	1.81
	5	1.77	2.24
	10	3.17	3.44
	15	4.37	4.19
	25	6.25	5.07
	100	6.03	6.65
Mutant ΔEUK1	100	0.030	0.028
	150	0.039	0.037
	200	0.043	0.043
	300	0.052	0.052
	400	0.054	0.058
	500	0.058	0.062
	1000	0.076	0.073
	2000	0.080	0.080

* Rates reported for the wild type are averages of 4 experiments, rates listed for the mutant are averages of 2 experiments.

TABLE VI
(Continued)

	Variable	Value	Standard Error
Wild type:	V_{max} [a]	7.42×10^3	0.77×10^3
	K_m [b]	11.6	3.1
Mutant:	V_{max} [a]	0.088×10^3	0.003×10^3
	K_m [b]	212	23

[a] Expressed as picomoles of protons per minute per 10^9 cells.
[b] Expressed as μM concentration.

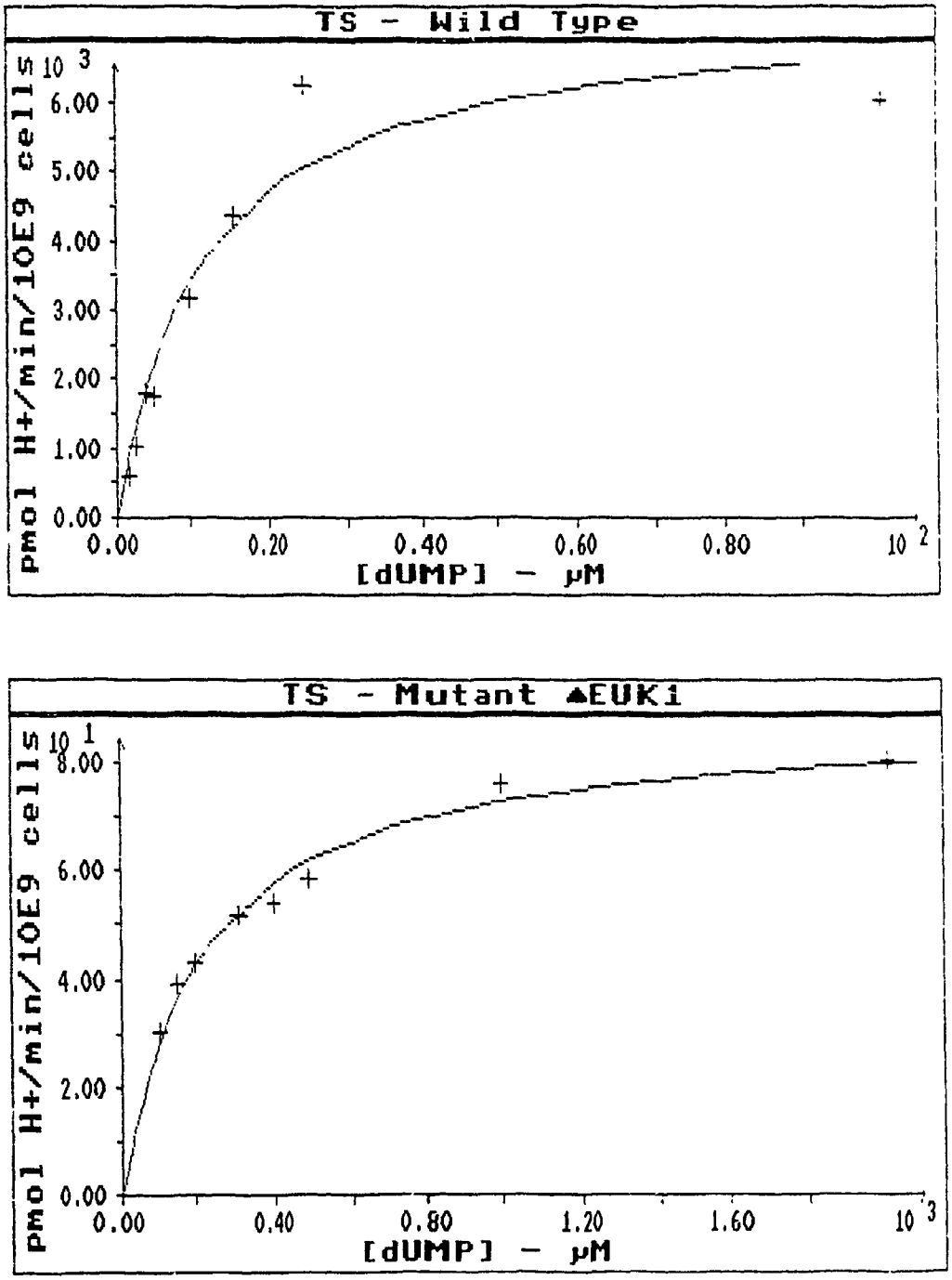

Figure 19. Michaelis-Menten plots of wild type and mutant ΔEUK1 thymidylate synthase activity versus substrate concentration, using data from Table VI.

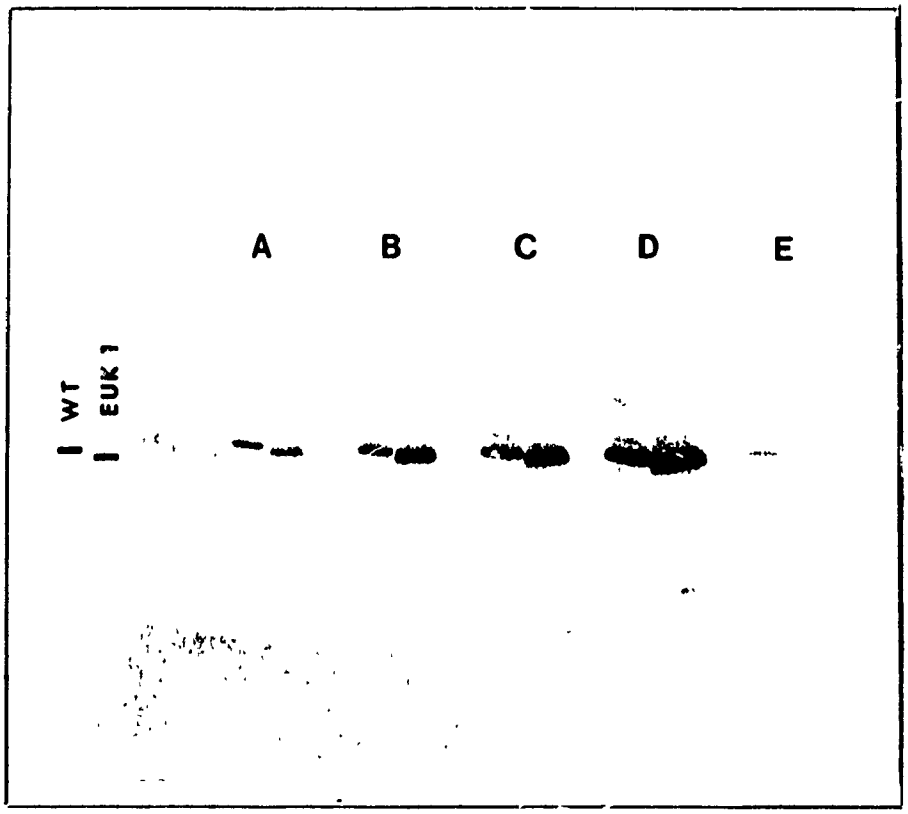

Figure 20. Immunoblot of protein extracts from cultures of yeast strain 280 transformed with either pEM54 (WT) or pEG13-E1 (ΔEUK1), which were used for the whole cell kinetic assays. The total protein loaded was 1.5 µg (A), 2.5 µg (B), 5.5 µg (C), 11 µg (D), and 1 µg (E). The mutant protein is the lower one in all pairs, its faster rate of migration reflecting the fact that it is smaller by 12 residues. Expression levels of the mutant protein appear to be at least as elevated as for the wild type, indicating that the lower activity is not due to lower amounts of enzyme.

Purification of Wild Type and Mutant ΔEUK1 Enzymes

The significant difference in K_m and V_{max} for the wild type and mutant enzymes obtained by performing *in situ* experiments suggested the possible occurrence of a structural deformation in the mutant. Confirmation of this conclusion required a more precise kinetic analysis using purified enzyme preparations. The use of pure enzyme offers several advantages; 1) it allows the performance of spectrophotometric assays, which although less sensitive than the radiochemical assay, are carried out continuously, thus providing more points and greater accuracy, and 2) it eliminates unforeseen variables in whole cell systems which could conceivably contribute to observed results.

For the purification procedure, wild type and mutant thymidylate synthase were expressed in *E.coli*, using the the strategy of Climie and Santi (1990). To optimize expression in *E. coli*, the yeast promoter was dropped out and the *E. coli lac Z* promoter used instead. Also, an *E. coli* ribosomal binding site (AGGAGG) was introduced ca. 10 bases upstream of the start codon (Figure 12). The new constructs denoted as pEGRBS-WT and pEGRBS-E1 were expressed in the *E.coli thyA* deletion strain 264, to avoid any background from the *E.coli* thymidylate synthase. This strain harbors a deletion of ca. 390 bases in the coding region of the *thyA* gene (Montfort and Pedersen-Lane, 1984) and is therefore not expected to produce any thymidylate synthase.

Purification of the wild type enzyme was done in 2 steps, using first a Q-sepharose anion exchange column followed by a hydroxyapatite affinity column. The TS peak emerging from the second column was virtually free of other contaminating proteins (Figure 21, panels

A to C). Purification of the mutant enzyme however, required a third column, a Cibacron-blue sepharose affinity column, to remove the numerous contaminants remaining after passage through the first two columns (Figure 21, panels D to G). The yields of enzyme obtained for the wild type and mutant were ca. 15 mg and 23 mg respectively.

TABLE VII: PURIFICATION OF MUTANT ENZYME

	Total Protein (mg)	Total Volume (ml)	Total Activity (units x 10^3)	Specific Activity* (units x 10^3/mg)	Yield %	Purification -fold
Crude extract	1080	180	295	0.273	100	-
Q-sepharose pooled fractions	319	110	124	0.390	42	1.4
Hydroxyapatite pooled fractions	103	45	91	0.875	31	3.2
Cibacron-blue pooled fractions	23	7.75	63	2.722	21	10

Purification scheme of mutant enzyme obtained from ca. 28 grams of cells.

*Calculations for specific activities are shown in detail in Appendix H and I.
1 unit of activity is defined as 1 µmole of product per minute.

Figure 21

SDS-PAGE gels of the purification stages for wild type (left) and mutant ΔEUK1 (right) thymidylate synthase. The TS-band is indicated by a black line to the left of the gels. Molecular weights are indicated in kilodaltons to the right of gel A.

A. Wild type fractions collected from the Q-sepharose column. **B.** Wild type fractions collected from the hydroxyapatite column. **C.** Purified wild type enzyme after concentration on PEG 20000, 3 μg loaded. **D.** Mutant fractions collected from the Q-sepharose column. **E.** Mutant fractions collected from the hydroxyapatite column. **F.** Mutant fractions collected from the Cibacron-blue column. **G.** Lanes 1 and 5, crude extract of mutant enzyme; lanes 2 and 6, pooled mutant fractions 24-38 from Q-sepharose column; lanes 3 and 7, pooled mutant fractions 14-27 from hydroxyapatite column, lanes 4 and 8, pooled mutant fractions 11, 15, 16 and 17 from Cibacron-blue column. Total protein loaded in gel G was 5 μg for lanes 1 to 4 and 10 μg for lanes 5 to 8.

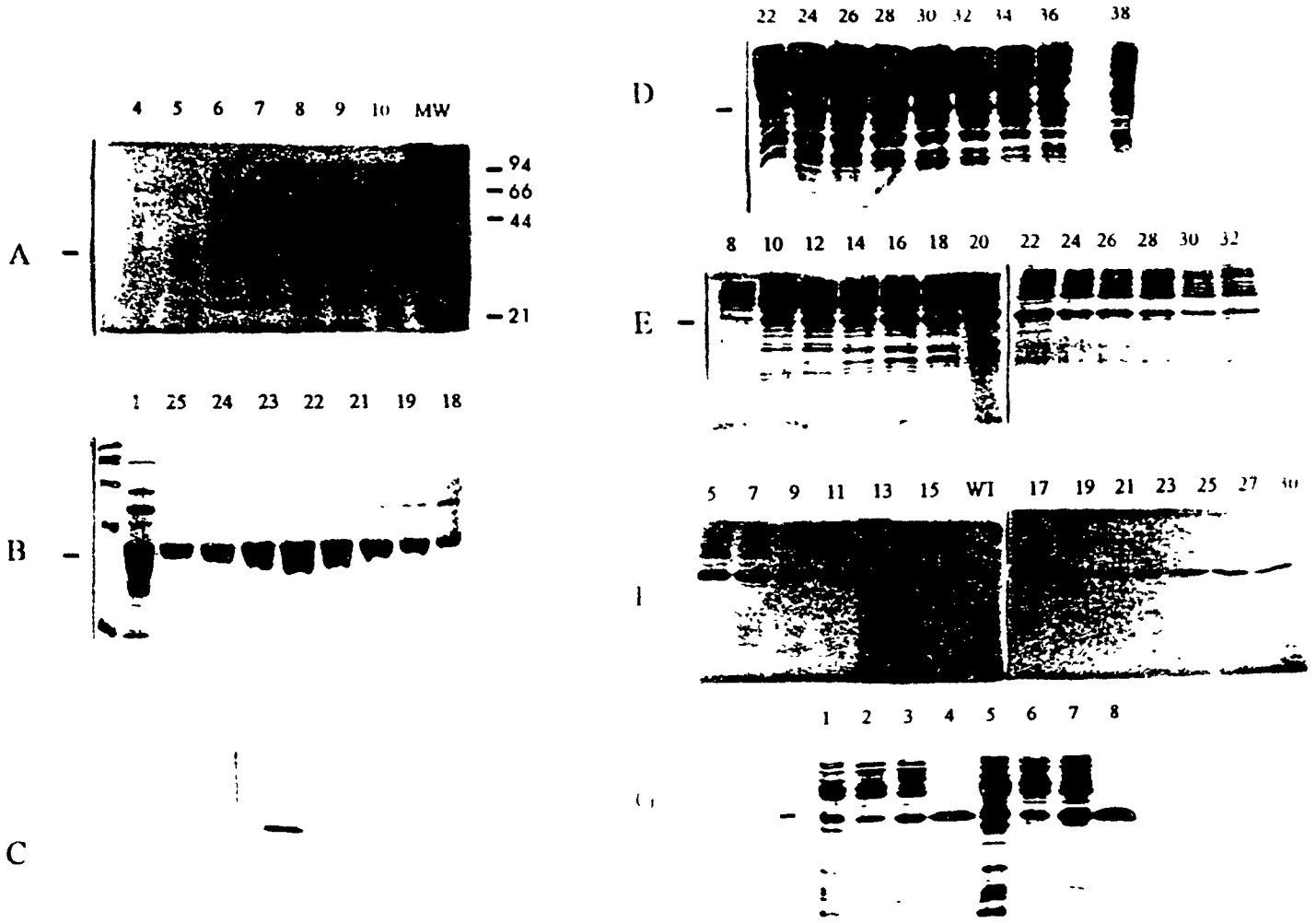
A
4 5 6 7 8 9 10 MW
94
66
44
21
B
1 25 24 23 22 21 19 18
C
D
22 24 26 28 30 32 34 36 38
E
8 10 12 14 16 18 20 22 24 26 28 30 32
5 7 9 11 13 15 WI 17 19 21 23 25 27 30
1 2 3 4 5 6 7 8

Kinetic Characterization of Mutant ΔEUK1 Using Purified Enzyme

Kinetic assays were carried out on both the wild type and mutant enzyme using a spectrophotometric method (Pogolotti *et al.*, 1986) which measures the appearance of dihydrofolate, the by-product of methylene-tetrahydrofolate in the synthesis of thymidylate. The use of this method together with purified enzymes, allowed a more accurate determination of the substrate K_m, and in addition, the cofactor K_m for both wild type and mutant enzymes. As with the radiochemical assay, significant differences were noted between the two enzymes, with the mutant having a 20-fold increase in K_m for substrate, a 10-fold increase in K_m for cofactor, and a 550-fold decrease in specific activity (Figures 22 and 23, Table X). Table X shows comparative values of these kinetic parameters published for yeast (Bisson and Thorner, 1981) , *E. coli* (Hardy and Nalivaika, 1992), *Lactobacillus casei* (Climie *et al.*, 1992), T4-Phage (LaPat-Polasko *et al.*, 1990), and human TS (Dev *et al.*, 1994).

TABLE VIII: MICHAELIS-MENTEN KINETICS FOR VARIABLE SUBSTRATE CONCENTRATIONS - SPECTROPHOTOMETRIC ASSAYS USING PURIFIED ENZYMES

	[dUMP] μM	Rate* Abs_{340}/min ($x10^3$)	Calculated ($x10^3$)
Wild type:	2.5	76	76
	3.75	93	88
	5	100	96
	10	96	109
	25	115	120
	50	127	124
	125	133	126
Mutant:	10	0.42	0.36
	25	0.81	0.67
	50	1.05	0.94
	75	0.99	1.09
	100	1.00	1.18
	150	1.12	1.29
	200	1.40	1.35
	250	1.49	1.39
	300	1.25	1.42
	500	1.57	1.48
	1000	1.55	1.52
	2000	1.66	1.55

*Rates are averages of several values - see Appendix E to G for raw data.

TABLE VIII
(Continued)

	Variable	Value	Standard Error
Wild type:	V_{max} [a]	128×10^{-3}	5×10^{-3}
	K_m [b]	1.71	0.35
Mutant:	V_{max} [a]	1.58×10^{-3}	0.07×10^{-3}
	K_m [b]	33.5	7.4

[a] Expressed as Abs_{340} per minute; see Appendix J for conversion to units of enzyme activity.
[b] Expressed as μM concentration.

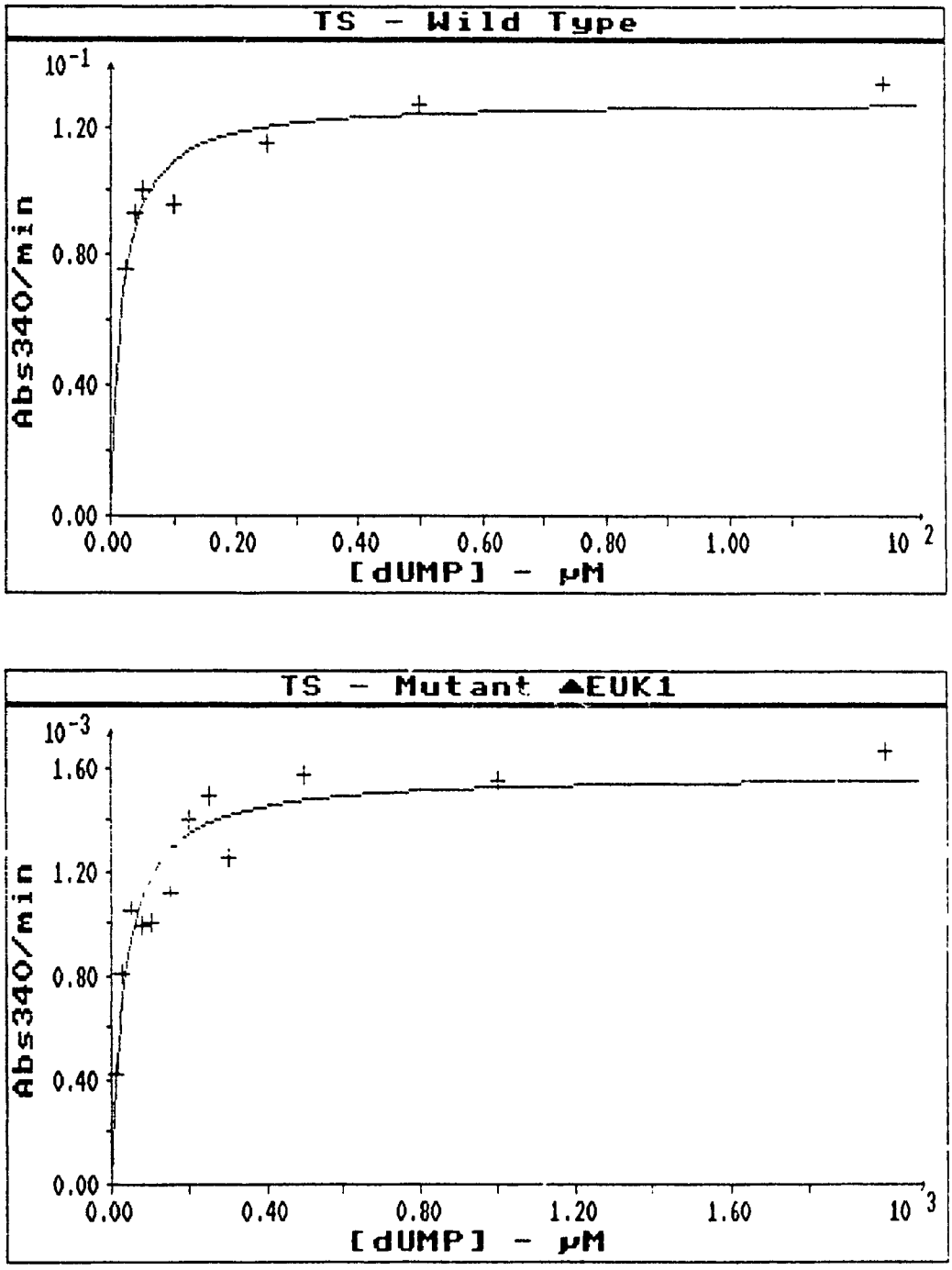

Figure 22. Michaelis-Menten plots for wild type and mutant ΔEUK1 thymidylate synthase using data from Table VIII.

TABLE IX: MICHAELIS-MENTEN KINETICS FOR VARIABLE COFACTOR CONCENTRATIONS - SPECTROPHOTOMETRIC ASSAYS USING PURIFIED ENZYMES

	[Folate] μM	Rate* Abs_{340}/min ($x10^3$)	Calculated ($x10^3$)
Wild type:	1.25	14	24
	2.5	35	41
	5	59	61
	7.5	76	74
	10	88	82
	15	97	93
	20	104	99
	50	116	113
	160	114	121
	200	118	122
Mutant:	10	0.15	0.19
	20	0.35	0.32
	30	0.42	0.42
	40	0.37	0.50
	50	0.61	0.56
	60	0.69	0.61
	80	0.73	0.69
	100	0.74	0.75
	160	0.79	0.85
	200	0.91	0.89

*Reported as average of 2 or 3 values in most cases; see Appendix G.

TABLE IX
(Continued)

	Variable	Value	Standard Error
Wild type:	V_{max} [a]	125 x 10^{-3}	4 x 10^{-3}
	K_m [b]	5.18	0.61
Mutant	V_{max} [a]	1.11x 10^{-3}	0.096 x 10^{-3}
	K_m [b]	49.1	10.9

[a] Expressed as Abs_{340} per minute; see Appendix J for conversion to units of enzyme activity.
[b] Expressed as μM concentration.

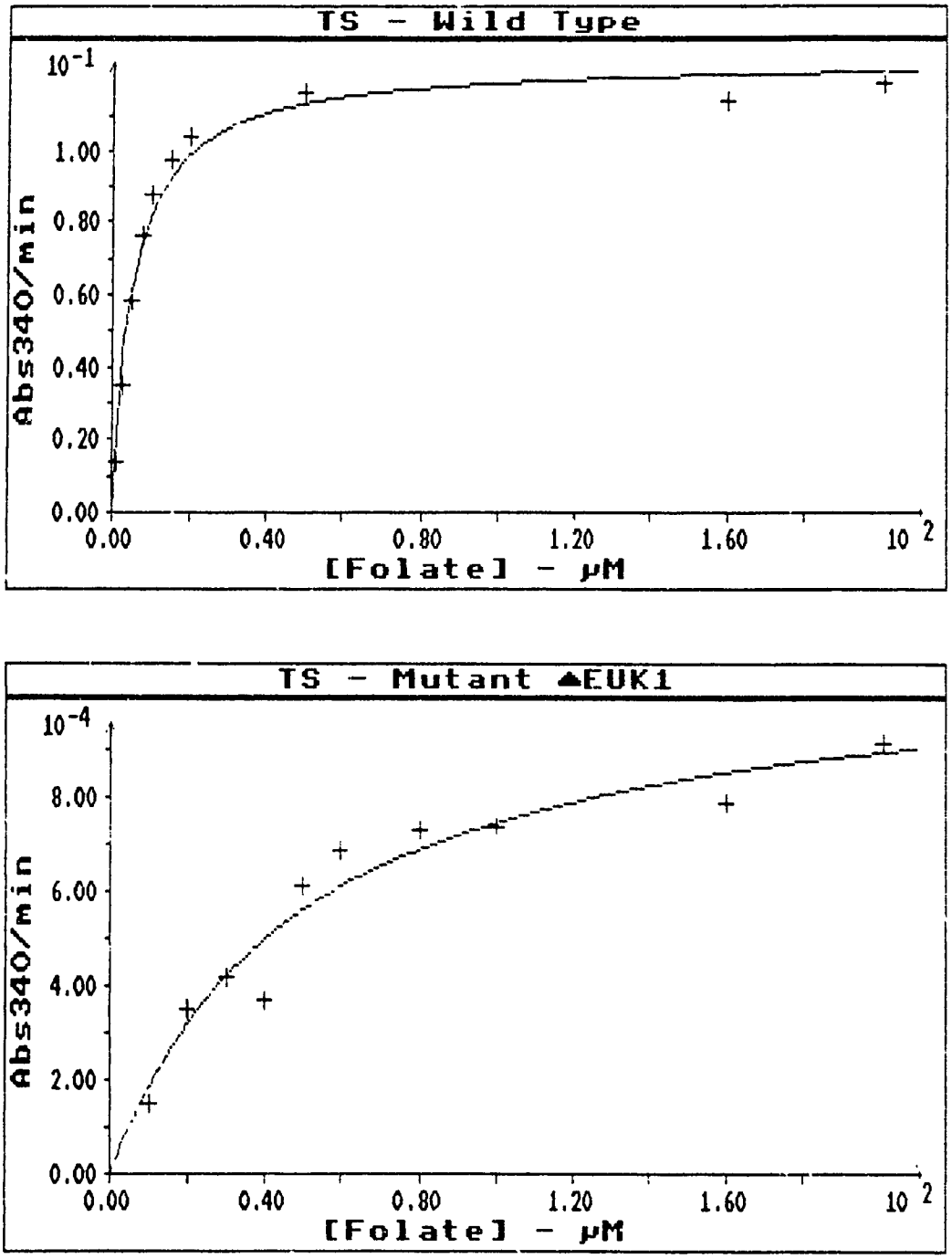

Figure 23. Michaelis-Menten plots for wild type and mutant ΔEUK1 thymidylate synthase using data from Table IX.

TABLE X: COMPARISON OF KINETIC PARAMETERS WITH OTHER PUBLISHED VALUES

	Specific Activity units/mg	K_m for dUMP µM	K_m for Folate µM
Wild type (this work)	1.48	1.71	5.18
Mutant ΔEUK1	0.0027	33.5	49.1
S.cerevisiae[a]	1.2	6	70
L.casei[b]	-	2.9	14
E.coli[c]	-	4.5	9.8
T4-Phage[d]	-	2.7	49.9
Human[e]	0.8-1.2	2.5	12

[a]Bisson and Thorner, 1981
[b]Climie *et al.*, 1992
[c]Hardy and Nalivaika, 1992
[d]LaPat-Polasko *et al.*, 1990
[e]Dev *et al.*, 1994

Section II: Mutants ΔEUK2a and ΔEUK2b

To probe the role of the peptide insert located at position 124 to 131 in yeast thymidylate synthase, the deletion mutants designated asΔEUK2a and ΔEUK2b were generated. Mutant ΔEUK2a harbors a full deletion of residues 124 to136, which encompasses the eukaryotic insert as well as the five residues immediately downstream. These were removed to eliminate a motif, Y-G-Q, found in several of the eukaryotic sequences. In addition, an aspartate replaces the histidine at position 121 (Table III, Figures 6 and 7). This substitution was made in order to generate a novel *Eco*RI restriction site that would permit convenient screening for mutants. The resulting mutant, ΔEUK2a, closely mimics the phage T4 enzyme in this region.

In mutant ΔEUK2b, the eukaryotic insert spanning residues 124 to 131 was removed, and residues 132 to 136 were replaced by the corresponding residues of *E.coli*, T-P-D-G-R.

Generation of Mutants ΔEUK2a and ΔEUK2b

Mutants ΔEUK2a and ΔEUK2b were constructed by the *in vitro* mutagenesis method of Kunkel *et al.*(1987). Single-stranded template DNA of phagemid pEM89 was obtained by infecting the *dut⁻ ung⁻* strain CJ236 (which incorporates uridylate into newly synthesized DNA), with helper phage M13K07 . Second-strand synthesis was carried out *in vitro*, using T4 DNA polymerase and a synthetic primer which encompassed the region to be deleted (Figure 15A). The double-stranded phagemid was then transformed into the *dut⁺ ung⁺* strain

XL1-Blue, in which the wild type uridylate-containing strand is selected against, thereby enriching for the mutagenized strand. Transformants containing the *TMP1-ΔEUK2a* gene were screened by *Eco*RI restriction analysis, since the histidine to aspartate codon substitution created a 5th *Eco*RI site on the phagemid. Of 48 colonies screened, 4 had the new 500 base pair *Eco*RI fragment, indicating a low mutational frequency (8%).

Mutant ΔEUK2b was generated in the same way, using the mutagenized *TMP1-ΔEUK2a* gene as template, to insert the *E.coli* sequence and restore histidine 121 (Figure 15B). Transformants containing the *TMP1-ΔEUK2b* gene were then screened by *Eco*RI restriction analysis since this new mutant would only have 4 *Eco*RI fragments as a result of the aspartate to histidine 121 substitution. Of 34 transformants tested, 7 lacked the 500 bp *Eco*RI fragment characteristic to ΔEUK2a DNA, but only 2 were confirmed by sequencing.

One sample each of ΔEUK2a and ΔEUK2b was sequenced in its entirety to ascertain that no mutations other than those designed were present on the gene.

Activity of ΔEUK2a and ΔEUK2b in *E. coli* and *S. cerevisiae*

Mutants ΔEUK2a and ΔEUK2b were transformed into thyA$^-$ *E.coli* strain 264 and Tmp$^-$ yeast strain 280. Since selection in yeast was done using the *TRP1* marker, and since strain 280 showed a high Trp$^+$ reversion frequency, a new strain having a disrupted *TRP1* gene, designated as 3236, was derived from strain 280 (see Materials & Methods).

Table XI shows that neither mutant was able to complement either *E.coli* or yeast. To determine whether inability to complement *E.coli* was due to low expression from the

pEMBL-derived constructs, the mutants were expressed in *E. coli* from high copy pUC-derived pEGRBS plasmids, which optimize expression by using the *lac Z* promoter and an *E.coli* ribosomal binding site. Only the wild type *TMP1* and mutant *TMP1-ΔEUK1* genes complemented *E.coli* with this vector. The mutant genes were also transformed into thyA$^+$ *E.coli* (DH5α) and Tmp$^+$ yeast (2379) to determine whether they had any effect on normal thymidylate synthesis. Both *E.coli* and yeast grew well without thymidylate supplement when harboring either mutant gene, therefore the mutations are not dominant. Figure 24 shows cell patches of the transformants listed in Table XI, on selection plates with and without thymidylate supplement.

Expression of ΔEUK2a and ΔEUK2b in *E.coli* and *S.cerevisiae*

To determine whether the mutant proteins were being expressed, immunoblot analyses were performed using both *E.coli* and yeast protein extracts. High levels of wild type thymidylate synthase, as well as all three mutant enzymes, were detected in *E.coli* extracts containing the pEGRBS vectors (Figure 25A). In yeast, high levels of wild type thymidylate synthase and TS-ΔEUK1 were detected, while TS-ΔEUK2a and TS-ΔEUK2b bands were barely discernible, although large amounts of breakdown product were observed in all extracts (Figure 25B).

TABLE XI: GROWTH OF *E.coli* AND *S.cerevisiae* STRAINS TRANSFORMED WITH *TMP1-ΔEUK2a* OR *TMP1-ΔEUK2b* GENES

Vector	*TMP1* gene	*E.coli* 264 ($thyA^-$)	Yeast 3236 (Tmp^-)	*E.coli* DH5α ($thyA^+$)	Yeast 2379 (Tmp^+)
pEM89	wild type	+++	+++	n/d[a]	+++
pEG89-E2a	*ΔEUK2a*	-	-	n/d	+++
pEG89-E2b	*ΔEUK2b*	-	-	n/d	+++
pNG22	none	n/d	-	n/d	n/d
YEp13	none	-	n/d	n/d	n/d
pEGRBS-WT	wild type	+++	n/a[b]	+++	n/a
pEGRBS-E1	*ΔEUK1*	+++	n/a	+++	n/a
pEGRBS-E2a	*ΔEUK2a*	-	n/a	+++	n/a
pEGRBS-E2b	*ΔEUK2b*	-	n/a	+++	n/a

[a] Not done
[b] Not applicable

Ability to complement was assessed by patching single colony transformants grown with thymidine (for *E.coli*) or thymidylate (for yeast) onto minimal media without these supplements (see Figure 24).

+++ Good healthy growth; thick, uniform patches
- No growth; absence of patches

Figure 24

A. Various transformants of *E.coli* strains 264 and DH5α on minimal media with ampicillin. Colonies grown on rich media with ampicillin and thymidine were picked and patched onto plates that lacked thymidine (1a, 2a, 3a) and then onto plates with thymidine (1b, 2b, 3b).

Top: Transformants of *E.coli* thyA⁻ strain 264
1. pEM89 (*E.coli*/yeast shuttle with wild type *TMP1*)
2. pEG89-E2a (same as 1. but with *TMP1-ΔEUK2a*)
3. pEG89-E2b (same as 1. but with *TMP1-ΔEUK2b*)
4. YEp13 (E.*coli*/yeast shuttle - no *TMP1* gene)

Middle: Transformants of *E.coli* thyA⁻ strain 264
1. pEGRBS-WT (*E.coli* high copy plasmid with wild type *TMP1*)
2. pEGRBS-E1 (same as 1. but with *TMP1-ΔEUK1*)
3. pEGRBS-E2a (same as 1. but with *TMP1-ΔEUK2a*)
4. pEGRBS-E2b (same as 1. but with *TMP2-ΔEUK2b*)
5. YEp13 (*E.coli*/yeast shuttle - no *TMP1* gene)

Bottom: Transformants of *E.coli* thyA⁺ strain DH5α
1. pEGRBS-WT (see above)
2. pEGRBS-E1
3. pEGRBS-E2a
4. pEGRBS-E2b

B. Various transformants of yeast strains 3236 and 2379 on selection media. Colonies grown on selection plates supplemented with thymidylate were patched onto plates without (1a, 2a) and with thymidylate (1b, 2b).

Top: Transformants of yeast Tmp⁻ strain 3236
1. pEM89 (see above)
2. pEG89-E2a
3. pEG89-E2b
4. pNG22 (E.coli/yeast shuttle - no *TMP1* gene)

Bottom: Transformants of yeast Tmp⁺ strain 2379
1. pEM89
2. pEG89-E2a
3. pEG89-E2b

A

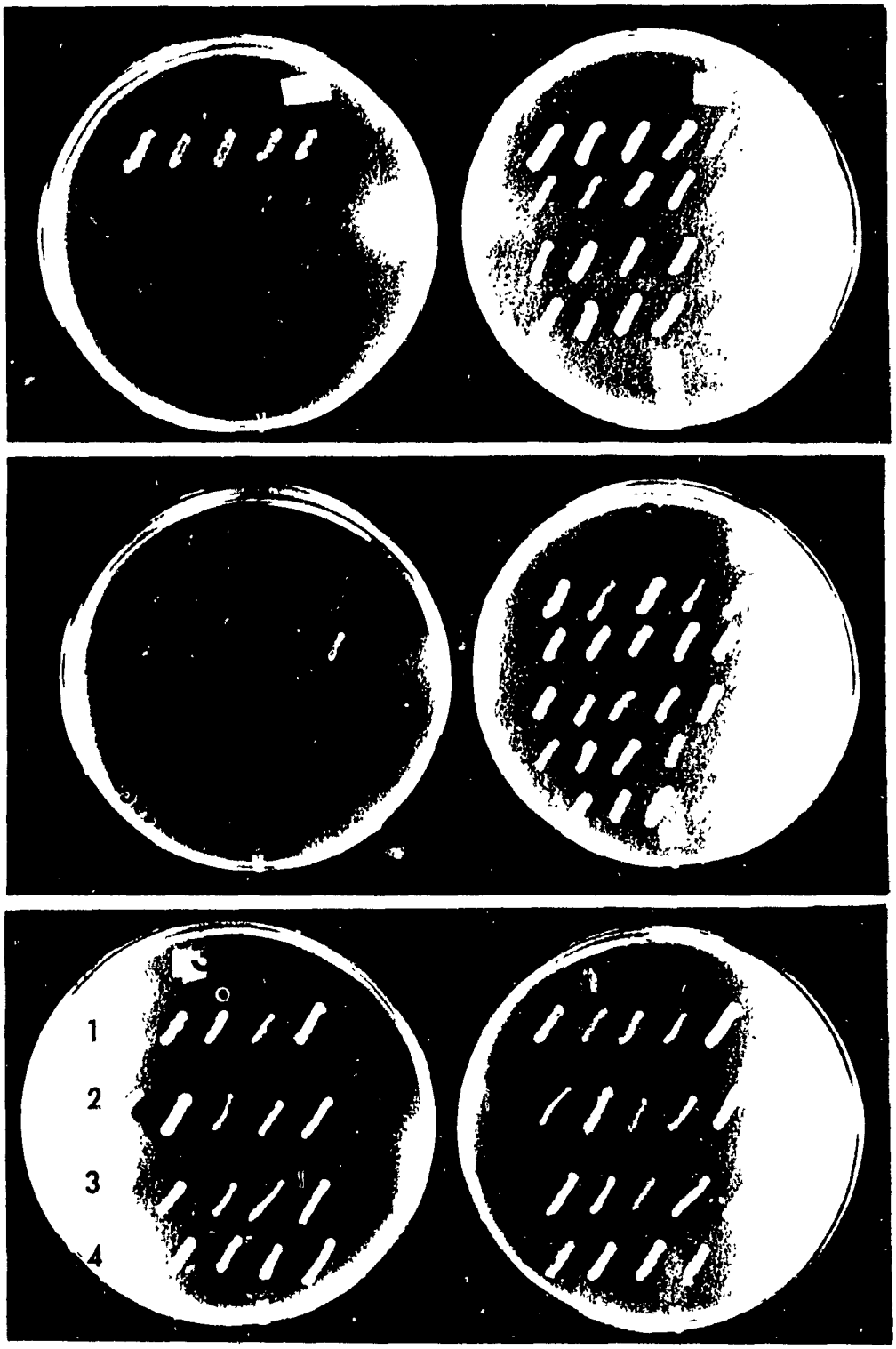

B

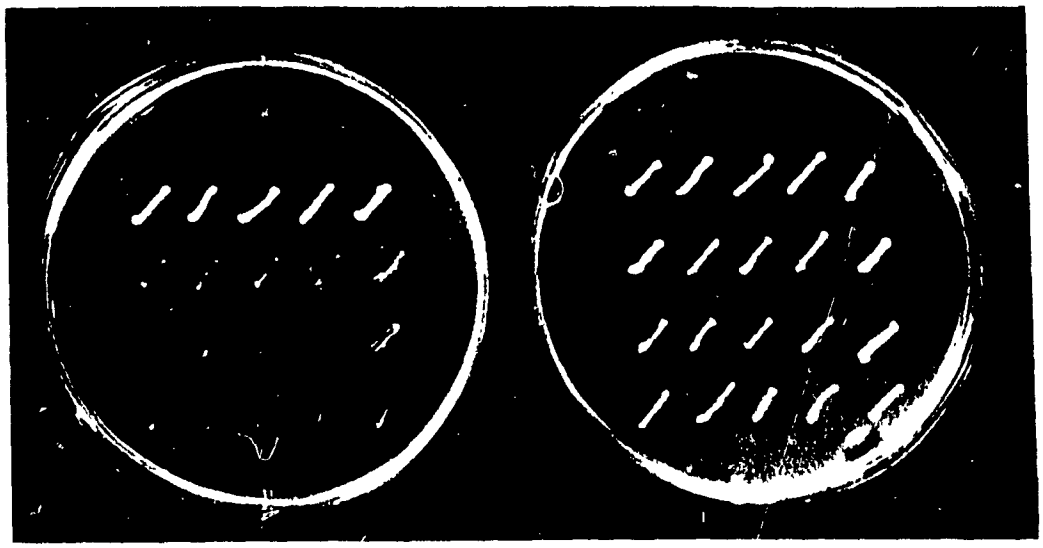

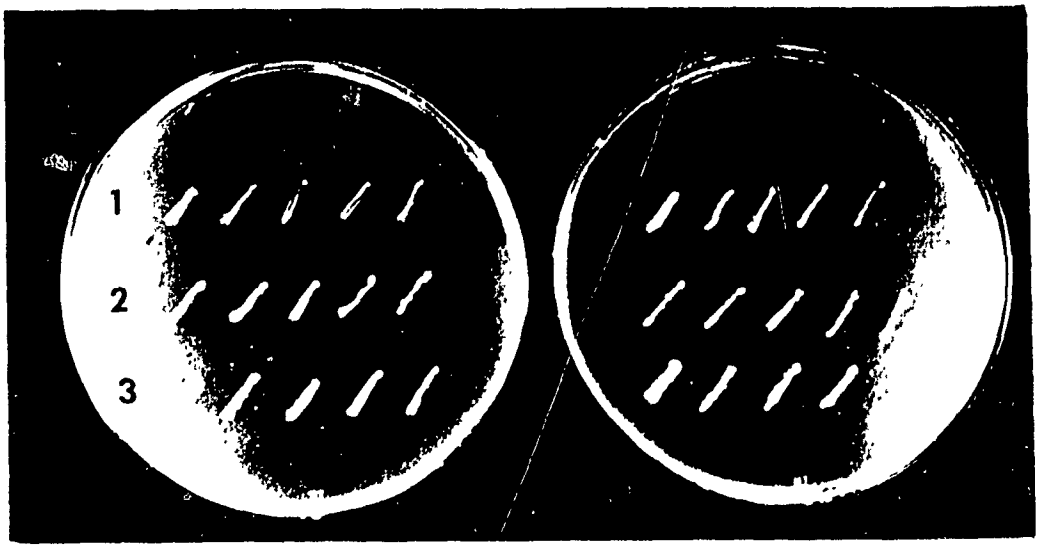

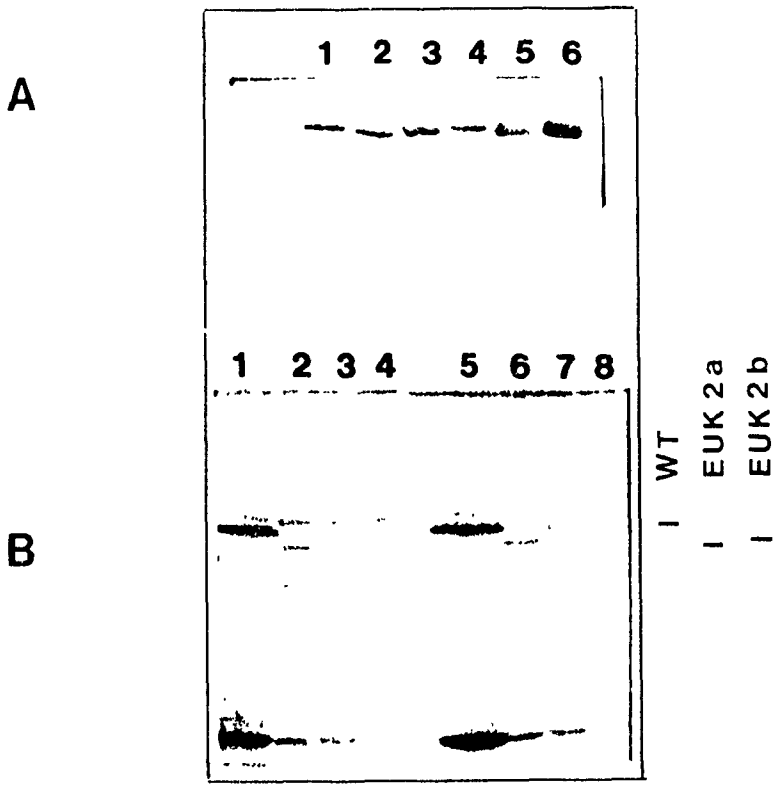

Figure 25. **A.** Immunoblot of wild type and mutant yeast thymidylate synthase. Lanes 5 and 6 are purified mutant ΔEUK1 and wild type enzymes respectively, 1.5 μg loaded for each. Lanes 1 to 4 are mutants ΔEUK2b, ΔEUK2a, ΔEUK1 and the wild type enzyme respectively, expressed from pEGRBS plasmids in *E. coli* strain 264. The amount of total protein loaded was 5 μg for each lane. **B.** Immunoblot of wild type TS (lanes 1 and 5), mutant ΔEUK2a (lanes 2 and 6) and ΔEUK2b (lanes 3 and 7), expressed from plasmids pEM89, pEG89-E2a and pEG89-E2b respectively in yeast strain 3236. Lanes 4 and 8 are extracts of cultures harboring plasmid pNG22, which has no *TMP1* gene. The total protein loaded was 17 μg for lanes 1 to 4, and 34 μg for lanes 5 to 8.

Activity of Mutants ΔEUK2a and ΔEUK2b as Detected by Radiochemical Assays

Although mutants ΔEUK2a and ΔEUK2b were unable to complement TS-deficient yeast or *E.coli* strains even when the genes were overexpressed, this did not preclude the possibility that some activity might be detectable by the sensitive tritium release method, as was the case for some *L.casei* mutants described by Schellenberger *et al.* (1994).

Radiochemical assays were performed on permeabilized whole cells of various cultures, essentially as described in Materials and Methods for mutant ΔEUK1. The results are shown in Table XII. Although some activity was detected for mutants ΔEUK2a and ΔEUK2b, the levels were minute and in the same range as the chromosomally encoded mutant, *tmp1-6*. The activity of ΔEUK2b was 3.4-fold higher than that of ΔEUK2a, but was still 100-fold lower than the chromosomally expresssed wild type level. Compared to the wild type enzyme expressed from the same plasmid, pEM89, the activities of ΔEUK2a and ΔEUK2b were reduced 1700-fold and 500-fold respectively.

Immunoblots of ΔEUK2a and ΔEUK2b cultures used for the assays (data not shown) indicated similar results as those in Figure 25. The protein bands of these two mutants were slightly fainter than the chromosomally expressed wild type protein loaded in the same amount. The wild type protein expressed from the same plasmid as ΔEUK2a and ΔEUK2b, pEM89, revealed a band that was at least ten times more intense than those of the mutants, even though only 5 μg total protein were loaded compared to 30 μg for the mutants.

TABLE XII: COMPARISON OF ACTIVITIES OF WILD TYPE AND MUTANT TS

TMP1 gene	Vector	Yeast Host Strain	Activity[a] pmol H^+/ min/10^9 cells	Relative Activity[b]
1. *tmp1-6*	chromosome	280	0.1	0.0012
2. *TMP1-ΔEUK2a*	pEG89-E2a	3236	0.2	0.0024
3. *TMP1-ΔEUK2b*	pEG89-E2b	3236	0.7	0.0082
4. *TMP1-ΔEUK1*	pEG13-E1	559	35	0.41
5. *TMP1-WT*	chromosome	HR125-5D	85	1
6. *TMP1-WT*	pEM54	559	854	10.04
7. *TMP1-WT*	pEM89	3236	336	3.95
8. *TMP1-WT*	pEM54	HR125-5D	643	7.96

[a] Activities were measured using the tritium release method and permeabilized whole cells. The first 5 samples were assayed over a time span of 105 minutes while the last 3 were assayed for 25 minutes. Five time points were used for all samples and were in the linear portion of the reaction. All assays were performed using 1400 μM THF (racemic mixture) and 100 μM dUMP, labeled at 45 dpm/picomole.

[b] Activities are calculated relative to sample 5, the chromosomally expressed wild type TS.

DISCUSSION

Section I: Mutant ΔEUK1

The region referred to as loop 1 in this work contains an insert of variable length in several of the thymidylate synthases sequenced so far. In the eukaryotes, this insert has a length of 12 residues. Although the sequence of the insert is variable, some residues are largely conserved; 6 of the 12 positions are occupied by no more than 2 different residues in all the eukaryotes (Figure 6). For example leucine 98 is absolutely conserved, glycine 102 and arginine 106 are conserved in 10 of the 12 eukaryotes, and position 97 is occupied by either tyrosine or its closest structural relative, phenylalanine. Among the six residues immediately upstream of the insert, a conserved motif, N-G-S-R, appears in most of the eukaryotes.

The only 3-dimensional structure of a eukaryotic thymidylate synthase published so far is that of the *L. major* bifunctional enzyme (Knighton *et al.*, 1994). This structure reveals that part of the eukaryotic insert forms a helix spanning residues 94 to 101 (yeast numbering), and that Phe97 (Tyr in yeast) interacts with the C-terminal valine in a ternary complex of the enzyme with F-dUMP and CB3717. No residues in the region that we denote as loop 1 have yet been shown to contribute to ligand binding or to catalysis. However, position 92 of the preceding helix, occupied by asparagine or tryptophan in 17 of 18 known sequences, interacts hydrophobically with the quinazoline ring of CB3717 in the *E.coli* complex (Matthews *et al.*, 1990a) and with the pterin ring of the cofactor in the *L.casei*

complex (Finer-Moore *et al.*, 1990).

To investigate the function of the eukaryotic insert, we constructed the mutant ΔEUK1, in which the entire yeast sequence from residues 91 to 108 is deleted, and the sequence E-W-A-D-E-N from *E.coli* is inserted. The deletion thus encompasses both the eukaryotic insert and the N-G-S-R motif.

Complementation of Mutant ΔEUK1 in *E. coli* and *S.cerevisiae*

The mutant allele *TMP1-ΔEUK1*, expressed from a variety of vectors, was tested for its ability to complement *E.coli* and *S.cerevisiae*, to determine whether the deletion had an effect on activity in either organism. Since all eukaryotes sequenced thus far have an insert at this position, while some prokaryotes (including *E.coli*) do not, we hypothesized that removal of the insert might have consequences in yeast that would not be observed in *E.coli*. The results however did not support this notion; complementation results were parallel in both organisms.

The mutant allele complemented *E.coli* only when expressed from a pUC-derived plasmid, pTL830-E1, and not when expressed from either the yeast episomal or centromeric plasmids (Figure 18A). This suggested that complementation of thy A⁻ *E.coli* required high levels of expression, since pUC plasmids are maintained in very high copy numbers in this host. It has been observed in our lab that expression levels of the *TMP1* gene can be affected by the orientation of the gene in certain plasmids, or by the nature of the sequences that flank the *TMP1* promoter. In this case however, the inability of the mutant allele to complement

E.coli when expressed from the yeast shuttle vectors was not related to the nature of the construct itself. This is demonstrated by the complementation obtained with the wild type gene on the same constructs. These results reflect a very significant difference between the wild type and mutant enzyme activities, which seems to be compensated for when the genes are expressed from the pUC plasmid, presumably due to increased levels of expression. This conclusion was corroborated by the complementation results in yeast. Cell growth was somewhat impaired when the mutant allele was expressed from the centromeric plasmid pEG50-E1, as compared to the episomal plasmid pEG13-E1 (Figure 18B). While the difference was not as dramatic as in *E.coli*, it did however suggest that higher levels of mutant enzyme are required to fully complement Tmp$^-$ yeast strains than what are normally expressed chromosomally.

Kinetic Characterization of Mutant ΔEUK1 Using Permeabilized Whole Yeast Cells

Since the complementation results clearly indicated that the mutant enzyme had reduced biological activity, the nature of the impairment, whether structural or functional, was investigated. For example, a functional impairment could result from the removal of a localization sequence, which would impede the enzyme's translocation to its proper destination within the cell, thus reducing its efficacy. Alternately, structural damage would reduce the enzyme's competence at synthesizing product.

We addressed the latter possibility by performing assays *in situ* with permeabilized whole cells, using the tritium-release assay. Preliminary experiments revealed a ten-fold

reduction in the enzymatic activity of the mutant as compared to the wild type (data not shown). However, since these assays were performed as end-point rather than time-course assays, we could not determine whether we were within linear ranges of the reactions for either the mutant or wild type enzyme, hence the comparison could not be considered to truly reflect the difference between the two enzymes. To obtain a more accurate assessment, time-course assays were performed, and enzyme rates were determined in the linear portions of the reactions. In addition, assays were done at various substrate concentrations in order to compare the V_{max} and K_m of the two enzymes. Both parameters were found to be significantly affected in the mutant enzyme, which exhibited a 20-fold increase in K_m and a 100-fold decrease in V_{max} (Table VI). This apparent decrease in mutant enzyme activity was not due to lower levels of enzyme being expressed in the cells. This was verified by immunoblot analysis of the cultures used for the assay, which showed equivalent densities for the mutant and wild type protein bands (Figure 20). The reduced activity of the mutant is thus not due to reduced expression.

These results suggested a probable structural perturbation in the dUMP binding site and the catalytic site. However, since the assays were done *in situ*, we could not rule out the involvement of other cellular components in contributing to these effects. For example, a higher K_m could reflect the mutant's inability to participate in a nucleotide channeling complex, possibly caused by the impairment of a signal for protein interaction or subcellular localization, rather than a disturbance at the binding site.

Purification of Wild Type and Mutant ΔEUK1 Enzymes

To resolve with certainty whether we had a structural mutant, the purification of both wild type and mutant enzyme was undertaken. The determination and comparison of steady-state kinetic parameters using purified enzymes eliminates unpredictable factors provided by the cellular environment, and is generally considered as a reliable indication of kinetic differences between mutant and wild type enzymes.

The enzymes were purified by column chromatography using a Q-sepharose anion exchanger followed by a hydroxyapatite affinity column. While the wild type enzyme emerged from the anion exchange column as an early peak between 70 and 140 mM KCl, prior to elution of the main protein peak, a significant shift was observed with the mutant, which co-eluted with the main protein peak between 300 and 500 mM KCl. This was not surprising, since the modification engineered into the mutant enzyme probably increases the net negative charge of the protein (discussed later), presumably resulting in tighter binding of the enzyme to the positively charged groups on the sepharose matrix. Since the hydroxyapatite column did not suffice to eliminate all the co-eluting contaminants, several other procedures were attempted, including FPLC, to no avail. Success was finally achieved with a Cibacron-blue affinity column, using the method described by Bisson and Thorner (1981). This particular dye has been shown by these authors to act as a competitive inhibitor of thymidylate synthase which can bind at both the substrate and the cofactor binding site. However, since the K_i for substrate is ca. 10-fold lower than for cofactor, it is difficult to elute TS from a Cibacron-blue column if binding has occurred via the dUMP binding site. For

this reason, it is necessary to saturate the dUMP site with substrate, to ensure that TS will bind to the dye via the cofactor binding site so that it can easily be eluted from the column. Initially, TS peaks were not retrieved from this column when using a 0.1 mM concentration of dUMP in the buffer as recommended by Bisson and Thorner. Since the radiochemical assays had indicated a possible decrease in substrate affinity for the mutant enzyme, dUMP concentration was increased to 4 mM, resulting in the emergence of a clean, albeit broad, TS peak from the Cibacron-blue column (Figure 21, panel F). This supported the earlier results suggesting that the mutant enzyme had undergone a structural deformation affecting the substrate binding site.

Kinetic Characterization of Mutant ΔEUK1 Using Purified Enzyme

Purified wild type and mutant enzymes were assayed spectrophotometrically to determine the K_m for substrate and cofactor. The mutant enzyme had a substrate K_m of 33.5 μM, compared to 1.7 μM for the wild type enzyme (Table VIII). This 20-fold increase reflects a similar difference as was observed with the *in situ* experiments, although the actual values are not in agreement. The higher values obtained *in situ*, 212 μM and 11.6 μM for mutant and wild type enzymes respectively, may be due to inadequate or delayed diffusion of the substrate into the permeabilized cells or cellular site of dTMP synthesis. Nonetheless, both sets of experiments imply that the substrate-binding site has been altered by the deletion of the EUK1 insert. Similarly, a 10-fold difference was observed in cofactor K_m between mutant (49.1 μM) and wild type enzyme (5.2 μM) (Table IX). This further substantiates that

the mutant enzyme has undergone an important structural perturbation affecting the active site.

The specific activity obtained for the mutant enzyme (0.0027 units/mg protein) was ca. 550 times less than that obtained for the wild type (1.48 units/mg protein) (Table X). This does not necessarily reflect, however, the actual difference in k_{cat} between the two enzymes, since the concentration of titratable active sites was not determined. It is quite conceivable that the mutant enzyme underwent more damage during the purification procedure due to the additional manipulations required by the extra purification step, or simply because it is instrinsically less stable hence more fragile than the wild type enzyme. Although this possibility has not been resolved, the *in situ* experiments corroborate the occurrence of a significant reduction in turnover rate in the mutant, since V_{max} was 100 times lower than for the wild type (88 versus 7420 pmol H^+/min/10^9 cells). In addition, radiochemical assays performed during various stages of the purification procedure always gave much higher specific activities for the wild type enzyme than for equivalent amounts of mutant enzyme (data not reported).

The steady-state kinetic parameters of the mutant ΔEUK1 and wild type enzymes were compared to other published values (Table X). The K_m value for dUMP for the wild type enzyme obtained in this work (1.7 μM) was lower than the value published by Bisson and Thorner (6 μM). This discrepancy may reflect a difference in assays or assay buffers since Bisson and Thorner obtained their data with the tritium-release method. Nonetheless, all reported values for substrate K_m are in the same range, 1.7 μM to 6 μM, which is significantly lower than the value obtained for mutant ΔEUK1, at 33.5 μM.

Our cofactor K_m value for the wild type enzyme (5.2 μM) was ca. 13-fold lower than the value obtained by Bisson and Thorner (70 μM), who report however, that assays using crude extract exhibited biphasic kinetics for cofactor binding, with values of 9 μM and 70 μM. Their explanation for this discrepancy is that they used a monoglutamylated form of folate for their experiments, which has a lower affinity for TS than polyglutamylated folates, and which may have been converted in part to polyglutamylated forms in the crude extracts, hence giving rise to biphasic kinetic results. Furthermore, they report unpublished data where they used pentaglutamylated folate with purified enzyme and obtained a K_m value of 7μM, which is very close to our result. This does not resolve the discrepancy with our results however, since we also used monoglutamylated folate.

Our cofactor K_m value for the mutant (49.1 μM) was again significantly higher than that obtained for the wild type enzyme, or those published for other enzymes, with the exception of T4-phage which is reported at 49.9 μM. It is interesting that the T4-phage enzyme has such as high cofactor K_m, since it is also known to participate in multi-enzyme complexes, a fact which could conceivably compensate for the decreased affinity by increasing the effective folate concentration in the vicinity of the enzyme. The EUK1 deletion does not alter the yeast enzyme in such a way as to mimic the corresponding region of T4-TS, but it does however result in changing the net charge in that region from +3 to -3 (sequence shown in Figure 6), which is close to the charge of -2 for T4-TS. Specifically, in T4-TS this sequence (residues 91-105, yeast numbering) contains 3 acidic side chains (E, E, D) and 1 basic side chain (K), while the mutant harbors 3 acidic residues (E, D, E) and no basic residues, compared to the yeast wild type TS which has 2 acidic groups (E, D) and 5

basic side chains (R, K, K, R, K). Although this region is not part of the main folate-binding loop, the net increase in acidic side chains perhaps has a peripheral repelling effect on the negatively charged glutamates of the cofactor. The fact that *E.coli*-TS, which also carries a net charge of -3 in this region, has a significantly lower cofactor K_m (9.8 μM) than does T4-TS, would then necessarily be attributed to covariances elsewhere in the protein that would offset the effect of the negative charge on folate binding.

Schellenberger *et al.* (1994) have recently reported a similar deletion of the large insert (residues 90-139, *L.casei* numbering) in the thymidylate synthase of *L. casei*. In contrast to our yeast mutant ΔEUK1, the *L. casei* mutant was unable to complement a TS-deficient *E. coli* strain, and showed no detectable activity using either the spectrophotometric or tritium release assays. Variations of the mutant harboring in addition to the deletion, *E.coli*-like substitutions in the adjacent sequences, revealed that the replacement by an aspartate of one residue in particular, phenylalanine 87, partially restored activity. Thus the exposure of this normally buried phenylalanine had a drastic effect on the function of the *L. casei* enzyme. The dysfunction of our mutant, however, cannot be attributed to a similar reason, since position 87 (94, yeast numbering) has been replaced, perhaps fortuitously, by an aspartate as part of our attempt to mimic this portion of the *E.coli* enzyme. On the other hand, the wild type yeast enzyme is already rich in hydrophilic residues in this region, and the substitution of an *E.coli* sequence was perhaps an unnecessary precaution.

The active *L.casei* mutants of Schellenberger and coworkers were still unable to complement *E.coli*, but low levels of activity were detectable with the radiochemical assay, enabling the determination of kinetic parameters. In contrast to our results, these showed that

that the deletion affected cofactor binding to a greater extent than dUMP binding, with K_m increased 34-fold and 6-fold respectively in their most active mutant. While k_{cat} was also significantly reduced, dehalogenation assays, which measure the thiol-dependent conversion of halogenated substrate analogs to dUMP in the absence of cofactor (Garrett *et al.*, 1979), and are considered analogous to the first step of the TS reaction, showed less difference between the mutant and wild type enzymes. The results of Schellenberger and coworkers, taken together with ours, seem to indicate that the loop 1 inserts in various thymidylate synthases could have species-specific structural functions that complement variations elsewhere in the respective proteins.

Conclusions - Mutant ΔEUK1

Our results suggest that the amino acid sequence spanning residues 91 to 108 in yeast TS is an important structural feature of the enzyme. Although it is not directly implicated in the formation of the catalytic or substrate binding sites, its presence apparently makes a significant contribution to the enzyme's affinity for ligands and its turnover rate.

It is surprising that mutant ΔEUK1, whose enzymatic activity is so greatly impaired, is able to complement a TS-deficient yeast strain even when expressed from a single-copy plasmid; particularly since an *L.casei* mutant with a 27-fold reduction in k_{cat} does not complement *E.coli* when expressed from a high copy pUC vector (similar to our pEGRBS plasmids shown in Figure 13). This suggests that if the deleted sequence does have a secondary role in the yeast cell, such a role is probably non-essential; for example, it is

unlikely that an enzyme with drastically reduced synthesis efficiency could satisfy cellular requirements for dTMP, if in addition it is incapable of reaching its normal cellular destination, as would ensue from the removal of a localization signal.

As mentioned earlier, thymidylate synthase from phage T4 is known to form a multienzyme complex with other viral and host proteins involved in nucleotide synthesis (Mathews *et al.*, 1988). Whether or not this phenomenon occurs in eukaryotes is still a subject of controversy, since evidence both supporting and contradicting this notion has been reported. Our complementation results do not appear to support the existence of a nucleotide channeling complex in yeast, since the impaired ability to complement TS-deficiency observed in the ΔEUK1 allele encoded on a single-copy plasmid, was overcome by increasing the gene dosage. If yeast TS were stochiometrically involved in a multi-enzyme complex it would seem that excess TS molecules would be excluded from the nucleotide-synthesis agglomerates, and hence would be unable to contribute to the rate of dTMP synthesis.

Section II: Mutants ΔEUK2a and ΔEUK2b

The surface loop referred to in this work as loop 2, which harbors the eukaryotic insert spanning residues 124 to 131, exists in all thymidylate synthases sequenced so far, but varies in size from 5 residues (in phage T4) to 18 residues (in all the eukaryotes sequenced to date). The 3-dimensional structures of TS show that the almost absolutely conserved arginine 120 and aspartate 139 form a salt bridge which circularizes the loop, and which, perhaps more importantly, may help align the flanking helices along a common longitudinal axis (Hardy *et al.*, 1987; Matthews *et al.*, 1990a).

To address the possible role of this insert, we generated two deletion mutants. In mutant ΔEUK2a, the loop has been reduced from its largest naturally occurring form (18 amino acids) to its smallest (5 amino acids) by the removal of residues 124 to 136. Furthermore, histidine 121 has been replaced by an aspartate. In mutant ΔEUK2b histidine 121 is unaltered, and the decrease in size is less drastic (10 amino acids) since the *E.coli* sequence T-P-D-G-R has been substituted for the yeast sequence 124-136.

Activity of Mutants ΔEUK2a and ΔEUK2b in *E.coli* and *S.cerevisiae*

Since ΔEUK2a failed to show any biological activity in the complementation assays, we conjectured that the drastic decrease in the size of the loop might present packing problems that would have a bearing on the alignment of the adjacent helices, which would in turn destabilize the overall structure. Alternately or conjointly, the introduction of an

aspartate at position 121 could interfere with the formation of the salt linkage between arginine 120 and aspartate 139. It remained perplexing however, that the diminished loop and asparate substitution would create such havoc in the yeast enzyme while being tolerated in T4-TS. One possible reason is that a loop of 5 residues or less, more properly defined as a turn, usually accomodates side chains by projecting them to the outside, since the main chain is too short to circumscribe them (Leszczynski and Rose, 1986). Perhaps this situation, while normal for T4-TS, is impractical in the context of the yeast enzyme, either for steric reasons or because the T4 version of the loop is mostly hydrophobic. In T4-TS, this loop has been implicated in the formation of an interaction surface for other proteins that participate in a multi-enzyme nucleotide synthesis complex (Finer-Moore *et al.*, 1994), which would presumably result in burying these hydrophobic residues. Perhaps in the yeast enzyme they are exposed to solvent, creating an energetically unfavorable situation.

We attempted to rectify this problem by creating mutant ΔEUK2b, in which the loop was increased to 10 residues by the introduction of the *E.coli* sequence T-D-G-P-R, and in which histidine 121 was restored. Surprisingly, these modifications did not restore sufficient activity to the enzyme to enable complementation of TS-deficient yeast or *E.coli* strains.

To determine whether the ΔEUK2a and ΔEUK2b mutations are dominant, plasmids harboring these mutant alleles were transformed into yeast and *E.coli* strains with genomically encoded wild type thymidylate synthase. Growth of *E.coli* strain DH5α was unimpeded by the presumably elevated numbers of inactive mutant enzyme molecules present in the cells. This was surprising since mutant protein molecules were expected to greatly outnumber the *E.coli* wild type enzyme, a fact which could conceivably lead to competition

for the substrates and/or formation of heterodimers with impaired activity relative to wild type homodimers. That this was not the case may be an indication that these mutants have a poor affinity for the substrates, and that either they are unable to form heterodimers with the *E.coli* enzyme, or, the mutant moiety of such heterodimers in no way interferes with the function of the wild type subunit. Similarly, ΔEUK2a and ΔEUK2b did not seem to hinder the growth of a yeast strain with chromosomally expressed wild type TS. This was somewhat anticipated, since our results so far seem to indicate that yeast cells do not maintain high levels of these mutant proteins (see below).

Expression of Mutants ΔEUK2a and ΔEUK2b in *E.coli* and *S.cerevisiae*

We considered the possibility that the inactivity of mutants ΔEUK2a and ΔEUK2b was due to low protein levels, which could be the consequence of inefficient transcription or translation and/or unstable transcripts or protein. This was investigated by immunoblot analysis of the wild type and mutant proteins expressed in yeast under similar conditions. The results indicated that the mutant protein bands were much lower in intensity than the wild type band (Figure 25B). In contrast to this, when expressed in *E.coli* using the high expression pEGRBS vectors, the ΔEUK2a and ΔEUK2b proteins gave signals that were as strong as those of the wild type and mutant ΔEUK1 proteins (Figure 25A).

We have not resolved the cause of the reduced levels of mutant protein bands in the yeast extracts. The smaller molecular weight species appearing in all lanes are presumably breakdown products of TS, but we have not determined whether this degradation occurs *in*

vivo or whether it is an artifact of the protein extraction procedure. The total amount of intact TS and breakdown product is much higher for the wild type than for the mutants, a fact which may reflect decreased levels of transcription, unstable transcripts, or inefficient translation for the mutants. This question can only be satisfactorily resolved by future Northern blot analysis. Although decreased *in vivo* levels of mutant TS could be a contributing factor to the lack of complementation ability, other immunoblots (data not shown) have revealed that mutant enzyme levels are approximately equivalent to genomic wild type levels, hence reduced expression alone cannot account for the loss of activity. Moreover, overexpression of ΔEUK2a and ΔEUK2b in *E.coli* led to mutant protein levels that were comparable to those of the wild type and ΔEUK1 proteins, but the inability to rescue TS-deficient *E.coli* strain 264 persisted.

Activity of ΔEUK2a and ΔEUK2b as Determined by Radiochemical Assays

Since the complementation assay failed to detect any activity in mutant ΔEUK2a and ΔEUK2b, the more sensitive tritium release assay was used to further test these two mutants. The results, shown in Table XII, demonstrate that ΔEUK2a and ΔEUK2b may have 500-fold and 125-fold reduced activities respectively, compared to wild type TS expressed at approximately the same level. However, we do not know whether the immunoblots truly reflect the amounts of mutant enzyme within the cells, or if the mutants are more susceptible to *in vitro* degradation incurred by the protein extraction procedure. Therefore, relative activities of the mutant enzymes could actually be less than 0.2% and 0.8% of the

chromosomally expressed wild type.

Comparing the activities of these two mutants to the wild type enzyme expressed from the same parent plasmid in the same yeast strain is an impractical undertaking for the following reasons. We cannot properly estimate the relative amounts of the mutant and wild type enzymes in the cells for this set of experiments, since we cannot gauge whether the extent of *in vitro* degradation is equivalent for all three enzymes. Furthermore, it is difficult to accurately assess the relative thymidylate synthase levels on the immunoblot due to the vast difference in band intensities (Figure 25B) between the mutant and wild type proteins. Finally, the activities for the highly expressed wild type enzymes reported in Table XII are probably less than the actual values by 5 or 10-fold. This conclusion is based on the fact that earlier results which were repeated several times (see Table VI) indicated an activity of ca. 6000 pmol H^+/min/10^9 cells, for strain 559 transformed with pEM54, using the same conditions as for the assays reported in Table XII. While the activity of pEM54 transformants is ca. 7-fold lower in Table XII than in Table VI, the activity of pEG13-E1 transformants is comparable in both tables (35 versus 30 pmol H^+/min/10^9cells at 100 μM dUMP). Failure to achieve maximal rate when using highly expressed wild type enzyme is a problem that has occurred from time to time and may be attributed to oxidation of the highly unstable cofactor, which then becomes limiting in a system where thymidylate synthase activity is high. This does not seem to affect the rate of the slower mutant enzyme ΔEUK1 however, hence the slower rates reported in Table XII (samples 1 to 5) are probably valid. A more accurate and reliable evaluation of the activities of mutants ΔEUK2a and ΔEUK2b will require the purification of these enzymes and should eliminate most of the problems encountered using whole cells or

crude protein extracts.

Structure of Loop 2 in Other Organisms

The nature of the inactivation of the yeast enzyme by the alterations described for mutants ΔEUK2a and ΔEUK2b remains unclear. As discussed earlier, the loop in question occurs in variable lengths and composition in the thymidylate synthases of different species. This variability may reflect the fact that the loop is precisely tailored to fulfill a species-specific role. In support of this, the 3-dimensional structures for the *E.coli*, *L. major* and T4 enzymes reveal structural differences in the region of the loop, although in all cases, it appears as a surface protruberance located at the dimer interface. In *E.coli* it is projected toward its counterpart on the opposite subunit, such that the sister loops are intimately associated, with proline 104 and proline 104' placed adjacent to each other (Matthews *et al.*, 1990a). In contrast to this, the *L. major* loop, which is 8 residues longer than the *E.coli* version, is oriented away from its partner and interacts with the N-terminal of the dihydrofolate reductase domain of the bifunctional enzyme (Knighton *et al.*, 1994). In T4-TS, the diminution of the loop, together with strategically placed inserts elsewhere in the protein, may provide a somewhat flatter surface on that face of the enzyme, thus facilitating interaction with other proteins involved in the multi-enzyme complex (Finer-Moore *et al.*, 1994). The occurrence of such a diversity of conformations for this structural feature of TS makes it difficult to predict its structure in the yeast wild type enzyme or the ΔEUK2a and ΔEUK2b mutants. Although yeast is more closely related to *L. major* than to the bacterial

species, its thymidylate synthase lacks a dihydrofolate reductase domain and it would therefore seem unnecessary for the extended loop to fold back on itself if the sole purpose of this were to allow interaction with DHFR. This singular orientation of the insert may however serve another function in yeast TS, analogous to that described by Knighton *et al.* for the *L. major* enzyme. These authors report that the conformation of the loop is stabilized by burying the aromatic side chains of 3 residues that are conserved in the eukaryotic sequences, Phe117, Tyr126, and Tyr133 (yeast numbering). While Tyr126 and 133 have been deleted in ΔEUK2a and ΔEUK2b, Phe117 is still present and possibly exposed in the abridged versions of the loop. The fact that this residue is replaced by hydrophilic amino acids (Lys or Ser) in the prokaryotes lends support to the notion that exposing Phe117 to solvent may be the reason for the inactivation of the mutants. Furthermore, as was discussed earlier Schellenberger *et al.* (1994) have reported a deletion mutant of *L.casei* TS whose activity was partially restored simply by substituting an aspartate for phenylalanine 87, which is normally buried in the wild type enzyme.

Conclusions - ΔEUK2a and ΔEUK2b

The modifications which we have engineered into loop 2 of yeast thymidylate synthase abolish the mutant genes' ability to complement TS-deficiency by dramatically decreasing the rate of dTMP synthesis of the enzyme.

The elucidation of the mechanism by which the enzyme is so severely impaired remains a challenging problem. We have yet to address such questions as enzyme stability,

dimerization, catalytic site and ligand binding site integrity, and even localization for these mutants. Resolving this enigma should begin with the generation of 2 new derivatives of ΔEUK2a and ΔEUK2b in which Phe117 would be replaced by a hydrophilic residue, in an attempt to increase the activities of these mutants. Purification of the 4 mutants should then enable a more detailed and accurate characterization of enzyme activity using either the radiochemical or spectrophotometric method, as well as assessment of dimer formation and enzyme stability.

LITERATURE CITED

Alani, E., L. Cao, and N. Kleckner. 1987. A method for gene disruption that allows repeated use of *URA3* selection in the construction of multiply disrupted yeast strains. Genetics **116**: 541-545.

Ausubel, F., R. Brent, R. Kingston, D. Moore, J. Seidman, and K. Struhl. 1989 Harvard Medical School: Current Protocols in Molecular Biology, John Wiley & Sons, N.Y.

Aull, J.I., R.B. Loeble, and R.B. Dunlap. 1974. The carboxypeptidase-dependent inactivation of thymidylate synthetase. J. Biol. Chem. **249**: 1167-1172.

Baldari, C., and G. Cesareni. 1985. Plasmids pEMBLY: new single-stranded shuttle vectors for the recovery and analysis of yeast DNA sequences. Gene **35**: 27-32.

Belfort, M., G. Maley, J. Pedersen-Lane, and F. Maley. 1983. Primary structure of the *Escherichia coli thyA* gene and its thymidylate synthase product. Proc. Natl. Acad.Sci. USA **80**: 4914-4918.

Belfort, M., and J. Pedersen-Lane. 1984. Genetic system for analyzing *Escherichia coli* thymidylate synthase. J. Bacteriol. **160**: 371-378.

Bellisario, R.L., G.F. Maley, D.U. Guarino, and F. Maley. 1979. The primary structure of *Lactobacillus casei* thymidylate synthetase: II . The complete amino acid sequence of the active site peptide, CNBr4. J. Biol.Chem. **254**: 1296-1300.

Beverley, S.M., T.E. Ellenberger, and J.S. Cordingley. 1986. Primary structure of the gene encoding the bifunctional dihydrofolate reductase-thymidylate synthase of *Leishmania major*. Proc. Natl. Acad. Sci. USA **83**: 2584-2588.

Bisson, L.F., and J. Thorner. 1977. Thymidine 5'-monophosphate-requiring mutants of *Saccharomyces cerevisiae* are deficient in thymidylate synthetase. J. Bact. **132**: 44-50.

Bisson, L.F., and J. Thorner. 1981. Thymidylate synthetase from *Saccharomyces cerevisiae*. J. Biol. Chem. **256**: 12456-12462.

Boeke, J., F. Lacroute, and G. Fink. 1984. A positive selection for mutants lacking orotidine-5'-phosphate decarboxylase activity in yeast: 5-fluoro-orotic acid resistance. Mol. Gen. Genet. **197**: 345-346.

Bradford, M.M. 1976. A rapid and sensitive method for the quantitation of microgram quantities of protein utilizing the principle of protein-dye binding. Anal. Biochem. **72**: 248-254.

Bradshaw, T.P., and R.B. Dunlap. 1993. Characterization of a novel form of thymidylate synthase: a heterodimer isolated after specific chemical modification of the immobilized native enzyme. Biochem. **32**: 12774-12781.

Broach,J.R., J.N. Strathern, and J.B. Hicks. 1979. Transformation in yeast: development of a hybrid cloning vector and isolation of the *CAN1* gene. Gene **8**: 121-133.

Bullock, W.O., J.M. Fernandez, and J.M. Short. 1987. XL1-Blue: a high efficiency plasmid transforming *recA Escherichia coli* strain with beta-galactosidase selection. BioTechniques **5**: 376-381.

Bures, A.K., H.H. Daron, and J.L. Aull. 1991. Inhibition of thymidylate synthase by glyceraldehyde 3-phosphate. Int. J. Biochem. **23**: 733-736.

Bzik, D.J., W. Li, T. Horii, and J. Inselburg. 1987. Molecular cloning and sequence analysis of the *Plasmodium falciparum* dihydrofolate reductase-thymidylate synthase gene. Proc. Natl. Acad. Sci. USA **84**: 8360-8364.

Casadaban, M., A. Martinez-Arias, S.K. Shapira, and J. Chou. 1983. β-Galactosidase gene fusions for analyzing gene expression in *Escherichia coli* and yeast. Methods in Enzymol. **100**: 293-308.

Carreras, C.W., S. Climie, and D.V. Santi. 1992. Thymidylate synthase with a C-terminal deletion catalyzes partial reactions but is unable to catalyze thymidylate formation. Biochem. **31**: 6038-6044.

Carreras, C.W., P.M. Costi, and D.V. Santi. 1994. Heterodimeric thymidylate synthases with C-terminal deletion on one subunit. J. Biol. Chem. **269**: 12444-12446.

Cella, R., D. Carbonera, R. Orsi, G. Ferri, and P. Iadarola. 1991. Proteolytic and partial sequencing studies of the bifunctional dihydrofolate reductase-thymidylate synthase from *Daucus carota*. Plant Mol. Biol. **16**: 975-982.

Chu, E., D.M. Koeller, J.L. Casey, J.C. Drake, B.A. Chabner, P.C. Elwood, S. Zinn, and C. Allegra. 1991. Autoregulation of human thymidylate synthase messenger RNA translation by thymidylate synthase. Proc. Natl. Acad. Sci. USA **88**: 8977-8981.

Chu, F.K., G.F. Maley, F. Maley, and M. Belfort. 1984. Intervening sequence in the thymidylate synthase gene of bacteriophage T4. Proc. Natl.Acad. Sci. USA **81**: 3049-3053.

Climie, S., and D.V. Santi. 1990a. Chemical synthesis of the thymidylate synthase gene. Proc. Natl. Acad. Sci. USA **87**: 633-637.

Climie, S., L. Ruiz-Perez, D. Gonzalez-Pacanowska, P. Prapunwattana, S.W. Cho, R. Stroud, and D.V. Santi. 1990b. Saturation site-directed mutagenesis of thymidylate synthase. J. Biol. Chem. **265**: 18776-18779.

Climie, S., C.W. Carreras, and D.V. Santi. 1992. Complete replacement set of amino acids at the C-terminus of thymidylate synthase: Quantitative structure-activity relationship of mutants of an enzyme. Biochem. **31**: 6032-6038.

Danenberg, K.D., and P.V. Danenberg. 1979. Evidence for a sequential interaction of the subunits of thymidylate synthetase. J.Biol. Chem. **254**: 4345-4348.

Danenberg, P.V., and K.D. Danenberg. 1978. Effect of 5,10-methylene-tetrahydrofolate on the dissociation of 5-fluoro-2'-deoxyuridylate from thymidylate synthetase: evidence for an ordered mechanism. Biochem. **17**: 4018-4024.

Dente, L., G. Cesareni, and R. Cortese. 1983. pEMBL: a new family of single-stranded plasmids. Nucl. Acids Res. **11**: 1645-1655.

Dev, I.K., B.B. Yates, J. Leong, and W.S. Dallas. 1988. Functional role of cysteine-146 in *Escherichia coli* thymidylate synthase. Proc. Natl. Acad. Sci. USA **85**: 1472-1476.

Dev, I.K., W.S. Dallas, R. Ferone, M. Hanlon, D.D. McKee, and B.B. Yates. 1994. Mode of binding of folate analogs to thymidylate synthase. J. Biol. Chem. **269**: 1873-1882.

Edman, U., J.C. Edman, B. Lundgren, and D.V. Santi. 1989. Isolation and expression of the *Pneumocystis carinii* thymidylate synthase gene. Proc. Natl. Acad.Sci. USA **86**: 6503-6507.

Fauman, E.B., E.E. Rutenber, G.F. Maley, F. Maley, and R.M. Stroud. 1994. Water-mediated substrate/product discrimination: the product complex of thymidylate synthase at 1.83Å. Biochem. **33**: 1502-1511.

Finer-Moore, J.S., W.R. Montfort, and R.M. Stroud. 1990. Pairwise specificity and sequential binding in enzyme catalysis: thymidylate synthase. Biochem. **29**: 6977-6986.

Finer-Moore, J.S., E.B. Fauman, P.G. Foster, K.M. Perry, D.V. Santi, and R.M. Stroud. 1993. Refined structures of substrate-bound and phosphate-bound thymidylate synthase from *Lactobacillus casei*. J. Mol. Biol. **232**: 1101-1116.

Finer-Moore, J.S., G.F. Maley, F. Maley, W.R. Montfort, and R.M. Stroud. 1994. Crystal structure of thymidylate synthase from T4 phage: component of a deoxy-nucleoside triphosphate-synthesizing complex. Biochem. **33**: 15459-15468.

Galivan, J.H., G.F. Maley, and F. Maley. 1976. Factors affecting substrate binding in *Lactobacillus casei* thymidylate synthetase as studied by equilibrium dialysis. Biochem.**15**: 356-362.

Garrett, C., Y. Wataya, and D.V. Santi. 1979. Thymidylate synthetase. Catalysis of dehalogenation of 5-bromo- and 5-iodo-2'-deoxyuridylate. Biochem. **18**: 2798-2803.

Garvey, E.P., and D.V. Santi. 1985. Limited proteolysis of the bifunctional thymidylate synthase-dihydrofolate reductase from *Leishmania tropica*. Proc. Natl. Acad. Sci. USA **82**: 7188-7192.

Greenwood, M.T., E.M. Calmels, and R.K. Storms. 1986. Growth-rate-dependent regulation of the expression and inactivation of thymidylate synthase in *Saccharomyces cerevisiae*. J. Bact. **168**: 1336-1342.

Grumont, R., W.L. Washtien, D. Caput, and D.V. Santi. 1986. Bifunctional thymidylate synthase-dihydrofolate reductase from *Leishmania tropica*: sequence homology with the corresponding monofunctional proteins. Proc. Natl. Acad. Sci. USA **83**: 5387-5391.

Hall, M.N., L. Hereford, and I. Herkowitz. 1984. Targeting of *E.coli* beta-galactosidase in yeast. Cell **36**: 1057-1065.

Hanahan, D. 1983. Studies on transformation of *Escherichia coli* with plasmids. J. Mol. Biol. **166**: 557-580.

Hardy, L.W., J.S. Finer-Moore, W.R. Montfort, M.O. Jones, D.V. Santi, and R.M. Stroud. 1987. Atomic structure of thymidylate synthase: target for rational drug design. Science **235**: 448-455.

Hardy, L.W., and E. Nalivaika. 1992. Asn^{177} in *Escherichia coli* thymidylate synthase is a major determinant of pyrimidine specificity. Biochem. **89**: 9725-9729.

Harrap, K.R., A.L. Jackman, D.R. Newell, G.A. Taylor, L.R. Hughes , and A.H. Calvert. 1989. Thymidylate synthase: a target for anticancer drug design. Adv. Enzyme Regul. **29**: 161-179.

Honess, R.W., W. Bodemer, K.R. Cameron, H.H. Niller, B. Fleckenstein, and R.E. Randall. 1986. The A+T-rich genome of *Herpesvirus saimiri* contains a highly conserved gene for thymidylate synthase. Proc. Natl. Acad. Sci. USA **83**: 3604-3608.

Hughes, D.E., O.A. Shonekan, and L. Simpson. 1989. Structure, genomic organization and transcription of the bifunctional dihydrofolate reductase-thymidylate synthase gene from *Crithidia fasciculata*. Mol. Biochem. Parisitol. **34**: 155-166.

Iwakura, M., M. Dawata, K. Tsuda, and T. Tanaka. 1988. Nucleotide sequence of the thymidylate synthase B and dihydrofolate reductase genes contained in one *Bacillus subtilis* operon. Gene **64**: 9-20.

Kamb, A., J.S. Finer-Moore, A.H. Calvert, and R.M. Stroud. 1992a. Structural basis for recognition of polyglutamyl folates by thymidylate synthase. Biochem. **31**: 9883-9890.

Kamb, A., J.S. Finer-Moore, and R.M. Stroud. 1992b. Cofactor triggers the conformational change in thymidylate synthase: implications for an ordered binding mechanism. Biochem. **31**: 12876-12884.

Kammen, H.O. 1966. A rapid assay for thymidylate synthetase. Anal. Bioch. **17**: 553-556.

Kenny, E., T. Atkinson, and B.S. Hartley. 1985. Nucleotide sequence of the thymidylate synthetase gene ($ThyP^3$) from the *Bacillus subtilis* phage Φ3T. Gene **34**: 335-342.

Keyomarsi, K., J. Samet, G. Molnar, and A.B. Pardee. 1993. The thymidylate synthase inhibitor, ICI D1694, overcomes translational detainment of the enzyme. J. Biol. Chem. **268**: 15142-15149.

Knighton, D.R., C.C.Kan, E. Howland, C.A. Janson, Z.Hostomska, K.M. Welsh, and D.A. Matthews. 1994. Structure of and kinetic channeling in bifunctional dihydrofolate reductase-thymidylate synthase. Struct. Biol. **1**: 186-194.

Kunkel, T.A., J.D. Roberts and R.A. Zakour. 1987. Rapid and efficient site-specific mutagenesis without phenotypic selection. Meth. Enzymol. **154**: 367-382.

Lagosky, P.A., G.R. Taylor, and R.H. Haynes. 1987. Molecular characterization of the *Saccharomyces cerevisiae* dihydrofolate reductase gene. Nucleic Acids. Res. **15**: 10355-10371.

LaPat-Polasko, L., G.F. Maley, and F. Maley. 1990. Properties of bacteriophage T4 thymidylate synthase following mutagenic changes in the active site and folate binding region. Biochem. **29**: 9561-9572.

Lazar, G., A. Hong, and H.M. Goodman. 1993. The origin of the bifunctional dihydrofolate reductase-thymidylate synthase isogenes of *Arabidopsis thaliana.* Plant J. **3**: 657-668.

Lehninger, A.L., D.L. Nelson, and M.M. Cox. 1993. Principles of Biochemistry. (Worth Publishers, New York). pp 726-732.

Leszczynsky, J.F., and G.D. Rose. 1986. Loops in globular proteins: a novel category of secondary structure. Science **234**: 849-855.

Lockshin, A., and P.V. Danenberg. 1979. Thymidylate synthetase and 2'-deoxyuridylate form a tight complex inthe presence of pteroyltriglutamate. J. Biol. Chem. **254**: 12285-12288.

Lu,Y.-Z, P.D. Aiello, and R.G. Matthews. 1984. Studies on the polyglutamate specificity of thymidylate synthase from fetal pig liver. Biochem. **23**: 6870-6876.

Luo, M.Z., P. Piffanelli, L. Rastelli, R. Cella. 1993. Molecular cloning and analysis of a cDNA coding for the bifunctional dihydrofolate reductase-thymidylate synthase of *Daucus carota.* Plant Mol. Biol. **22**: 427-435.

Luche, R.M., and R. Sumrada. 1990. A *cis*-acting element present in multiple genes serves as a repressor protein binding site for the yeast *CAR1* gene. Mol. & Cell. Biol. **10**: 3884-3895.

Maley, G.F., R.L. Bellisario, D.U. Guarino, and F. Maley. 1979a. The primary structure of *Lactobacillus casei* thymidylate synthetase: I. The isolation of cyanogen bromide peptides 1 through 5 and the complete amino acid sequence of CNBr 1, 2, 3, and 5. J. Biol. Chem. **254**: 1288-1295.

Maley, G.F., R.L. Bellisario, D.U. Guarino, and F. Maley. 1979b. The primary structure of *Lactobacillus casei* thymidylate synthetase: III. The use of 2-(2-nitrophenyl sulfenyl)-3-bromoindolenine and limited tryptic peptides to establish the complete amino acid sequence of the enzyme. J. Biol. Chem. **254**: 1301-1304.

Maley, F., J. Pedersenlane, and L.M. Changchien. 1995. Complete restoration of activity to inactive mutants of *Escherichia coli* thymidylate synthase - evidence that *Escherichia coli* thymidylate synthase is a half-the-sites activity enzyme. Biochem. **34**: 1469-1474.

Maniatis, T., E.F. Fritsch, and J. Sambrook. 1989. Molecular Cloning: A Laboratory Manual. Cold Spring Harbor Laboratory Press, Cold Spring Harbor.

Mathews, C.K., and M.B. Slabaugh. 1986. Eukaryotic DNA Metabolism. Are deoxyribonucleotides channeled to replication sites? Exp. Cell Research **162**: 285-295.

Mathews, C.K., L.K. Moen, Y. Wang, and R.G. Sargen. 1988. Intracellular organization of DNA precursor biosynthetic enzymes. Trends Biochem. Sci. **13**: 394-397.

Matthews, D.A., K. Appelt, and S.J. Oatley. 1989. Stacked beta-bulges in thymidylate synthase account for a novel right-handed rotation between opposing beta-sheets. J. Mol. Biol. **205**: 449-454.

Matthews, D.A., K.Appelt, S.J. Oatley, and N.H. Xuong. 1990a. Crystal structure of *Escherichia coli* thymidylate synthase containing bound 5-fluoro-2'-deoxyuridylate and 10-propargyl-5,8-dideazafolate. J. Mol. Biol. **214**: 923-936.

Matthews, D.A., J.E. Villafranca, C.A. Janson, W.W. Smith, K. Welsh, and S. Freer. 1990b. Stereochemical mechanism of action for thymidylate synthase based on the X-ray structure of the covalent inhibitory ternary complex with 5-fluoro-2'-deoxyuridylate and 5,10-methylenetetrahydrofolate. J. Mol. Biol. **214**: 937-948.

McIntosh, E.M., R.W. Ord, and R.K. Storms. 1988. Transcriptional regulation of the cell cycle-dependent thymidylate synthase gene of *Saccharomyces cerevisiae*. Mol. Cell. Biol. **8**: 4616-4624.

Michaels, M.L., C. W. Kim, D.A. Matthews, and J. H. Miller. 1990. *Escherichia coli* thymidylate synthase: amino acid substitutions by suppression of amber nonsense mutations. Proc. Natl. Acad. Sci. **87**: 3957-3961.

Montfort, W.R., K.M. Perry, E.B. Fauman, J.S.Finer-Moore, G.F. Maley, L. Hardy, F. Maley, and R.M. Stroud. 1990. Structure, multiple site binding, and segmental accommodation in thymidylate synthase on binding dUMP and an anti-folate. Biochem. **29**: 6964-6977.

Mullis, G.T., and F. Faloona. 1987. Specific synthesis of DNA *in vitro* via a polymerase catalyzed chain reaction. Meth. Enzymol. **155**: 335-350

Perry, K.M., E.B. Fauman, J.S. Finer-Moore, W.R. Montfort, G.F. Maley, F. Maley, and R.M. Stroud. 1990. Plastic adaptation toward mutations in proteins: structural comparison of thymidylate synthases. Proteins: Struct. Funct. and Gen. **8**: 315-333.

Perry, K.M., C.W. Carreras, L.C. Chang, D.V. Santi, and R.M. Stroud. 1993. Structures of thymidylate synthase with a C-terminal deletion: role of the C-terminus in alignment of 2'-deoxyuridine 5'-monophosphate and 5,10-methylenetetrahydrofolate. Biochem. **32**: 7116-7125.

Perryman, S.M., C. Rossana,T. Deng., E.F. Vanin., and L.F. Johnson. 1986. Sequence of a cDNA for mouse thymidylate synthase reveals striking similarity with the prokaryotic enzyme. Mol. Biol. Evol. **3**: 313-321.

Pogolotti, A.L.Jr., P.V. Danenberg, and D.V. Santi. 1986. Kinetics and mechanism of interaction of 10-propargyl-5,8-dideazafolate with thymidylate synthase. J. Med. Chem. **29**: 478-482.

Pookanjanatavip, M., Y. Yuthavong, P.J. Greene, and D.V. Santi. 1992. Subunit complementation of thymidylate synthase. Biochem. **31**: 10303-10309.

Poon, P.P. 1993. The periodically expressed *TMP1* gene is subject to START-dependent and START-independent regulation, and thymidylate synthase is localized to the nuclear periphery. PhD. thesis, Concordia University, Montreal, Quebec.

Poon, P.P., and R.K. Storms. 1994. Thymidylate synthase is localized to the nuclear periphery in the yeast *Saccharomyces cerevisiae.* J. Biol. Chem. **269**: 8341-8347.

Richter, J., I. Puchtler, and B. Fleckenstein. 1988. Thymidylate synthase gene of *Herpesvirus atales.* J. Virol. **62**: 3530-3535.

Roos, D.S. 1993. Primary structure of the dihydrofolate reductase-thymidylate synthase gene from *Toxoplasma gondii.* J. Biol. Chem. **268**: 6269-6280.

Rose, M.D., P. Novick, J.H. Thomas, D. Botstein, and G.R. Fink. 1987. A *Saccharomyces cerevisiae* genomic plasmid bank based on a centromere-containing shuttle vector. Gene **60**: 237-243.

Rouch, D.A., L.J. Messerotti, S.L. Loo, C.A. Jackson, and R.A. Skurry. 1989. Trimethoprim resistance transposon *Tn*4003 from *Staphylococcus aureus* encodes genes for a dihydrofolate reductase and thymidylate synthetase flanked by three copies of IS257. Mol. Microbiol. **3**: 161-175.

Sabatini, D.D., G. Kreibich, T. Morimoto, and M. Adesnik. 1982. Mechanisms for the incorporation of proteins in membranes and organelles. J. Cell. Biol. **92**: 1-22.

Saiki, R.K., D.H. Gelfand, S. Stoffel, S.J. Scharf, R. Higuchi, G.T. Horn, K.B. Mullis, and H.A. Erlich. 1988. Primer-directed enzymatic amplification of DNA with a thermostable DNA polymerase. Science **239**: 487-491.

Sanger, F., S. Nicklen, and A.R. Coulson. 1977. DNA sequencing with chain-terminating inhibitors. Proc. Natl. Acad. Sci. USA **74**: 5463-5467.

Schellenberger, U., P. Balaram, V.S.N.K. Francis, B.K. Shoichet, and D.V. Santi. 1994. Partial restoration of activity to *Lactobacillus casei* thymidylate synthase following inactivation by domain deletion. Biochem. **33**: 5623-5629.

Schiestl, R.H., and R.D. Gietz. 1989. High efficiency transformation of intact yeast cells using single-stranded nucleic acids as a carrier. Curr. Gen. **16**: 339-346.

Schiffer, C.A., V.J. Davisson, D.V. Santi, and R.M. Stroud. 1991. Crystallization of human thymidylate synthase. J. Mol. Biol. **219**: 161-163.

Short, J.M., J.M. Fernandez, J.A. Sorge, and W.D. Huse. 1988. λ ZAP: A bacteriophage λ expression vector with *in vivo* excision properties. Nucleic Acids. Res. **16**: 7583-7600.

Singer, S.C., C.A. Richards, R. Ferone, D. Benedict, and P. Ray. 1989. Cloning, purification, and properties of *Candida albicans* thymidylate synthase. J. Bacteriol. **171**: 1372-1378.

Storms, R.K., R.W. Ord, M.T. Greenwood, B. Mirdamadi, F.K. Chu, and M. Belfort. 1984. Cell cycle-dependent expression of thymidylate synthase in *Saccharomyces cerevisiae*. Mol. Cell. Biol. **4**: 2858-2864.

Stroud, R.M., and J.S. Finer-Moore. 1993. Stereochemistry of a multistep/bipartite methyl transfer reaction: thymidylate synthase. FASEB **7**: 671-677.

Struhl, K., D.T. Stinchcomb, S. Scherer, and R.W. Davis. 1979. High frequency transformation of yeast: autonomous replication of hybrid DNA molecules. Proc. Natl. Acad. Sci. USA **76**: 1035-1039.

Takeishi, K., S. Kaneda, D. Ayusawa, K. Shimizu, O. Gotoh, and T. Seno. 1985. Nucleotide sequence of a functional cDNA for thymidylate synthase. Nucleic Acids Res. **13**: 2035-2043.

Taslimi, P. 1995. Identification of thymidylate synthase as the molecular target of 5-fluoro-orotic acid, FOA, in yeast and isolation and partial characterization of FOA resistant mutants. Master's thesis, Concordia University, Montreal, Quebec.

Taylor, G.R., P.A. Lagosky, R.K. Storms and R.H. Haynes. 1987. Molecular characterization of the cell cycle-regulated thymidylate synthase gene of *Saccharomyces cerevisiae*. J. Biol. Chem. **262**: 5298-5307.

Thompson, R., R.W. Honess, L. Taylor, J. Morran, and A.J. Davison. 1987. *Varicella-zoster* virus specifies a thymidylate synthase. J. Gen. Virol. **48**: 1449-1455.

Vieira, J., and J. Messing. 1982. The pUC plasmids, and M13mp7 derived system for insertion mutagenesis and sequencing with synthetic universal primer. Gene **19**: 259-268.

Vieira, J., and J. Messing. 1987. Production of single-stranded plasmid DNA. Meth. Enzymol. **153**: 3-11.

APPENDIX

Preparation of cofactor (6R,S)-CH_2-H_4folate

100 mg of tetrahydrofolate (purchased from Sigma) was dissolved in 20 ml of buffer containing 30 mM $NaHCO_3$ pH 9.5, 150 mM HCHO*, 100 mM β -mercaptoethanol, while stirring over ice, shielded from light, and with N_2 bubbling through.

The active concentration of cofactor (6R-CH_2-H_4folate) was determined by reacting 0.05 units of *L.casei* thymidylate synthase with 200 μM (6R,S)-CH_2-H_4folate and 150 μM dUMP in TS assay buffer (50 mM TES, 25 mM $MgCl_2$, 6.5 mM HCHO, 1 mM EDTA, 75 mM β -mercaptoethanol) and measuring the amount of 7,8-dihydrofolate produced, at Abs_{340}.

$$\text{Maximal } Abs_{340} - \text{Baseline } Abs_{340} = \Delta Abs_{340}$$

$$\text{Concentration} = \frac{\Delta Abs_{340} \times \text{dilution factor}}{\varepsilon_{340} \times \text{pathlength}}$$

$$[6R\text{-}CH_2\text{-}H_4\text{folate}] = \frac{0.3148 \times 45.45}{6400\ M^{-1}cm^{-1} \times 1\ cm} = 2.227 \times 10^{-3}\ M$$

*HCHO concentration in original protocol was 15 mM, and was inadvertently increased 10-fold in this preparation

RAW DATA FOR KINETIC ASSAYS USING TRITIUM RELEASE METHOD AND PERMEABILIZED CELLS

		'Picomoles of protons released per 10E9 cells - wild type enzyme							
TIME IN MINUTES		[1.5 uM] dUMP	[2.5 uM] dUMP	[3.75 uM] dUMP	[5 uM] dUMP	[10 uM] dUMP	[15 uM] dUMP	[25 uM] dUMP	[100 uM] dUMP
	Set 1								
0		0	0	0	0	0	0	0	0
1		477	409	1196	914	1493	1865		
2		983	784	2458	1947	3316	3658	4729	
3		1437	1202	3695	3258	4935	5767		
4		1941	1608	4920	4123	6538	7912	9909	10650
6								15425	
8								20157	20795
12									29558
16									38688
Pmol/min/10E9 cells:		**484**	**401**	**1233**	**1059**	**1651**	**1972**	**2550**	**2407**
	Set 2								
0		0	0	0	0	0	0	0	0
1		713	1072	1803	1120	1915	2265		
2		1478	2193	3237	2274	4032	4990	5881	
3		2254	3246	5045	3659	6142	7268		
4		2928	4273	6404	4873	8200	9759	11967	15098
6								17787	
8								23464	28338
12									41008
16									50878
Pmol/min/10E9 cells:		**739**	**1072**	**1605**	**1228**	**2063**	**2452**	**2942**	**3191**

B

RAW DATA FOR KINETIC ASSAYS USING TRITIUM RELEASE METHOD AND PERMEABILIZED CELLS

		'Picomoles of protons released per 10E9 cells - wild type enzyme							
TIME IN MINUTES		[1.5 uM] dUMP	[2.5 uM] dUMP	[3.75 uM] dUMP	[5 uM] dUMP	[10 uM] dUMP	[15 uM] dUMP	[25 uM] dUMP	[100 uM] dUMP
	Set 3								
0		0	0	0	0	0	0	0	0
1		270	2098	2883	3269	4511	7958		
2		583	3962	5537	6635	9778	16792	26334	
3		904	5828	7917	9942	14489	24397		
4		1217	6885	9892	13093	19528	31674	50299	38170
6								72247	
8								84729	74743
12									114227
16									141984
Pmol/min/10E9 cells:		**306**	**1749**	**2481**	**3285**	**4903**	**7978**	**10768**	**9418**
	Set 4								
0		0	0	0	0	0	0	0	0
1		825	873	1708	1553	3842	4434		
2		1626	1789	3693	2952	7893	9545	19671	
3		2496	2622	5599	4676	12249	15153		
4		3165	3544	7330	6031	16188	19955	29899	26382
6								54567	
8								70295	72816
12									109023
16									113923
Pmol/min/10E9 cells:		**799**	**883**	**1855**	**1518**	**4078**	**5062**	**8724**	**9117**

RAW DATA FOR KINETIC ASSAYS USING TRITIUM RELEASE METHOD AND PERMEABILIZED CELLS

		'Picomoles of protons released per 10E9 cells - mutant enzyme							
TIME IN MINUTES		[100 uM] dUMP	[150 uM] dUMP	[200 uM] dUMP	[300 uM] dUMP	[400 uM] dUMP	[500 uM] dUMP	[1000 uM] dUMP	[2000 uM] dUMP
	Set 1								
0		0	0	0	0	0	0	0	0
20		453	599	614	709	745	649	900	1292
45		1148	1284	1559	1861	2008	1989	2359	2500
65		2048	2302	2953	3185	3119	3341	4928	4230
85		2823	3463	3939	4669	4785	5050	6382	6473
Pmol/min/10E9 cells:		**42**	**54**	**59**	**70**	**69**	**77**	**100**	**99**
	Set 2								
0		0	0	0	0	0	0	0	0
20		406	506	513	659	753	706	760	1095
45		868	1106	1232	1530	1794	1642	2300	2707
65		1101	1537	1702	2163	2444	2698	3259	4062
85		1339	1874	2053	2776	3364	3284	4413	5147
Pmol/min/10E9 cells:		**19**	**24**	**27**	**34**	**39**	**40**	**53**	**62**

RAW DATA FOR SPECTROPHOTOMETRIC ASSAYS - WILD TYPE - KM FOR DUMP

	ZERO	ORDER	FIT		FIRST	ORDER	FIT	
[dUMP] uM	Rate= Abs/min	Std. Dev.	Corr. Coeff.	Rate=k Y=A e	Std. Dev.	Corr. Coeff.	Abs.	Abs.
125.00	0.12766	0.0010	0.9993	0.24068		0.9995	0.63493	0.13076
125.00	0.13838	0.0014	0.9988	0.25320		0.9996	0.64526	-0.17825
50.00	0.11670	0.0006	0.9991	0.72772			0.26824	-0.13434
50.00	0.14271	0.0003	0.9993					
50.00	0.12630	0.0006	0.9992	0.67057			0.24256	-0.27924
50.00	0.12360	0.0006	0.9992	0.56068	0.0041	0.9972	0.27167	-0.19980
25.00	0.11497	0.0004	0.9970	1.44986	0.0020	0.9948	0.11681	-1.87650
10.00	0.08547			1.06968	0.0022	0.9943	0.14579	-0.57710
10.00	0.04690			1.97529	0.0010	0.9873	0.04098	-0.14150
10.00	0.09708	0.0003		5.85716	0.0007	0.9899	-0.02298	
10.00	0.04148	0.0003	0.9714	1.68168	0.0007	0.9942	0.04693	-0.12963
10.00	0.10567	0.0003	0.9884	2.30036	0.0008	0.9974	0.03487	-0.16163
5.00	0.11082	0.0002	0.8837	6.39272	0.0005	0.9954	-0.00536	-0.62399
5.00	0.09084	0.0003	0.9892	4.87811	0.0004	0.9947	0.00420	-0.26850
5.00	0.09931	0.0003	0.9516	5.12947	0.0006	0.9934	-0.00342	-0.43082
5.00	0.09960	0.0003	0.9739	6.07808	0.0004	0.9963	-0.05877	-0.88705
3.75	0.08685	0.0003	0.9892	5.83357	0.0004	0.9951	0.00329	-0.21048
3.75	0.09389	0.0020	0.9834	6.61500	0.0004	0.9953	0.02887	-0.36501
3.75	0.09799	0.0004	0.9751	5.87299	0.0004	0.9970	0.00430	-0.30774
2.50	0.07514	0.0003	0.9592	9.42625	0.0003	0.9945	-0.00702	-0.67883
2.50	0.08316	0.0002	0.9754	8.00706	0.0003	0.9943	-0.00478	-0.12028
2.50	0.06839	0.0003	0.9943	8.42723	0.0004	0.9885	-0.00924	-0.25924

RAW DATA FOR SPECTROPHOTOMETRIC ASSAYS - MUTANT EUK1 - Km FOR dUMP

[dUMP] mM	Rate= Abs/min	Standard Deviation	Corr. Coeff.		[dUMP] mM	Rate= Abs/min	Standard Deviation	Corr. Coeff.
2.0000	0.00204	0.0003	1.0100		0.1500	0.00115	0.0009	0.9821
2.0000	0.00168	0.0004	0.9973		0.1500	0.00113	0.0002	0.9216
2.0000	0.00127	0.0002	0.9059		0.1500	0.00108	0.0002	0.9487
1.0000	0.00120	0.0001	0.9041		0.1000	0.00107	0.0005	0.9671
1.0000	0.00161	0.0003	0.9982		0.1000	0.00108	0.0002	0.8916
1.0000	0.00184	0.0004	0.9402		0.1000	0.00085	0.0002	0.9886
0.5000	0.00128	0.0003	0.9340		0.0750	0.00123	0.0010	0.9680
0.5000	0.00168	0.0006	0.9863		0.0750	0.00075	0.0001	0.9149
0.5000	0.00174	0.0002	1.0225		0.0750	0.00101	0.0003	0.8992
0.3000	0.00088	0.0005	0.7878		0.0500	0.00093	0.0003	1.0008
0.3000	0.00134	0.0003	0.9784		0.0500	0.00115	0.0002	0.9465
0.3000	0.00153	0.0002	0.9862		0.0500	0.00106	0.0004	0.9884
0.2500	0.00143	0.0002	0.9504		0.0250	0.00081	0.0021	0.8318
0.2500	0.00165	0.0010	0.9705		0.0250	0.00096	0.0002	0.9162
0.2500	0.00140	0.0003	0.9600		0.0250	0.00067	0.0002	0.9768
0.2000	0.00116	0.0002	1.0477		0.0100	0.00058	0.0002	0.9314
0.2000	0.00120	0.0006	0.9614		0.0100	0.00036	0.0005	1.0631
0.2000	0.00140	0.0002	0.9585		0.0100	0.00031	0.0003	1.2994

RAW DATA FOR SPECTROPHOTOMETRIC ASSAYS - Km FOR FOLATE

WILD TYPE					MUTANT EUK1			
[Folate] uM	Rate= Abs/min	Standard Deviation	Corr. Coeff.		[Folate] uM	Rate= Abs/min	Standard Deviation	Corr. Coeff.
1.25	0.01352	0.0001	0.9375		200	0.00099	0.0005	0.9674
1.25	0.01417	0.0001	0.8881		200	0.00082	0.0007	0.9799
2.5	0.03574	0.0002	0.961		160	0.00079	0.001	0.9482
2.5	0.0344	0.0001	0.979		100	0.00074	0.0005	0.9961
5	0.06841	0.0001	0.9943		80	0.00073	0.0005	0.9858
5	0.0489	0.0001	0.9993		60	0.00069	0.0006	0.9654
7.5	0.07779	0.0001	0.9973		50	0.0006	0.0003	0.983
7.5	0.07428	0.0001	0.9976		50	0.00062	0.0005	0.9919
10	0.11051	0.0001	0.999		40	0.00037	0.0006	0.9813
10	0.06563	0.0001	0.9996		30	0.00042	0.0004	0.9659
15	0.09234	0.0001	0.9984		20	0.00036	0.0002	0.9914
15	0.10249	0.0001	0.9985		20	0.00034	0.0001	0.9878
20	0.11014	0.0001	0.9997		10	0.00015	0.0001	0.9747
20	0.09711	0.0003	0.9989		10	0.00021	0.0001	0.9922
50	0.1142	0.0006	0.9992		10	0.0001	0.0003	0.8296
50	0.11864	0.0009	0.9985					
160	0.1138	0.0003	0.9998					
200	0.11828	0.0011	0.9991					

DATA FOR TABLE VII

Protein Concentrations

Protein concentrations were measured by the Bradford method, using BSA as standard and correcting for BSA by dividing all values by 2 (Maniatis *et al* , 1989).

Crude extract:	12 µg/µl ÷ 2 = 6 µg/µl
Q-sepharose pool:	5.8 µg/µl ÷ 2 = 2.9 µg/µl
Hydroxyapatite pool:	4.6 µg/µl ÷ 2 = 2.3 µg/µl
Cibacron- blue fraction #5*	5.4 µg/µl ÷ 2 = 2.7 µg/µl

*Enzyme was collected from Cibacron-blue column in 7 fractions which were concentrated separately. Assays of these fractions showed that they all had equivalent specific activities, i.e. equivalent dpms were obtained from amounts that gave same band intensities on a Western blot. Activity of fraction #5 is therefore indicative of the activity of the entire stock.

Assays

Amount of protein used per reaction:

Crude extract:	91 µl = 546 µg
Q-sepharose pool:	192 µl = 557 µg
Hydroxyapatite pool:	60 µl = 138 µg
Cibacron-blue #5:	14 µl = 38 µg

Reaction volume: 600 µl for crude extract and Q-sepharose pools
400 µl for hydroxyapatite pool and Cibacron-blue #5

Volume of aliquots taken at various time points: 180 µl

Volume of charcoal supernatant counted: 180 µl (of 620 µl total volume)

Activity of tritiated dUMP: 49.5 dpm/pmole

Sample calculation of specific activity: (for crude extract)

Activity per sample = 644 dpm/min (see next page)
Protein per sample = 180÷ 600 x 546 µg = 164 µg

$$\frac{644 \text{ dpm/min} \times 620 \text{ µl}}{180 \text{ µl} \times 49.5 \text{ dpm/pmol} \times 164 \text{ µg}} = 0.2732 \text{ pmol/min/µg}$$

	Rxn #	dpms at time = 15 min	dpms at time = 25 min	dpms at time = 35 min
Crude extract	1	12575	19646	25605
	2	12838	18995	24731
	3	11768	17911	23386
Q-sepharose pool	1	10260	20027	30155
	2	10290	19139	28779
Hydroxyapatite pool	1		15764	24635
	2		17161	24665
	3		15686	23491
Cibacron-blue #5	1		12869	20404
	2		15503	22257
	3		12836	19696
Blank	1			650
	2			734

Activities of samples in dpms/min (calculated by linear regression analysis)

Crude extract:	644
Q-sepharose pool:	935
Hydroxyapatite pool:	780
Cibacron-blue #5:	665

Specific activities of samples:

	pmoles/min/μg protein	units*/mg protein
Crude extract:	0.2732	0.2732×10^{-3}
Q-sepharose pool:	0.3896	0.3896×10^{-3}
Hydroxyapatite pool:	0.8754	0.8754×10^{-3}
Cibacron-blue #5:	2.7220	2.7220×10^{-3}

*1 unit of activity is defined as 1 μmole of product per minute

Calculation of TS specific activity from spectrophotometric assay results

Calculated: $V_{max} = 0.128844$ Abs/min

Convert Abs_{340} to moles/liter of 7,8-H_2folate:

$$Abs = \varepsilon\ b\ C$$

where

C = concentration
b = pathlength
$\varepsilon_{340} = 6400$ for 7,8-H_2folate at pH 7.4

$$[7,8\text{-}H_2\text{folate}] = \frac{0.128844}{6400\ M^{-1}cm^{-1} \times 1\ cm} = 20.132 \times 10^{-6}\ \text{moles/liter}$$

20.132×10^{-6} moles/liter = 20.132×10^{-3} moles/ml

Specific activity = 20.132×10^{-3} moles/min/13.6 µg of protein

= 1.4803 µmoles/min/µg of protein

= 1.48 units/µg of protein

where 1 unit of activity is defined as 1 µmole of product per minute